



QEX

\$5

March/April 2010

www.arri.org

A Forum for Communications Experimenters

Issue No. 259



Jon Wallace presents more of his Amateur Radio astronomy work. Signals recorded with simple VLF receivers and displayed with a computer spectrogram program allow us to “see” the various types of natural radio signals that occur at 10 to 20 kHz.

KENWOOD

Listen to the Future

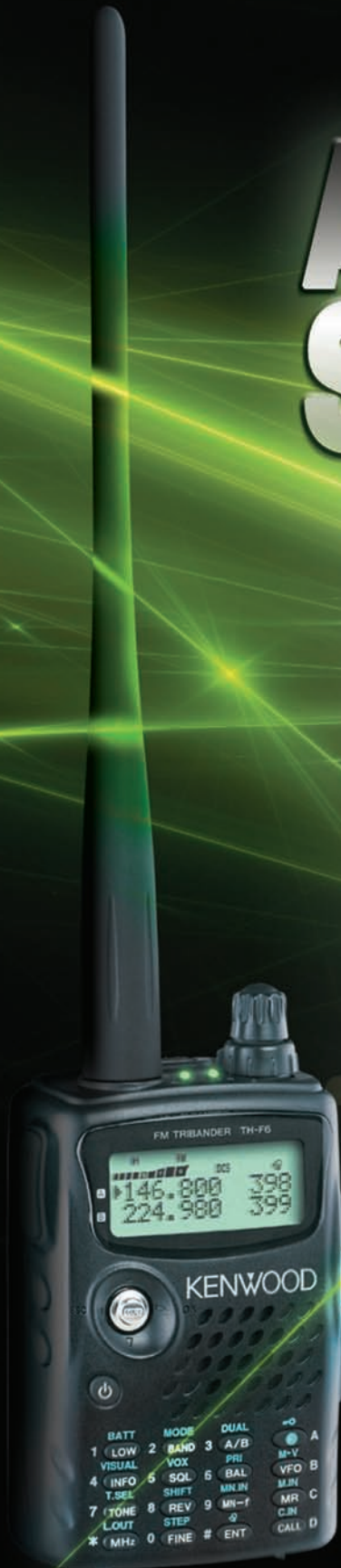
AIRWAVE SUPERIORITY

Never before has a compact HT offered as many features, and such high powered performance as the TH-F6A. Arm yourself with one today and gain your own airwave superiority.

- Triband 144/220/440 MHz all at 5W
- Receives 2 frequencies simultaneously even on the same band
- 0.1-1300MHz high-frequency range RX (B band)¹
- FM/FM-W/FM-N/AM plus SSB/CW receive
- Bar antenna for receiving AM broadcasts
- Special weather channel RX mode
- 435 memory channels, multiple scan functions
- 7.4V 2000mAh lithium-ion battery (std.) for high output² and extended operation
- 16-key pad plus multi-scroll key for easy operation
- Built-in charging circuitry for battery recharge while the unit operates from a DC supply
- Tough construction: meets MIL-STD 810 C/D/E standards for resistance to vibration, shock, humidity and light rain
- Large frequency display for single-band use
- Automatic simplex checker
- Wireless remote control function
- Battery indicator • Internal VOX • MCP software

¹Note that certain frequencies are unavailable. ²5W output

TH-F6A TRIBANDER



www.kenwoodusa.com



KENWOOD U.S.A. CORPORATION
Communications Sector Headquarters
3970 Johns Creek Court, Suite 100, Suwanee, GA 30024
Customer Support/Distribution

P.O. Box 22745, 2201 East Dominguez St., Long Beach, CA 90801-5745
Customer Support: (310) 639-4200 Fax: (310) 537-8235

ADS#36709



QEX (ISSN: 0886-8093) is published bimonthly in January, March, May, July, September, and November by the American Radio Relay League, 225 Main Street, Newington, CT 06111-1494. Periodicals postage paid at Hartford, CT and at additional mailing offices.

POSTMASTER: Send address changes to: QEX, 225 Main St, Newington, CT 06111-1494 Issue No 259

Harold Kramer, WJ1B
Publisher

Larry Wolfgang, WR1B
Editor

Lori Weinberg, KB1EIB
Assistant Editor

Zack Lau, W1VT
Ray Mack, W5IFS
Contributing Editors

Production Department

Steve Ford, WB8IMY
Publications Manager

Michelle Bloom, WB1ENT
Production Supervisor

Sue Fagan, KB1OKW
Graphic Design Supervisor

David Pingree, N1NAS
Senior Technical Illustrator

Advertising Information Contact:

Janet L. Rocco, W1JLR
Business Services
860-594-0203 – Direct
800-243-7768 – ARRL
860-594-4285 – Fax

Circulation Department

Cathy Stepina, QEX Circulation

Offices

225 Main St, Newington, CT 06111-1494 USA
Telephone: 860-594-0200
Fax: 860-594-0259 (24 hour direct line)
e-mail: qex@arrl.org

Subscription rate for 6 issues:

In the US: ARRL Member \$24,
nonmember \$36;

US by First Class Mail:
ARRL member \$37, nonmember \$49;

International and Canada by Airmail: ARRL member \$31, nonmember \$43;

Members are asked to include their membership control number or a label from their QST when applying.

In order to ensure prompt delivery, we ask that you periodically check the address information on your mailing label. If you find any inaccuracies, please contact the Circulation Department immediately. Thank you for your assistance.



Copyright © 2010 by the American Radio Relay League Inc. For permission to quote or reprint material from QEX or any ARRL publication, send a written request including the issue date (or book title), article, page numbers and a description of where you intend to use the reprinted material. Send the request to the office of the Publications Manager (permission@arrl.org).

March/April 2010

About the Cover

Jon Wallace continues with his “Amateur Radio Astronomy Projects.” The cover image shows two VLF radios — a Kiwa Earth Monitor and Brian Lucas’ ATMOS receiver. The computer spectrogram displays a sound file recording from the NASA INSPIRE Project (www.theinspireproject.org). This technique allows us to “see” the various types of natural radio signals that occur at 10 to 20 kHz.

In This Issue

Features

3 Design, Construction and Evaluation of the Eight Circle Vertical Array for Low Band Receiving®

By Joel Harrison, W5ZN and Bob McGwier, N4HY

19 Amateur Radio Astronomy Projects—A Whistler Radio

By Jon Wallace

23 Waveguide Filters You Can Build—and Tune—Part 3

By Paul Wade, W1GHZ

30 Doppler Tracking

By Chuck McConaghy, WA6SYE

38 On Maximizing the Tuning Range of SA/NE 602 IC Colpitts Oscillators

By John E. Post, KA5GSQ

44 An Inexpensive HF Power Meter with a Linear dB Scale

By Robert K. Zimmerman, VE3RKZ

Columns

47 Letters

48 In the Next Issue of QEX

Index of Advertisers

American Radio Relay League:..... Cover III
Down East Microwave Inc:.....48
Kenwood Communications:..... Cover II
National RF, Inc:48

Nemal Electronics International, Inc:.....37
RF Parts43, 45
Tucson Amateur Packet Radio:29
Yaesu USA Cov IV

The American Radio Relay League

The American Radio Relay League, Inc. is a noncommercial association of radio amateurs, organized for the promotion of interest in Amateur Radio communication and experimentation, for the establishment of networks to provide communications in the event of disasters or other emergencies, for the advancement of the radio art and of the public welfare, for the representation of the radio amateur in legislative matters, and for the maintenance of fraternalism and a high standard of conduct.



ARRL is an incorporated association without capital stock chartered under the laws of the state of Connecticut, and is an exempt organization under Section 501(c)(3) of the Internal Revenue Code of 1986. Its affairs are governed by a Board of Directors, whose voting members are elected every three years by the general membership. The officers are elected or appointed by the Directors. The League is noncommercial, and no one who could gain financially from the shaping of its affairs is eligible for membership on its Board.

"Of, by, and for the radio amateur," ARRL numbers within its ranks the vast majority of active amateurs in the nation and has a proud history of achievement as the standard-bearer in amateur affairs.

A *bona fide* interest in Amateur Radio is the only essential qualification of membership; an Amateur Radio license is not a prerequisite, although full voting membership is granted only to licensed amateurs in the US.

Membership inquiries and general correspondence should be addressed to the administrative headquarters:

ARRL
225 Main Street
Newington, CT 06111 USA
Telephone: 860-594-0200
FAX: 860-594-0259 (24-hour direct line)

Officers

President: JOEL HARRISON, W5ZN
528 Miller Rd, Judsonia, AR 72081

Chief Executive Officer: DAVID SUMNER, K1ZZ

The purpose of *QEX* is to:

- 1) provide a medium for the exchange of ideas and information among Amateur Radio experimenters,
- 2) document advanced technical work in the Amateur Radio field, and
- 3) support efforts to advance the state of the Amateur Radio art.

All correspondence concerning *QEX* should be addressed to the American Radio Relay League, 225 Main Street, Newington, CT 06111 USA. Envelopes containing manuscripts and letters for publication in *QEX* should be marked Editor, *QEX*.

Both theoretical and practical technical articles are welcomed. Manuscripts should be submitted in word-processor format, if possible. We can redraw any figures as long as their content is clear.

Photos should be glossy, color or black-and-white prints of at least the size they are to appear in *QEX* or high-resolution digital images (300 dots per inch or higher at the printed size). Further information for authors can be found on the Web at www.arrl.org/qex/ or by e-mail to qex@arrl.org.

Any opinions expressed in *QEX* are those of the authors, not necessarily those of the Editor or the League. While we strive to ensure all material is technically correct, authors are expected to defend their own assertions. Products mentioned are included for your information only; no endorsement is implied. Readers are cautioned to verify the availability of products before sending money to vendors.

Larry Wolfgang, WR1B

lwolfgang@arrl.org

Empirical Outlook

Life Changing Events

A number of recent stories have me thinking about events that can change lives. Most of us pay at least some lip service to the emergency communications aspects of Amateur Radio. After all, it's one of those important five purposes of the Amateur Radio service listed in the FCC Rules. Section 97.1(a) of the Rules says "Recognition and enhancement of the value of the amateur service to the public as a voluntary noncommercial communication service, particularly with respect to providing emergency communications." So, this must be pretty important. What does it mean to you, and how do you react in a communications emergency?

The devastation of the January earthquake in Haiti has caught the national and world news media attention for several weeks. When I first heard about the earthquake I wondered if there was any Amateur Radio communications activity, and tuned my radio to 20 meters and then 40 meters. Several nets had been listed in an ARRL bulletin, so I listened on those frequencies first. It was interesting to hear many stations checking in to ask how they could help, or to notify the net control stations that they were standing by to help. Stations at different locations might serve as important relay points if they could hear traffic that the NCS or other stations were not able to hear because of propagation conditions. I chose to listen without checking in. Why further clutter the airwaves with non-emergency communications? If I had heard a call from a station and no one else was acknowledging it, then I could have checked in and offered to help.

Frequencies were also announced for emergency communications, and we were asked to keep those frequencies clear. This request also at least implied that people were needed to monitor those frequencies for any emergency communications from Haiti. Again, silent monitoring seemed like the most appropriate response to me.

While I didn't hear any HH stations, it was certainly interesting to monitor some of the activity surrounding this disaster, and to hear some of the stories from Amateur Radio operators who went, or attempted to go to Haiti to offer communications assistance. I did not have a direct impact on any of that communications, and the events in Haiti might not seem to have directly impacted my life in a significant way, but many lives were definitely touched.

A series of significant snow storms also hit large sections of the US in the final week of preparing this issue of *QEX* for the printer. I wonder how many motorists were able to call for help, either for themselves or someone else by using Amateur Radio during those storms. How many emergency shelters relied upon Amateur Radio operators for communications links between the shelters and the base agency? What other important communications role did Amateur Radio play? In any case, those calls for help also depend on operators who are listening and able to respond to the requests.

I was also struck by the story about the man who took a "short cut" over some back roads in Colorado, and became stranded in his vehicle for 3 days, stuck in the snow. (This happened at about the same time the northeast was digging out of the first of those big snowstorms.) Might he have been able to make a call for help if he were a ham, with a mobile transceiver in his car? Perhaps it's a good case for a mobile HF installation, for the times we are out of repeater range.

On Sunday February 7, an explosion at a natural gas fired electric generating station under construction in Middletown, Connecticut claimed five lives and injured several more. This struck a little "closer to home" for me, because we lived in Middletown for the first seven years of my career at ARRL. While I didn't know any of the workers who were killed in that explosion, two were from nearby communities and one was an Amateur Radio operator from Missouri. I had never met Chris, NØHVK, but many hams in Connecticut had. A dedicated family man out of work, he came to Middletown to help build the power plant. While here, he became active with an Amateur Radio club and volunteered at a number of public service communications events and club activities. He apparently loved ham radio, and the friends he made among the hams in Connecticut probably made his time away from family and friends in Missouri a bit easier. From the stories told by the members of his club, he had also touched their lives in a significant way. We swell with pride at stories of lives and/or property saved by Amateur Radio communications, and we mourn at lives lost. Near or far, it doesn't matter.

We may not realize the impact our words and actions can have on others. I am sure we all do our best to have it be a positive impact, as much as possible.

Design, Construction and Evaluation of the Eight Circle Vertical Array for Low Band Receiving[©]

Copyright 2008, 2009

If you have the available real estate, this steerable array of vertical antennas may offer significant advantages.

In recent years, interest in DXing on the 160 and 80 meter amateur bands has increased. This has been driven by a number of factors including ARRL's DX Challenge Award and the expanded volume of low band antenna information in various publications and on the internet.¹ The impact of *ON4UN's Low Band DXing* book is not to be underestimated.² In addition, the large signal handling capability of Amateur Radio equipment has improved tremendously in the last two decades. These positive influences have prompted many radio amateurs to increase their knowledge of antenna and propagation characteristics on the low bands. Many have attempted to apply that knowledge by constructing and evaluating various antenna designs in different environments, and the authors are included in that group.

W5ZN has many years of experience in designing and evaluating antenna systems for amateur microwave applications and has presented numerous technical papers at conferences of the Central States VHF Society, Southeast VHF Society and the Microwave Update Conference, as well as co-authoring the chapter on multi-band feeds in the *W1GHZ Microwave Antenna Book*.^{3, 4, 5, 6} Using these designs at W5ZN resulted in first place finishes and new records in numerous contests. In 1987, after moving from a city lot to a 30 acre field he became interested in expanding his knowledge and

experience with receiving antennas for the Amateur Radio 160 and 80 meter bands.

N4HY has actively designed and modeled numerous antenna systems for multi-station amateur installations. He was AMSAT VP of Engineering for 3 years. Bob is the author of numerous papers about Amateur Radio for ARRL/TAPR Digital Communications Conferences, AMSAT Symposia and *QST*. He was previously an active member of the Frankfurt Radio Club but has been inactive in HF contesting for 15 years. He is active in VHF+ contesting. Bob is a proud member of the "Amateur Radio Geek Squad," and is a co-developer of the SDR code for Flex Radio's PowerSDR™.

The authors teamed up to refine the design, document the construction and evaluate the performance of the "W8JI Eight Circle Vertical Array" at Joel's station in north central Arkansas.

1.0 Design of the Eight Circle Array

The primary objective of any low band receiving array is to obtain a directivity pattern that will reduce the impact of various noise sources from multiple directions and locations. Antenna gain is not of specific importance in these designs since the sky noise is sufficiently high that not all of the gain in full size antennas and modern receivers can be used on the low bands. It is better to optimize directivity and ambient noise suppression in the antenna, and to optimize

the receivers for large signal handling and dynamic range. It is not the intent of this paper to discuss all of these topics. We suggest that a thorough study and understanding of *ON4UN's Low Band DXing*, Fourth Edition, by John Devoldere, ON4UN, is a requirement prior to proceeding with any low band operation. (See Note 2.) Chapter 7 is prerequisite for any receiving antenna project. In addition, the specific theory related to end-fire and broad-side arrays in the same chapter must be read and understood as well. The Eight Circle Vertical Array system is based on this theory and cannot be used to its full potential without this knowledge. If you don't fully and completely understand this material, read it as many times as necessary to adequately comprehend it, along with the wave characteristics and mathematics that encompasses the design.

1.1 Element and Array Design

The 160 meter Eight Circle Vertical Array was designed by Tom Rauch, W8JI, and previewed in the Fourth Edition of *ON4UN's Low Band DXing*, Chapter 7, Section 1.30. The array is centered on a shortened top loaded vertical and described in the above reference in section 1.21.1. Additional information on small vertical arrays can be found on Tom Rauch's Web site.⁷

[After reading the "In the Next Issue of QEX" item in the Jan/Feb issue, Robert Zavrel, W7SX, sent me a note to tell me that he holds a patent on an eight-circle vertical

¹Notes appear on page 17.

array from work he did in 1994. Bob's patent is number 5,479,176: "Multiple-element driven array antenna and phasing method." Details are available on the US Patent Office Web site; patft.uspto.gov. The details are also available from several other patent search Web sites, including www.google.com/patents. — Ed.]

We wished to further evaluate the design of the array and also evaluate an 80 meter version that did not exist (at least at the time of the original analysis that was done before the Devoldere publication of details of the 160 m array in *Low Band DXing* and later presented to N2NT, W2GD, and K3LR). The most crucial missing piece of all is a step by step *how-to* in building, tuning, and using the antenna. None chose to build it at the time of the original analysis, so it was dropped until W5ZN declared an intention to do so. It is important to understand first and foremost that this is a receiving antenna. Like most receive antennas, it is designed only for this purpose and is wholly unsuitable for transmitting.

One of the ways we make sure it is unsuitable for transmit applications is to use impedance matching with a low-wattage-rated resistor. This resistor will do great things in this application; most prominently it will lower the Q and broaden the response of the antenna at good SWR and match it to widely available and inexpensive coaxial cable. This comes at the expense of gain, but in the overall communications system, coupled with analysis of the noise temperature of the bands (160 meters as well as 80 meters), gain is not the primary objective with a low band receiving antenna design, and its insertion loss is not harmful. At 160 meters, the array using the elements proposed will have plenty of gain at -8 dBi. This loss actually helps increase the IP^3 of the system — a very important thing on the low bands! As such, we believe you should not even need a pre-amp unless you are installing an incredibly long feed line run from the array center to the shack, or feel the need to have one just as a buffer between the antenna and the rigs. That will be for you to determine based on your specific installation. Numerous methods for determining this need have been previously published. (See Notes 2 and 7.) With the theoretical gain given above, this will equate to an MDS in, say, an FT-1000MP, that will be -120 dBm on this antenna. That is very low for both 160 and 80 meters.

This antenna array will exhibit nearly the same gain and directivity over the entire 160 meter band and even better results should be achieved on 80/75 meters from 3.5 to 3.8 MHz with the 80 meter version. The results of the 160 m construction and testing, presented later, do attest to the validity

of the analysis. Our recommendation is that the design be skewed toward the bottom of each band.

Of primary importance in the design of low band receiving antennas is the Directivity Merit Factor (DMF, referred to by ON4UN) or a better measure, Receiving Directivity Factor (RDF, the W8JI measure) which is the ratio in dB of the forward gain at a desired direction and take off angle to the average gain over the rest of the entire sphere around the antenna. (See Notes 2 and 7.) These two "Factors" are described in detail in Sections 1.8 through 1.10 of Devoldere's book. While this antenna array has some small side lobes (see Figure 9), they are really nothing to be concerned about and are better than most four squares and Yagi antennas. You can trade off some side lobes for better directivity, and this was done in the original analysis discussed above. A nine element circle array, design by John Brosnahan, WØUN, makes these side lobes smaller but it does not increase the directivity factor significantly and has a larger lobe upward, which is prone to sky noise.⁸ One benefit of the WØUN design is that it can also be used for transmitting, but this comes at the expense of a more complicated switching and phasing network than needed for the eight circle antenna. John's system phases a three element parasitic array with a broadside/end-fire cell.

The Eight Circle Vertical Array is inex-

pensive, easy to build and easy to feed, as the utilization of a broadside/end-fire array reduces the complexity of the switching system. An analysis of vertical elements shows why the short vertical element is ideal for low band receive applications.

First, the ground is much less important. There is little ground effect cancellation of radiation. These small vertical elements with a top hat are still quite sensitive and have a low feed point impedance after you cancel their capacitive reactance with a small inductor at the base. Since the antenna needs to be broadband, the feed is swamped with a resistor and we should make it as large as practical, consistent with the coaxial feed line impedance. This allows us to use the least expensive coax that will permit reliable, robust operation. In this case 75Ω cable is perfect, plentiful, and cheap. Therefore, a short element with a capacitive top and an inductive loading coil at the base with enough resistance to bring the mostly resistive impedance up to 75Ω is nearly ideal. The resistive swamping lowers the Q and increases the operating bandwidth with 75Ω cable.

1.2 Modeling the Individual Elements

The best approach is to use the W8JI element. There isn't a great deal of information published about this design, so Bob did our own modeling with *EZNEC/4 Professional*.

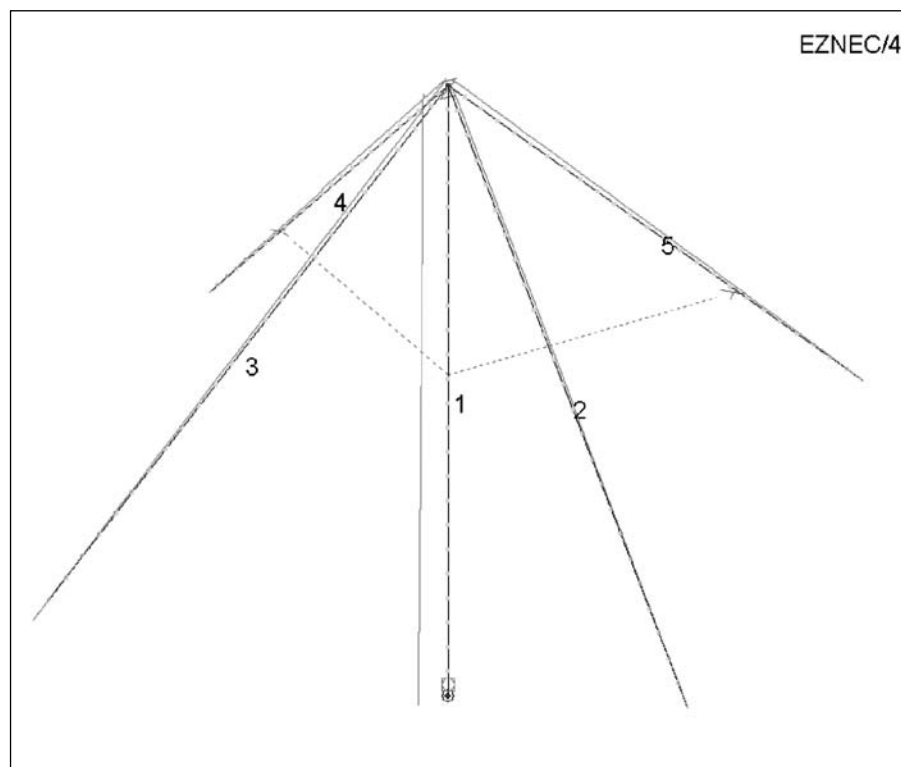


Figure 1 — This antenna drawing from *EZNEC/4 Pro* shows the analysis segments and bottom load as well as top-hat details of one element of the Eight Circle Vertical Array (no radials shown here).

Figure 1 shows the segment layout of the shortened vertical. This vertical contains some minor modifications from the W8JI design, based on Bob's studies.

The model shown in Figure 1 is from the W8JI site but has been slightly modified based on our analysis. The EZNEC/4 model files we used for our analysis are available for download from the ARRL QEX files Web site.⁹ Our model contains the correct number of segments and a better analysis of the loading of both the top-hat and base, and does an adequate job of modeling with the radial system. This determination was made because using *EZNEC/4 Pro* allows for good theoretical ground models. It is here we learned of the importance of the construction details over various quality grounds and how to achieve robust and predictable operation over all sorts of climates and soil conductivities. The 160 meter and 80 meter models are approached as lump resistance in the feed with lumped inductance, and no attempt is made to account for the resistance of the small inductors except when choosing the appropriate resistor. This is taken care of when we get to setup and tuning.

For 160 and 80 meters, the dimensions of the vertical and top hat wires are all 25 feet in length, with the top-hat wires also acting as guys, 25 feet from the base of the vertical. This allows the top-hat to serve as both capacitive top-loading and provide very good high angle rejection as well. Because the structure is ground mounted and four of the elements are active in each of the eight directions in a broadside/end-fire cell, the rejection above 45° is at least 9 dB down from the main lobe maximum. The suppression goes up with increasing angle and is a key feature of the top-hat because it acts as a shield against a large expanse of the sky and reduces sky noise above the antenna from reaching the receiver. The short, ground-mounted structure provides immunity from man-made noise in all but the immediate vicinity. So performance will be good so long as you minimize line of sight noise sources for the array.

The individual vertical structure is self resonant at 75 meters so we will need to bring the resonant frequency down with a small inductor. On 160 meters, our design indicated the load inductor to be 30 μH with enough resistance to give a low SWR at 1.85 MHz. This will provide less than 1.5:1 SWR from 1.8 to 1.9 MHz to 75 Ω coax. On 80 meters, the design indicates a 2 μH inductor will be required with the addition of enough resistance to give a low SWR from 3.5 to 3.8 MHz.

The 75 Ω feed point impedance was chosen because of the availability of inexpensive, readily available coax (cable TV installation)

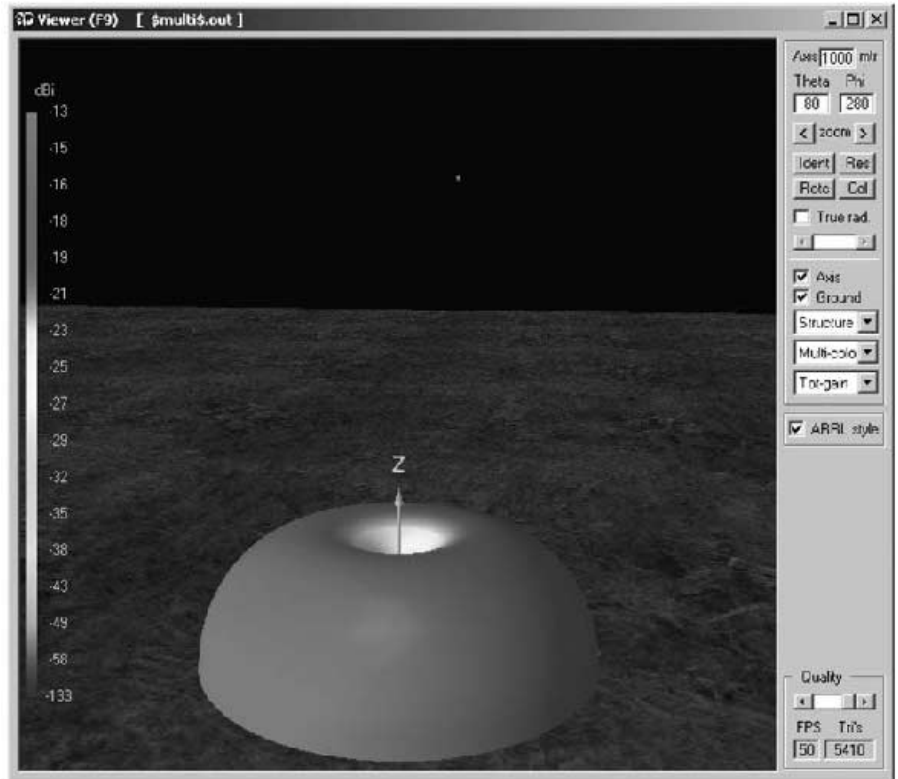


Figure 2 — This 3D radiation pattern for a single element from the array is captured from *4nec2*.

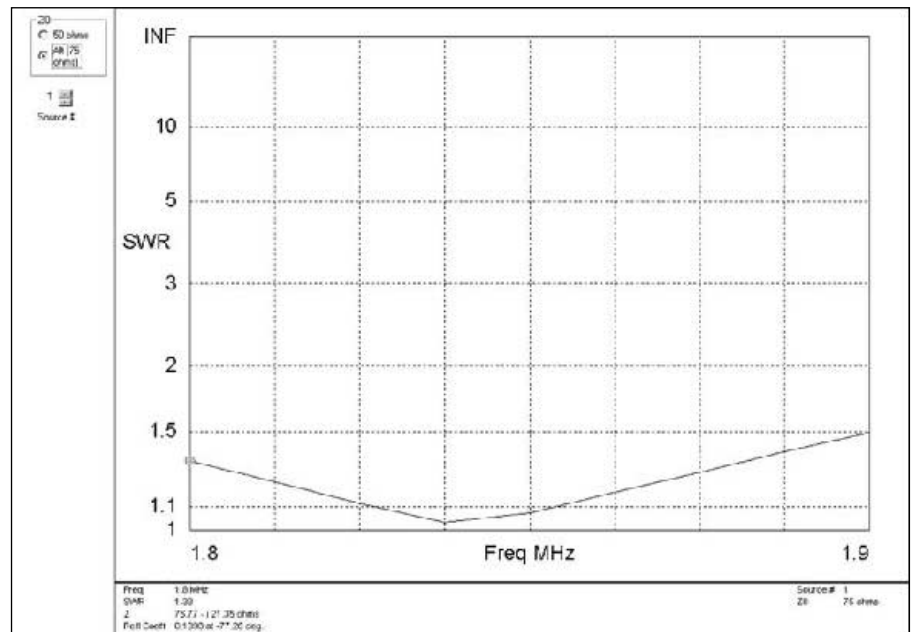


Figure 3 — This SWR profile is for one 160 meter vertical.

plus the higher resistance is used to broaden the SWR, since it is accomplished by lowering the Q . This helps guarantee the front end of your receiver sees the kinds of loads it needs to see to perform correctly.

The mounting is not critical and no special fixtures are needed to insulate the vertical element and top hat wires. You will not be able to tell the difference between an insulated bottom from one held off the ground by a fence post (non-conductive of course!).

The design uses a top-hat made from AWG no. 16 wire with the vertical element assumed to be a 1.25 to 1.5 inch diameter vertical pipe.

Even though ground resistance is not particularly important for radiation resistance, as mentioned earlier, you will need at least four $\frac{1}{8}$ to $\frac{1}{4} \lambda$ radials on each element in order to stabilize the feed point resistance over changing ground conditions year round. The exact number and length can be determined with some very easy tests after initial construction. That process will be covered later. Again, the ground system only needs to be good enough to provide a stable feed point resistance, since the object is not super efficiency and gain, but directivity and stability of the impedances in all seasons. This will permit the system to be close enough to “perfect” that the modeling applies consistently. Four radials are likely sufficient and that is what you should start with, but testing can easily be performed after construction to determine the exact number required. One each of these initial radials should be buried beneath each one of the top-hat wires. Depending on your location, just remember that if the radials are under more than just a few inches of water, they are effectively shielded from the antenna, and ineffective. Figure 2 shows the 3D pattern of one of the vertical elements at resonance using $4nec2dx$.

Figure 3 displays the SWR profile for Bob’s 160 meter design, computed by *EZNEC/4 Professional*, assuming perfect ground, 30 μH base inductor, resistor and 75 Ω coax.

The 80 meter design SWR profile, as computed by *EZNEC/4 Professional* assuming perfect ground, 2 μH base inductor, resistor and 75 Ω coax is shown in Figure 4.

1.3 Array Geometrics

The Eight Circle Vertical Array is comprised of broadside/end-fire cells. The circle’s dimension is determined by the broadside spacing and the end-fire spacing. Much analysis has been performed on the optimum broadside and end-fire spacing so rather than spend time in an effort to determine the same conclusions we will use those results. For those wishing to dig into the theory behind the spacing you can review Chapter 7 Section 1.11 and 1.12 of *ON4UN’s*

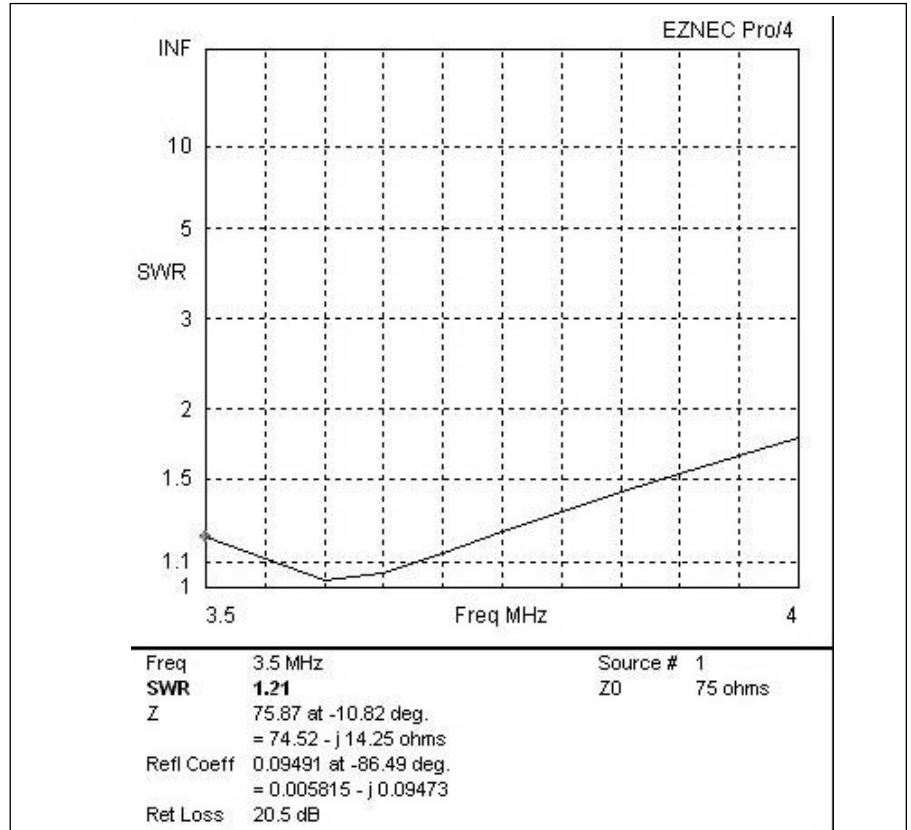


Figure 4 — Here is an SWR Profile for one 80 meter vertical.

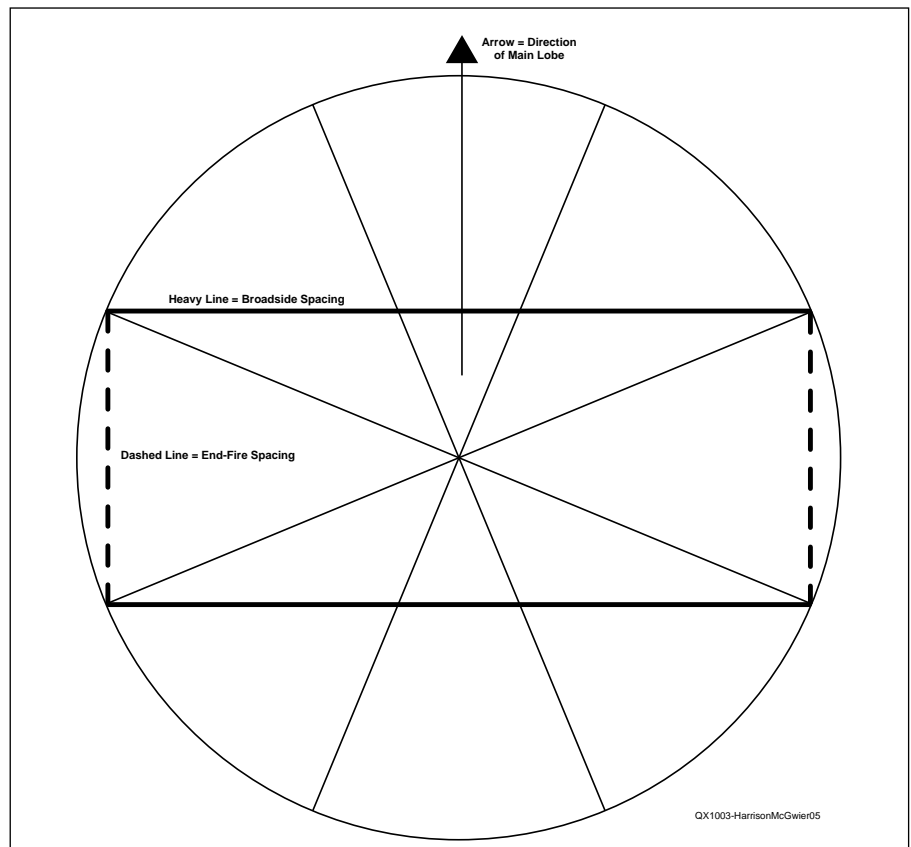


Figure 5 — This drawing shows the geometry of the Eight Circle Vertical Array of broadside/end-fire cells.

Low Band DXing.

The optimum broadside spacing for a takeoff angle of 24°, which yields the best attenuation off the sides, is 0.55 λ and yields an RDF of 13 dB. W8JI has suggested the possibility of using a slightly wider spacing of 0.65 λ. With this spacing, you will increase the number and/or size of the side lobes but in return you get a narrower 3 dB beamwidth. Bob calculated the RDF for this spacing to be 12.5 dB. For those in quiet areas, there is no doubt you should use 0.65 λ broadside spacing. If you live near a variety of noise sources you could use 0.55 λ broadside spacing to increase the rejection on as many of those sources as possible.

As depicted in Figure 5, once you decide on the broadside spacing and understand that the elements are going to land on a circle, the entire array geometry is determined.

The broadside dimension determines the entire circle as soon as it is specified. The end-fire spacing is determined by the broadside spacing and the circular array. The broadside spacing is the *only* degree of freedom in the entire design.

The crossing diameter lines represent the individual feed lines to each vertical antenna. These may be any equal electrical length pieces of 75 Ω coax. If you make them odd multiples of ¼ λ in length (¼ λ lengths of feed line will not reach the center feed point of the array) such as ¾ λ, then some nice opportunities are available for measuring antenna currents and voltages at the feed points. This is not necessary! They just have to all be equal lengths.

If the forward two elements are combined in phase and the back two elements are combined in phase then run through a phasing line and inverted in a 1:1 inverter transformer, then the antenna is beaming in the direction of the arrow.

The layout for this specific design is given in Table 1.

1.4 Feeding the Array

Feeding this array is relatively easy. The materials required are:

- One — 4:1 UNUN transformer.
- One — 1:1 Inverter transformer.
- Nine — DPDT relays.
- Two — 75 Ω coaxial phasing lines.

- These two pieces of 75 Ω coax are connected in parallel to form a 37.5 Ω phasing line. The final length will be discussed later, as there are trade-offs to consider.

Figure 6 shows the feed arrangement for the broadside/end-fire cell. Upon careful review, it becomes clear why this is so easy. The “front two antennas” consist of the two elements in the “front” of the four element cell coming to a Tee. The “back two antennas” are the back elements in the four element cell coming to a Tee. Two pieces of

Table 1
Eight-Circle Array Configuration

Band (Meters)	Broadside Spacing (λ)	(Meters)	(Feet)	Circle Diameter (ft)
160	0.55	90.1	296	320
160	0.65	106.5	350	378
80	0.55	46.5	152.5	165
80	0.65	55	180	194

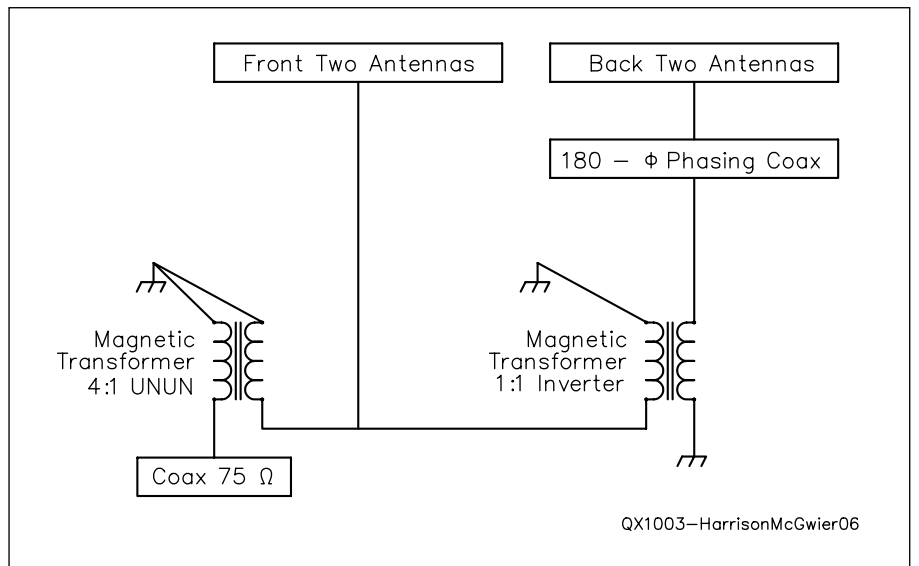


Figure 6 — Here is the feed arrangement for one cell.

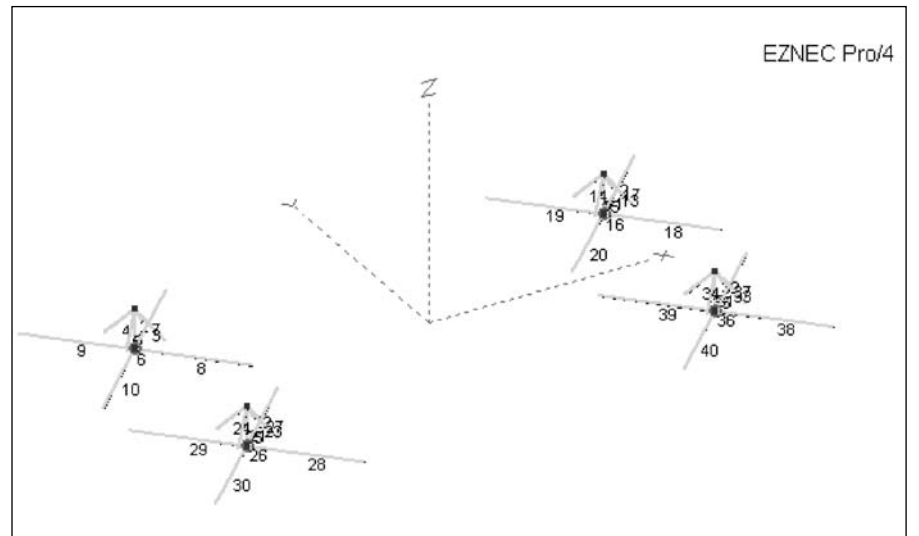


Figure 7 — The EZNEC/4 Pro model of an array of one 4-cell.

equal length 75 Ω coax are feeding the front two elements, which form a combined impedance of 37.5 Ω. The back two elements are the same and again form a combined impedance of 37.5 Ω, but with a phasing line (180° minus the desired phase angle) consisting of 75 Ω coax. The back two elements are then fed through an inverter, which allows us to feed them not with our phase angle, but with 180° minus the phase angle, which, among other things, allows for a shorter length of phasing line coax.

This phasing line consists of two equal length pieces of 75 Ω coax connected in parallel to produce a 37.5 Ω impedance to match the element feed line impedance (two 75 Ω feed lines in parallel to the back two elements), which should be 180° – 125°, or 55° in length. If you assume a 0.66 λ velocity factor, this would be a length of 54.2 ft (16.5 meters) for the 160 meter band and 28 ft (8.5 meters) for 80 meters. But remember, always measure your velocity factor or the delay, *do not assume!*

A simple collection of nine DPDT relays or four 4PDT relays with one DPDT can switch the array in eight directions. One of the nine, or the lone DPDT in the second example, does nothing but swap which side, front or back, sees the 180° minus phasing line coax.

1.5 Modeling the Complete Array Design

With the design assumptions now completed and understood, let us look at the results as an array. Figure 7 shows the *EZNEC/4 Professional* antenna model of a four cell broadside/end-fire array. Figures 8, 9 and 10 display the azimuth, elevation and 3D pattern for the 160 meter array and Figures 11, 12 and 13 show the azimuth, elevation and 3D pattern for the 80 meter array. The calculated RDF for the 160 meter array is at least 13 dB, as shown in the modeling figures that follow. Although the main sidelobe is >15 dB down from the highest gain point, RDF is about total contribution of power from behind the main lobe. The 80 meter model patterns show similar results.

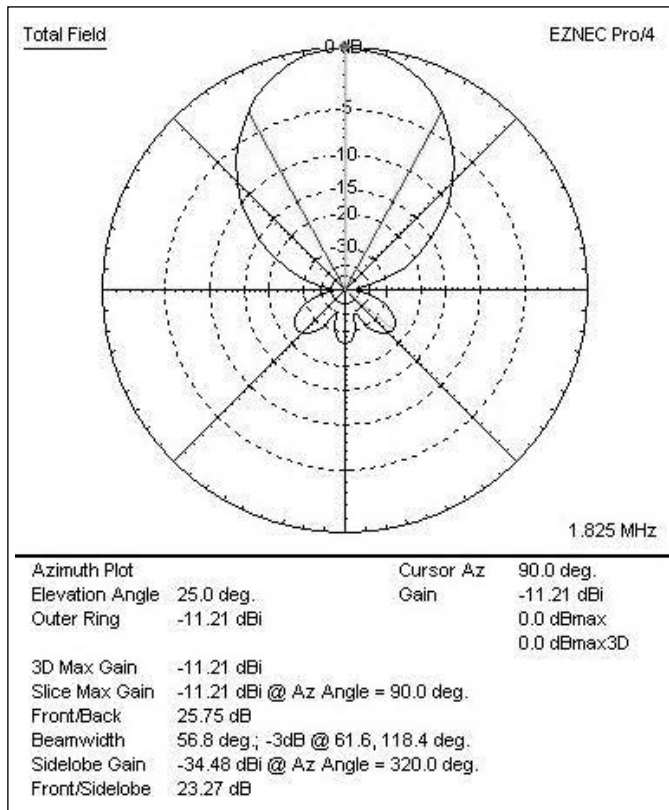


Figure 8 — The azimuth pattern for the 160 meter array.

2.0 Construction of the Eight Circle Vertical Array

Once the decision was made to erect a 160 meter Eight Circle Vertical Array at W5ZN, the construction phase began and involved numerous steps to ensure the design parameters were met.

2.1 Location and Physical Layout of the Array

The first step was to select an appropriate location and lay out the circle. Fortunately W5ZN has an area that seemed ideal for the array out in a field approximately 700 ft from the shack to the proposed center of the array. See Figure 14.

The location of the 160 meter transmit antenna, a shunt fed tower with HF Yagis seen in Figure 15, had to be taken into consideration. An existing barbed wire fence to the south of the proposed location

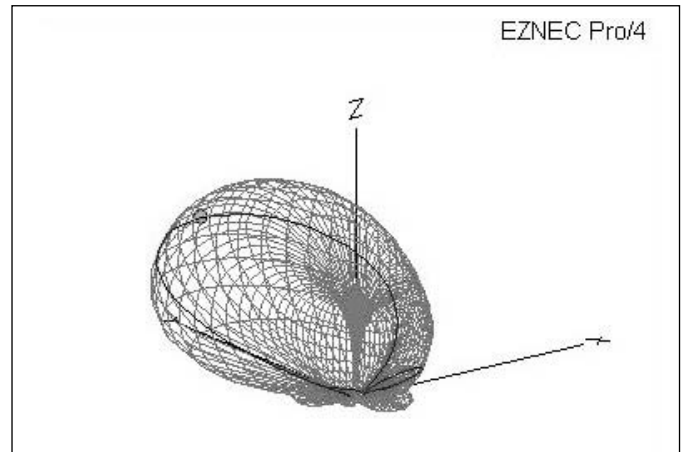


Figure 10 — This 3D plot shows the 160 meter radiation pattern.

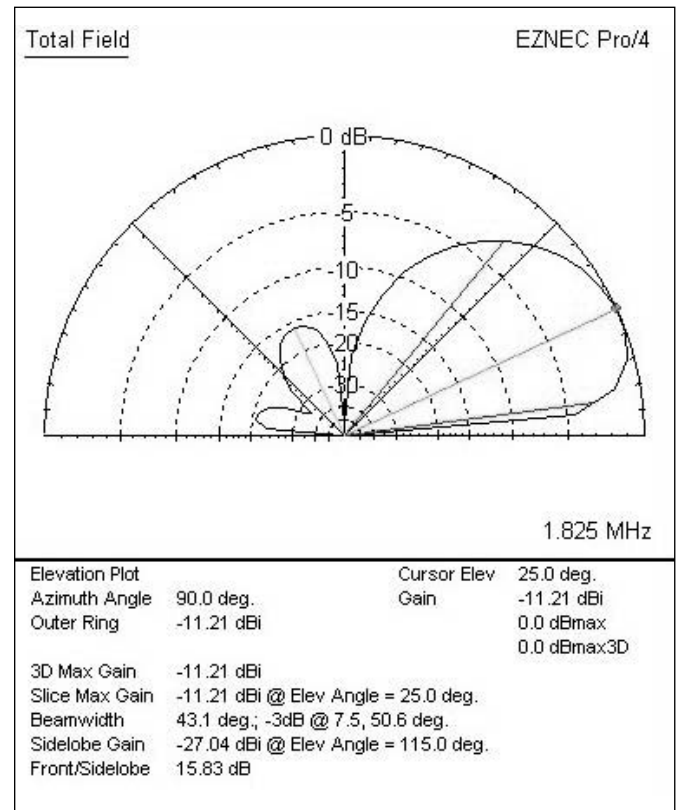


Figure 9 — Here is the elevation pattern for the 160 meter array.

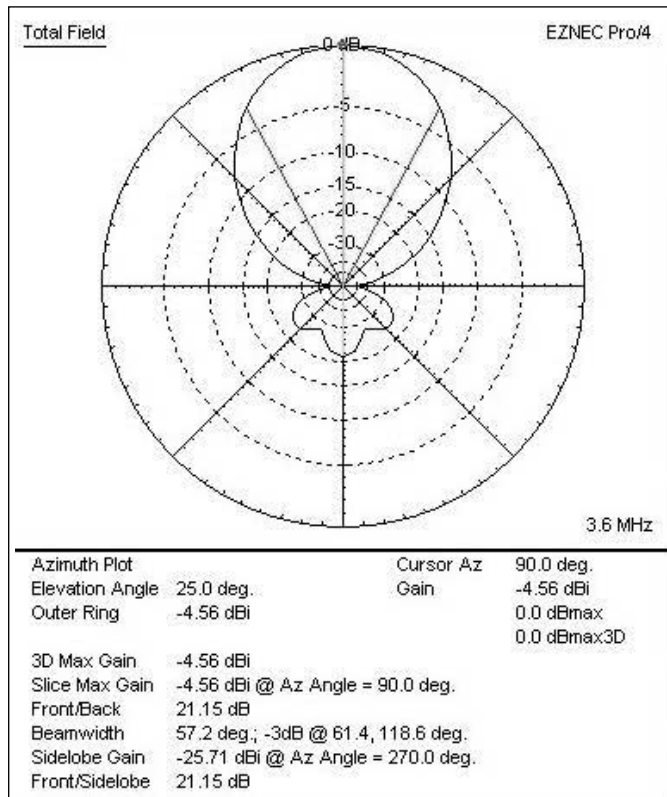


Figure 11 — Here is the azimuth pattern for the 80 meter antenna.

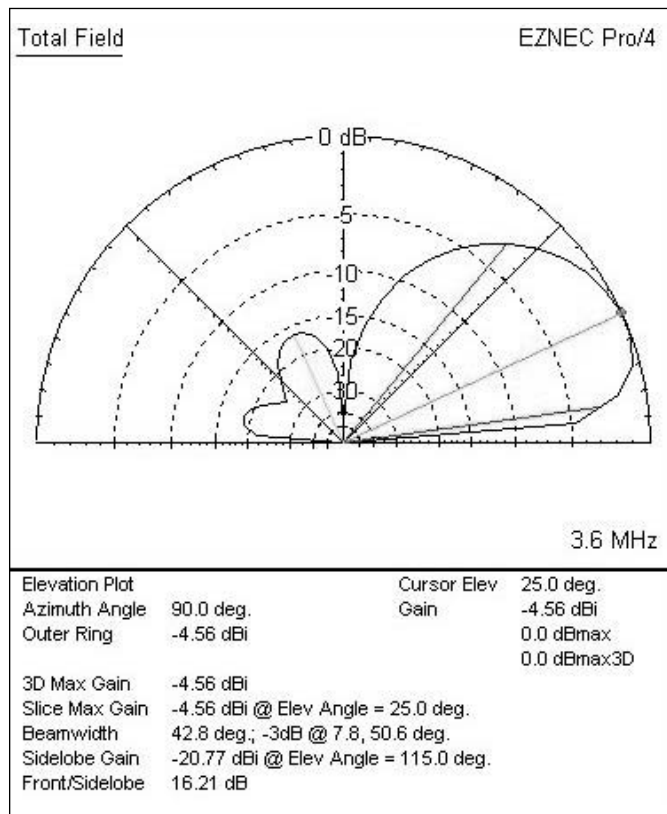


Figure 12 — This elevation pattern is for the 80 meter antenna.

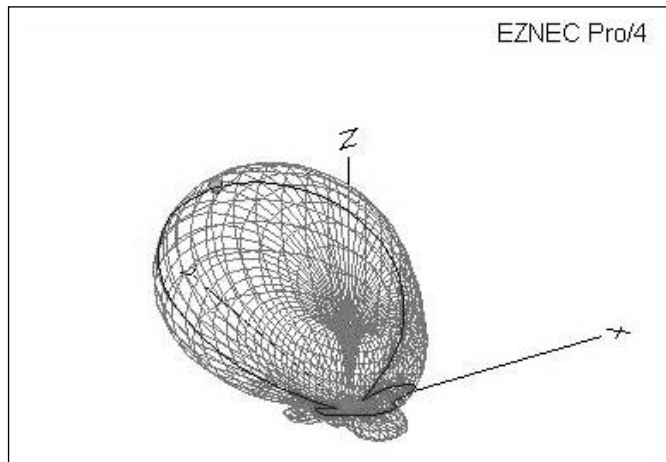


Figure 13 — Here is a 3D plot of the 80 meter radiation pattern.



Figure 14 — This photo shows the area selected for the Eight Circle Vertical Array.



Figure 15 — You can see the 160 meter transmit antenna (left tower) in this photo.



Figure 16 — Each vertical element is installed on 2x4 base.

also had to be evaluated. The western edge of the circle was measured to be 280 ft from the shunt fed transmitting tower, greater than $\frac{1}{2} \lambda$, and the southern edge was 75 feet from the barbed wire fence running east-west.

After consultation we concluded these distances should be adequate to prevent interaction with the array. Another concern we had was sloping ground, as can be seen in Figure 14. We concluded that, if the slope was less than approximately 10° , there should be no major deviation from the model. Prior to laying out the circle we needed to verify the slope angle of the ground. The most accurate way to accomplish this would be to use a transit, however a less expensive method that is somewhat less accurate but well within acceptable tolerances may be employed. A 4 ft level was placed on the ground at the western edge of the proposed circle pointing in the direction of the slope, assuring it was “level”. At the far eastern end of the proposed circle at the maximum point of the slope we vertically supported a 10 ft piece of white PVC pipe. While staring down the level to project a “level” straight line to the PVC pipe we marked this point on the pipe. We could then measure this distance down to the ground and use simple trigonometry to calculate the slope angle. We calculated that the sloping ground was no more than 2° , which is very acceptable.

Now that we verified that we had an acceptable location for the array, it was time to lay out the circle. Having identified the western edge of the circle by measuring its distance from the transmitting antenna, as

well as the southern edge of the circle by measuring its distance from the barbed wire fence, we began the layout. We had previously concluded we would use a broadside spacing of 0.55λ (296 ft), which results in a 320 ft diameter circle. We simply measured 160 ft (the radius of a 320 ft diameter circle) from each of the two previously identified edge points to a center point. From this now-identified center point we began measuring out 160 ft in 20 ft spacing segments, marking each edge point with an orange survey flag. In just a short time there was a 320 ft diameter orange flag circle in the field.

From this “circle” we could lay out the location of each vertical with a broadside spacing of 296 feet, physically spacing them equally around the circle so that a broadside array would project a main lobe in each of the eight directions of interest. The result is an end-fire spacing of 123 ft. Remember, the broadside spacing is the only degree of adjustment you have and the end-fire spacing is simply the result of the selection of the broadside spacing.

2.2 Element Supports

As noted earlier in the section on modeling, the material and method for supporting and insulating the vertical elements from the ground is insignificant. We used four 12 ft treated 2x4s and sawed them in half to produce eight 6 ft posts. Following this we dug a post hole about 18 inches deep, inserted the 2x4 and packed it in with Quikcrete to form a solid base. There’s no need to mix the Quikcrete with water, just use it as a fill-



Figure 17 — A close-up view of a vertical element sitting inside bottom support enclosure.

ing and packing material in the hole. It will absorb the moisture in the ground or during the next rainfall and the moisture will solidify the mix.

2.3 Element Material and Construction

The material used for the vertical elements and the construction technique is not critical as long as you stay within the dimensions of the model in order to replicate it. A variety of acceptable possibilities exist. In this section we will describe the procedure we followed. W8JI has very successfully used other materials (steel conduit and chain link fence top rails) and techniques that provide very strong elements mechanically, and excellent results as detailed on his Web site. (See Note 7.)

We chose to use aluminum tubing for the elements. There was no particular reason for this other than personal preference. We used 12 ft lengths of $\frac{1}{4}$ inch diameter aluminum tubing and a supply of $\frac{1}{8}$ inch diameter tubing that has a 0.058 inch wall thickness. As such, the $\frac{1}{8}$ inch diameter tubing fits right inside the $\frac{1}{4}$ inch tubing. Then the smaller diameter tubing was cut into 2 ft lengths and inserted 1 ft into one end of eight of the 12 ft lengths of the $\frac{1}{4}$ inch tubing. We secured the joint with no. 10 stainless steel screws and nuts. This provides 24 ft long elements. Next, we cut 18 inch lengths of $\frac{1}{8}$ inch diameter tubing, inserting it 6 inches into what would be the top end of each 24 ft long element and secured it with stainless steel screws and nuts. We now had very nice 25 ft elements. Four holes are drilled at the top, 90° apart in order to attach the top hat wires.

For top hat wires we used some AWG no. 16 speaker wire (16-2 stranded). Separating the two wires is very easy and this wire worked great. Again, there is flexibility with the material but stay with no. 16 gauge in



Figure 18 — One completed vertical.



Figure 19 — You can see the ground rod and radial attachment for a vertical in this photo.

Table 2
Vertical Element Self Resonance Measurement Results

Vertical	Self Resonance	Feed Point Impedance	160 Meter Feed Point Resistance (no matching)
1	3.90 MHz	20 j0 Ω	18 j321 Ω
2	3.85 MHz	19 j0 Ω	16 j321 Ω
3	3.90 MHz	22 j0 Ω	16 j321 Ω
4	3.92 MHz	21 j0 Ω	18 j328 Ω
5	3.92 MHz	18 j0 Ω	18 j328 Ω
6	3.90 MHz	18 j0 Ω	18 j328 Ω
7	3.90 MHz	18 j0 Ω	18 j321 Ω
8	3.90 MHz	22 j0 Ω	16 j315 Ω



Figure 20 — W5ZN measuring the self-resonance of the vertical elements.

order to replicate the design model. For guy lines we first used 50 pound fishing line. This worked well for a short period, however the lines began to break (they weren't stretched *that* tight), possibly from deer or other wild animals hitting them, so the fishing line was replaced with 1/8 inch Kevlar® rope. It does not stretch, it is perfect for guying vertical antennas and the Kevlar® rope has held nicely for several months now. We used tent stakes for the guy anchors.

After assembling the elements and top hat wires it was now time to mount the vertical elements to the 2x4 base supports. This can be accomplished in a variety of ways. At a local hardware store we located some plastic conduit clamps and some plastic housings

with an opening at the top, ideal for mounting the elements and also a means to weatherproof the feed line connections.

Figures 16, 17 and 18 show a 2x4 support, element attachment and completed element.

2.4 Ground Radial System

As described in the modeling section, some ground radials are required to stabilize the feed point impedance over changing ground conditions throughout the year.

At first we chose to bury four radial wires that were 65 ft long (1/8 λ on 160 meters) a few inches in the ground. These were laid out with one under each of the top hat wires. These wires aren't critical and they

don't necessarily have to be buried, but they do need to be lying on the ground as a minimum. A large supply of 16 gauge wire was acquired and used for radial wire.

For ground rods, all antenna and shack grounds are using 3/4 inch copper pipes. We purchased 10 ft lengths and then cut them in half. We placed an end cap over one end and then drove it into the ground. That is relatively easy to do in Arkansas, especially during the wet winter and spring months. Your specific area may prove difficult or prevent using this method entirely, and that is understood. Just get a good ground rod in the ground. The ground radials and outer shield of the coax connector are all connected to the ground rod. A solder connection is made to the copper pipe ground rod. Figure 19 shows the W5ZN ground radial system installation. It is important to note that the ground rod does nothing to improve the pattern or efficiency of the antenna. It is simply to provide a good dc ground.

2.5 Tuning the Individual Elements

Now that each vertical element was erected and the ground radial system installed, it was time to test and tune each element. Bob and Al Ward, W5LUA, traveled to Arkansas to assist with this process, and evaluate actual results with the designed/modeled results. Our first step was to check the self-resonance of each vertical. This is a simple process if you have an antenna analyzer similar to the MFJ-259B. Simply connect the analyzer directly to the vertical element and record the readings. Table 2 shows the results from each element while Figure 20 shows the measurements being taken. Needless to say, we were

all quite happy with the results, which clearly prove the design dimensions!

Now it was time to tune each element. The design indicated an inductor of 30 μH would be required to tune the element down to 160 meters and our resistor should be somewhere around 70 Ω . Our target was to center the zero reactance component between 1.8 and 1.9 MHz.

We had some small molded 27 μH and 31 μH inductors on hand, and some 75 Ω non-inductive resistors, so the first attempt was to try a 27 μH / 75 Ω combination. This produced a 160 meter feed point resistance of 100 $j0 \Omega$, clearly a sufficient amount of inductance but way too much resistance since 75 Ω was our target.

We then went to the resistor box and pulled out some 47 Ω resistors to try. These were not "non-inductive" but only measured about 1 μH , so we decided to give them a try. This combination worked pretty well. The feed point resistance came down to about 68 Ω but the zero reactance point didn't really move as we had expected, since we were using an "inductive" resistor. After scratching our heads for a bit we decided to check our "non-inductive" resistors and discovered they were anything but "non-inductive"! A case in point here: we did a search on the internet for "non-inductive" resistors and found just about all of our hits for "non-inductive" resistors came back to numerous ads that stated "non-inductive wire wound resistors." Huh? Obviously a wire wound resistor will not be "non-inductive" so beware! The resistors W5ZN had on hand, which were purchased from a popular surplus dealer, were very clearly marked and

identified as "non-inductive resistor," but they weren't. The good news is this is not really necessary for this application as long as you take the inductance of the resistor into account for the overall inductance/resistance combination. You should also be aware that the inductor will have some small amount of resistance as well but again just make sure you account for all of this in your inductor/resistor network. This is easily done when we calculate the overall reactance and SWR at the desired frequency.

Before you begin the tuning process it is a good idea to have a supply of 0.5 and 1.0 μH small molded inductors as well as some 1 to 3 Ω resistors on hand for fine tuning, especially if you're a perfectionist!

Once you have the element tuned to a reasonable point, it is now time to check the effectiveness of the ground radial system. This is easily done with an antenna analyzer similar to the MFJ unit. When the shell of the coax connector from the analyzer is attached to the radial system then the analyzer believes this is a perfect ground since there is zero ohms resistance (close enough). If, during the following test the value of the feed point impedance changes by more than 5%, the ground radial system is insufficient.

First, disconnect all of the ground radials, leaving only the ground rod connected to the cable shield and record the feed point impedance. Next, connect one ground radial and then the remaining three, recording the feed point resistance change at each step. If the change is less than 5%, then you have a very good ground radial system that should be stable under changing conditions throughout the year.

Table 3
Feed Point Resistance Change with Added Ground Radials. Readings Taken in October with Dry Ground.

Frequency	Ground Rod Only	1 Radial	2 Radials	4 radials	8 Radials
Self Resonance No RL Matching 80 Meters	38 $j30 \Omega$	32 $j0 \Omega$	30 $j0 \Omega$	30 $j0 \Omega$	20 $j0 \Omega$
No RL Matching 160 Meters	42 $j360 \Omega$	6 $j300 \Omega$	7 $j300 \Omega$	8 $j300 \Omega$	0 $j310 \Omega$
RL Matching For 160 Meter Resonance	110 $j0 \Omega$	80 $j15 \Omega$	81 $j12 \Omega$	80 $j10 \Omega$	78 $j0 \Omega$

Table 4
Feed Point Resistance Change with Added Ground Radials. Readings Taken in January with wet ground.

Frequency	Ground Rod Only	1 Radial	2 Radials	4 radials	8 Radials
Self Resonance No RL Matching 80 Meters	42 $j30 \Omega$	31 $j10 \Omega$	30 $j0 \Omega$	28 $j0 \Omega$	18 $j0 \Omega$
No RL Matching 160 Meters	40 $j363 \Omega$	5 $j306 \Omega$	5 $j306 \Omega$	5 $j307 \Omega$	0 $j323 \Omega$
RL Matching For 160 Meter Resonance	120 $j0 \Omega$	80 $j20 \Omega$	80 $j20 \Omega$	78 $j20 \Omega$	75 $j0 \Omega$

We did not. The change we experienced was greater, so we chose to add four more radials, bringing our total to 8 for each element. We continued the test by adding two, then the additional two and the change was now within 5% so we were satisfied we had a stable ground radial system. Table 3 shows the typical change in feed point resistance recorded for each of the verticals when adding radials in October with dry ground and Table 4 shows the typical change from readings taking in January with wet ground.

After completing the ground radial test we then performed some fine tuning and tweaking of the inductor/resistor values to bring the feed point resistance into our design range. Table 5 shows the final results along with the required individual inductance and resistance used as well as the total inductance and resistance of the network.

2.6 Feed lines and Phasing Lines

We are using 75 Ω coaxial cable feed line in this array. We chose to acquire “flooded” cable so it could be buried without the worry of moisture influx and deterioration. Good quality RG-6 flooded coax, along with very good F-connectors that work great in low band receiving applications are available from a few select Amateur Radio dealers. We recommend you bury the feed lines. If you choose not to, however, we recommend you use the flooded cable anyway just in case a wild animal wants to chomp on the coax. They most definitely will not enjoy the taste of the flooding compound and will look for another treat!

In order to accurately prepare our phasing lines we decided to measure the velocity factor of our RG-6 cable. Our test setup included an MFJ-259 Antenna Analyzer used as our signal generator and a dual trace oscilloscope to measure the signal time delay in a length of cable. We concluded the velocity factor of our cable to be about 80%. From this, we determined our 55° phasing lines should be 66 ft in length. Two of these were prepared, per the design.

We then prepared nine 75 Ω RG-6 coaxial lines of equal length (one each to feed each of the eight verticals and one spare), sufficient to run from the center point to each vertical element with about 5% extra to have some spare.

2.7 Switching Unit

The switching unit schematic is shown in Figure 22.

Rather than go through the time and expense of designing and manufacturing a circuit board, we chose to assemble a switching unit using point to point wiring. Figures 23 and 24 show the W5ZN unit.

The components for the switching unit aren't critical. Some chassis mount F connec-



Figure 21 — N4HY is very pleased with the design as compared to the actual results!

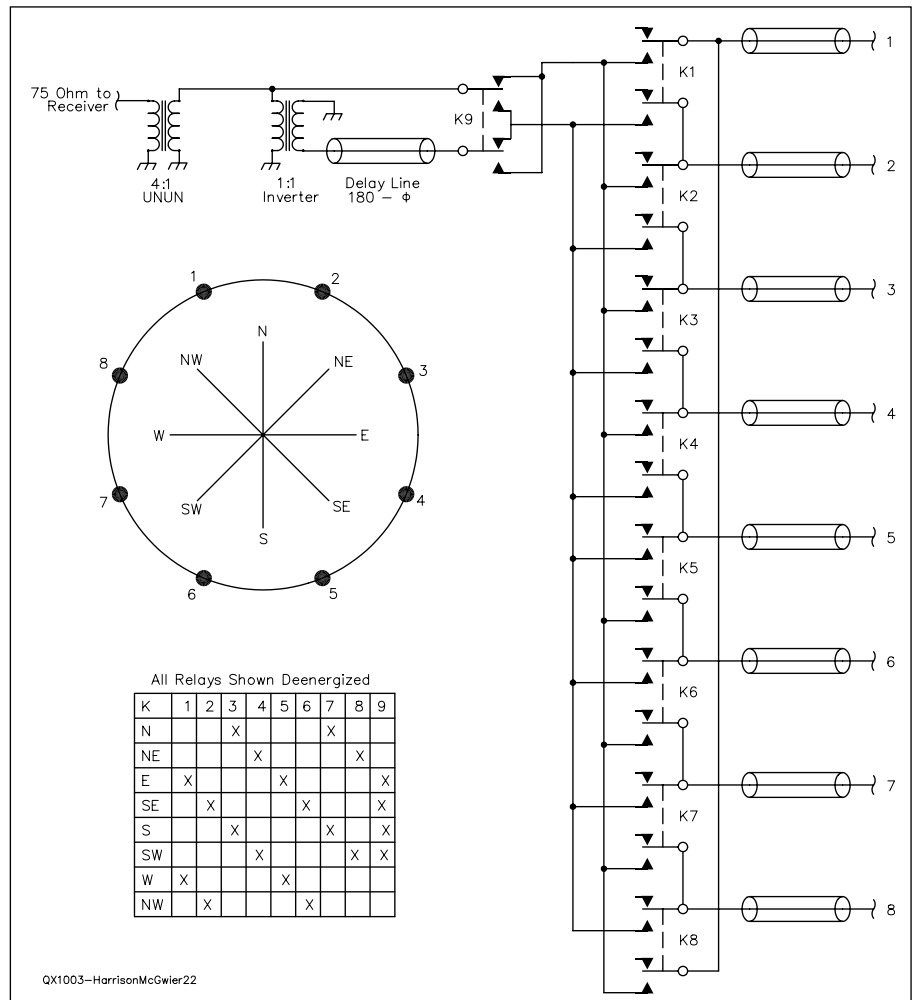


Figure 22 — This is a schematic drawing of the switching unit.

tors and simple (but good) enclosed 12 V dc relays will work just fine, and we used some small gauge enameled wire to connect everything. Don't use wire that is too small, which can become brittle and break, but don't use wire so large that it is too rigid and does not provide some flexibility. If you use point to point wiring, just remember the small pins on the relays are strong, but they won't stand up to a lot of stress. Even though is it not what we used, we recommend the use of small gauge stranded wire.

The relay unit was laid out on a piece of paper, and then a sheet of aluminum was used to mount the relays. We drilled the holes to mount the connectors. Epoxy glue was used to mount the relays upside down on the aluminum sheet, and some small, flexible enameled wire was used to connect everything.

After you have the switching unit assembled you can perform some simple tests to ensure everything is working fine. First, make sure all of the relays are working individually and then as a group in the proper sequence by using a simple continuity test with an ohm meter. Now you can inject a signal into the unit using an antenna analyzer or other weak signal source to verify that all of the other components are working. Figures 25, 26 and 27 show some of our test results.

The switching unit is really simple and straightforward, however there are a couple of points that need to be highlighted. First, make sure you note the wiring sequence "swap" when you go from relay 4 to relay 5. Again, this is a simple process, just make sure you are aware of it and wire it correctly, otherwise the unit will not switch the elements properly.

The second point is the 1:1 inverter and the 4:1 UNUN, which are very simple to construct. Binocular cores seem particularly useful for low band receive antenna applications. The Fair-Rite 2873000202 core that W8JI has popularized is easy to locate and purchase, easy to wind and works great. We used small gauge enameled wire, but this is not necessary and any small gauge wire

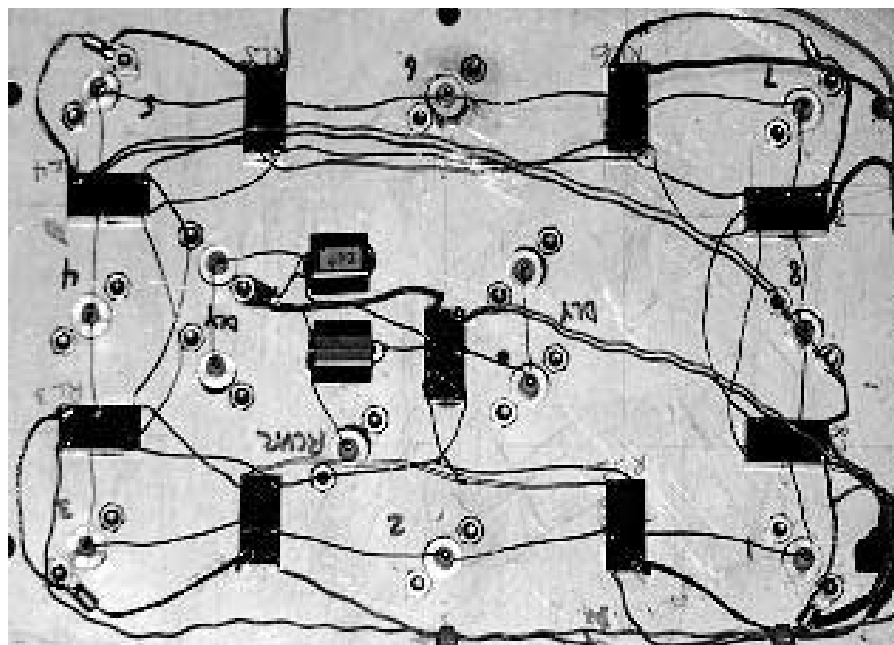


Figure 23 — This is a view of the component side of the switching unit.

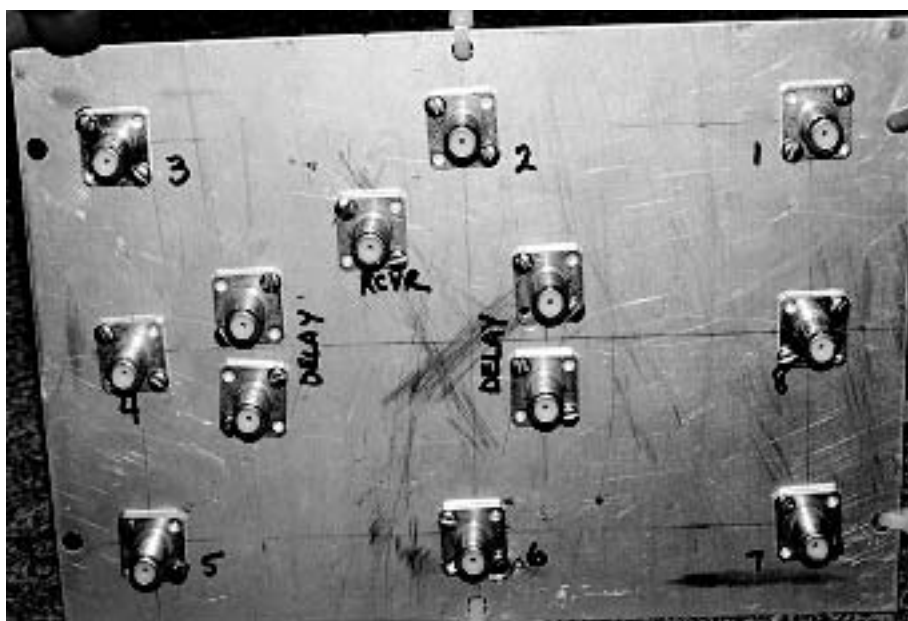


Figure 24 — This view shows the connector side of the switching unit.

Table 5
160 Meter Results After Tuning

Vert	1.800	1.830	1.860	1.890	j0 Bandwidth	Ind	Res	Total Ind and Res	
1	74 j13 Ω	75 j0 Ω	75 j0 Ω	76 j16 Ω	1.815 - 1.862	28 μH	56 Ω	28.4 μH	56.5 Ω
2	75 j10 Ω	75 j0 Ω	76 j0 Ω	77 j19 Ω	1.815 - 1.860	27.5 μH	55 Ω	28.6 μH	54 Ω
3	76 j15 Ω	76 j0 Ω	76 j0 Ω	76 j9 Ω	1.817 - 1.868	28 μH	54 Ω	28.6 μH	54.5 Ω
4	76 j15 Ω	75 j0 Ω	75 j0 Ω	76 j15 Ω	1.820 - 1.874	28 μH	53 Ω	28.3 μH	54 Ω
5	76 j17 Ω	75 j0 Ω	75 j0 Ω	76 j12 Ω	1.824 - 1.878	27.5 μH	53 Ω	28.0 μH	54 Ω
6	74 j11 Ω	74 j0 Ω	75 j0 Ω	76 j20 Ω	1.814 - 1.863	28 μH	55 Ω	28.5 μH	56 Ω
7	75 j15 Ω	74 j0 Ω	75 j0 Ω	75 j17 Ω	1.818 - 1.868	28 μH	53 Ω	28.5 μH	54 Ω
8	73 j16 Ω	73 j0 Ω	74 j0 Ω	74 j16 Ω	1.815 - 1.862	27.2 μH	56 Ω	27.7 μH	56.5 Ω

will work as long as it is insulated. For the 1:1 inverter just twist two wires together and make three passes through each hole in the core, to produce a 3 turn winding. Connect it as shown in Figure 22, making sure the ends of the two windings are reverse connected. For the 4:1 UNUN, just use four turns on the primary and two turns on the secondary. That is four passes through each hole for the primary winding and two passes through each hole for the secondary winding. This will give you a 2:1 voltage ratio, which equates to a 4:1 impedance ratio, and you're in business! You can check it on an oscilloscope and it will show a perfect 2:1 voltage ratio (the

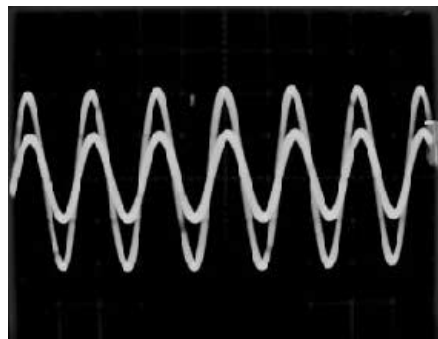


Figure 25 — This oscilloscope plot shows a 1.83 MHz signal through the 4:1 UNUN, showing a 2:1 voltage ratio (4:1 impedance ratio).

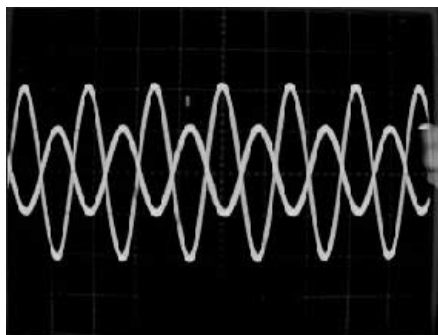


Figure 26 — Here is an oscilloscope plot of a 1.83 MHz signal through the 4:1 UNUN and 1:1 inverter (180°).

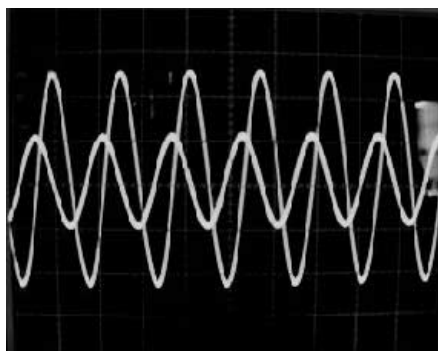


Figure 27 — The oscilloscope plot of a 1.83 MHz signal through 4:1 UNUN, 1:1 inverter and phase lines.

equivalent of a 4:1 impedance ratio).

Once the switching unit was installed, a ground rod is installed and connected to the aluminum sheet. Figure 28 shows the finished installation. A rubber trash can be used for weather proofing to protect the switching unit from the elements.

2.8 Switching Control

The control for the switching unit can be built in a number of different ways. Figure 29 shows the W5ZN method. Joel uses a diode matrix with an eight position pushbutton antenna relay control box. He prefers the pushbutton variety rather than rotary switches to eliminate a lot of “cranking” and switching through unwanted directions to prevent unnecessary relay activation. For control cable, we used 5 conductors of a CAT5 cable. Any 5 conductor cable will work fine to provide the proper dc relay voltage to the external unit. Joel’s run is approximately 600 ft from the shack.

3.0 Evaluation of the Eight Circle Vertical Array

Evaluation of any antenna system requires that you have a realistic understanding of what to expect! In the case of low band receiving antennas, some radio amateurs have erroneously assumed that after installing a Beverage or similar receiving antenna you will automatically begin to miraculously hear stations that never existed at your location before. The most important factor in being able to hear stations on the low bands is propagation characteristics. Joel listened for two 160 meter seasons as east coast stations boasted about how strong VQ9LA was without a peep of a signal into Arkansas. No receive antenna would have changed this. Finally one night the propagation came to W5 land and thanks to low noise receiving antennas VQ9LA is in the log at W5ZN. So don’t expect to begin to magically hear

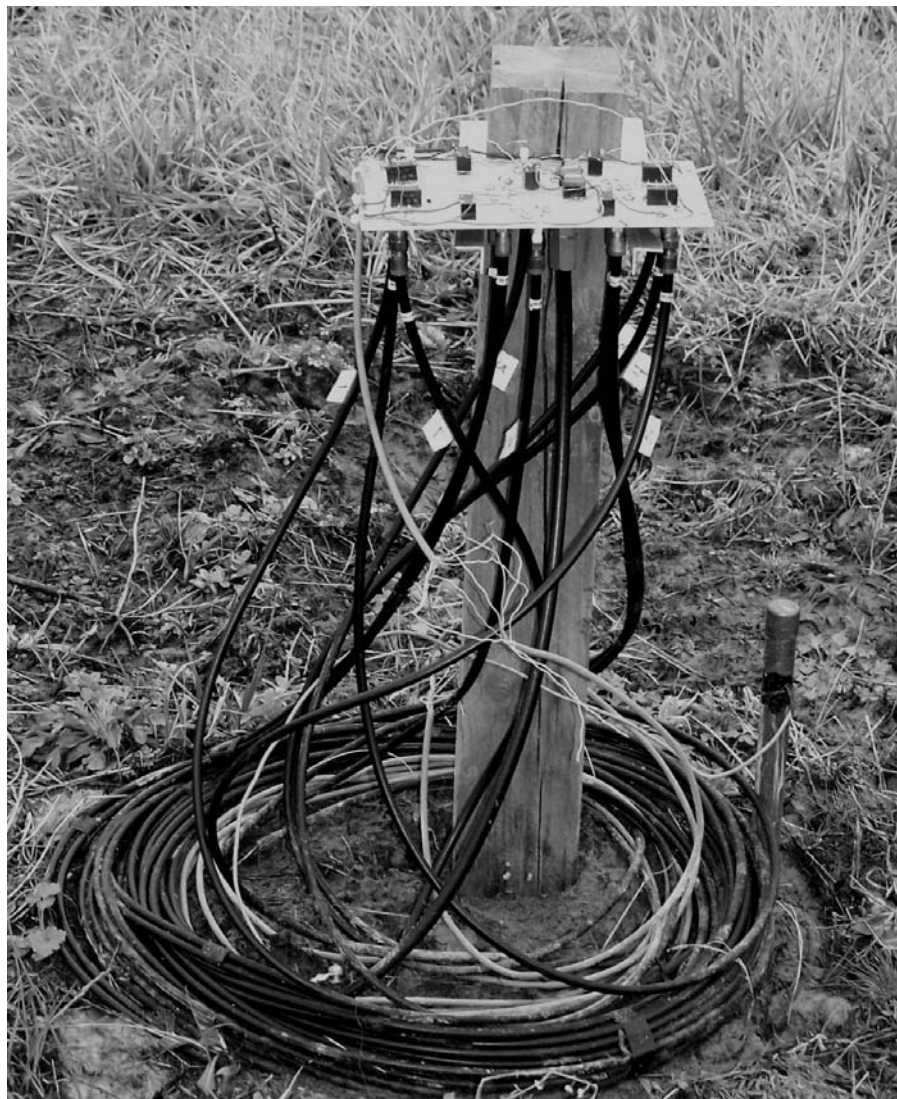


Figure 28 — This photo shows the switching unit installed at the center of the array.

stations that just never existed before. What should immediately become apparent is that your noise floor will decrease. Since DX signals on the low bands are weak signals, this component alone should allow you to hear stations that previously were buried in the noise.

Remember, your goal is to improve your DMF or RDF which will in turn reduce the amount of noise (both man-made and natural) and QRM collected by the receive antenna system in a particular direction and allow you to hear weak stations when propagation permits.

3.1 Noise Evaluation

Joel's first step in the evaluation was to record noise floor levels on the various 160 meter antennas installed at W5ZN. He has some significant noise sources in two directions, so a combination of low noise receiving antennas benefits him greatly. Table 6 shows a comparison of the noise floor for the W5ZN 160 meter antennas.

3.2 Signal Comparison, F/B Ratios, F/S Ratios

A comparison of on-the-air F/B and F/S measurements from various stations was per-

formed over several months and the results indicate the array is comparable to the modeling parameters produced.

The charts of Figures 30, 31, 32 and 33 depict signal comparisons between the Eight Circle Vertical Array and Joel's 880 ft Beverage antennas taken at different times of the day to different parts of the world. Obviously, the signal arrival angle will play an important part in signal strength and readability. The charts are typical for each DX station, however, and represent the ability to hear a station earlier than with the Beverages

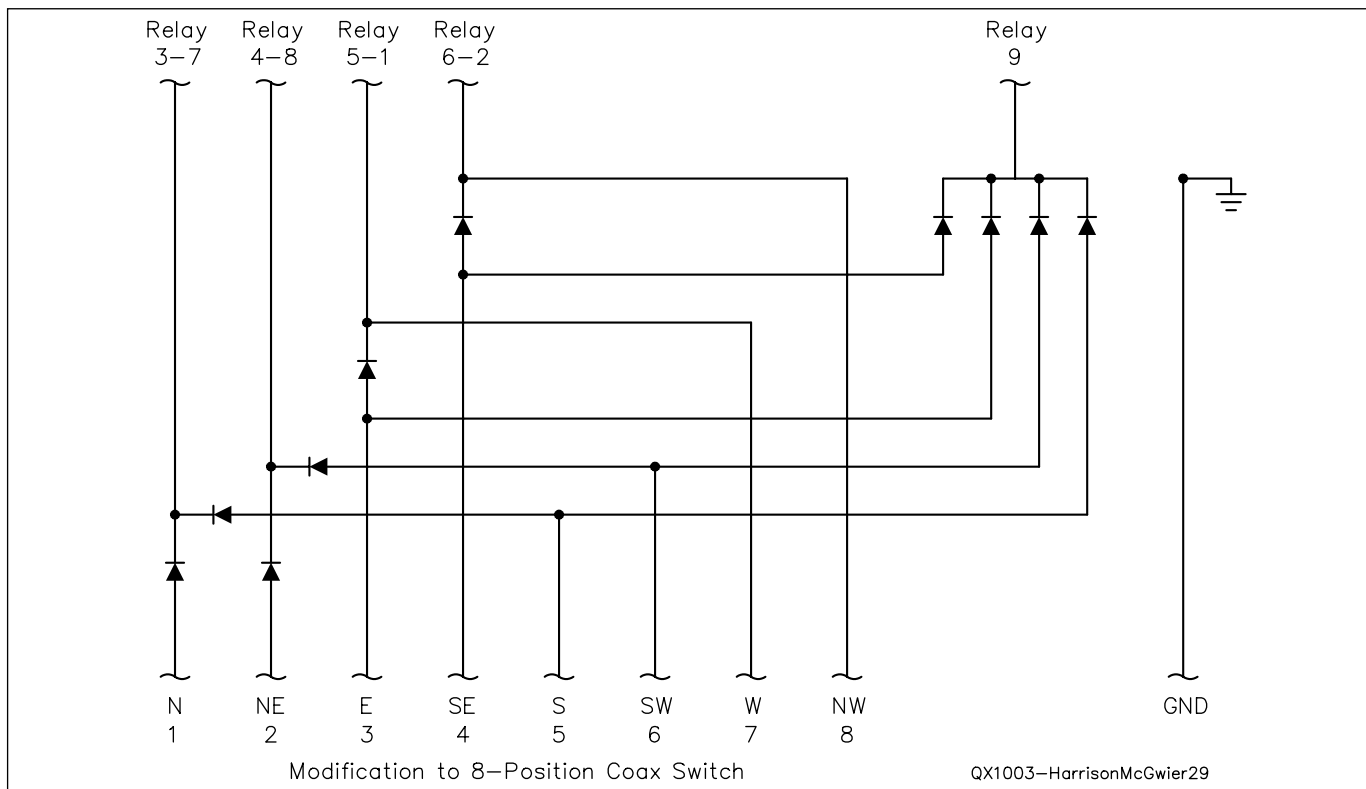


Figure 29 — Here is a switching control unit modification. Diodes are standard silicon diodes, 1N4004 or equivalent.

Table 6
Noise Floor Measurement Comparisons

Direction	Eight Circle Vertical Array	Beverage	K9AY Loop ¹	Shunt Fed 135 ft HF Tower	1/2 λ Inverted Vee ²
	Noise Floor	Noise Floor		160 Meter Xmit ²	
N	-129 dBm	-125 dBm	N/A	-100 dBm	-105 dBm
NE	-125 dBm	-120 dBm	-132 dBm	-100 dBm	-105 dBm
E	-125 dBm	-124 dBm	N/A	-100 dBm	-105 dBm
SE	-126 dBm	-123 dBm	-130 dBm	-100 dBm	-105 dBm
S	-126 dBm	-120 dBm	N/A	-100 dBm	-105 dBm
SW	-125 dBm	-120 dBm	-132 dBm	-100 dBm	-105 dBm
W	-126 dBm	-125 dBm	N/A	-100 dBm	-105 dBm
NW	-130 dBm	-128 dBm	-132 dBm	-100 dBm	-105 dBm

Noise Floor Measurements Comparing the Eight Circle Vertical Array, Beverages, Loop, Shunt-fed Tower and Inverted Vee at W5ZN. Measurements were taken with a 250 Hz bandwidth at a Sampling Rate of 48 kHz.

¹Loop has considerably less gain than the Beverage or Vertical Array which equates to not only a lower noise floor but much lower signal levels as well and traditionally requires a preamp.

²Omnidirectional.

and to also hear the station for a period of time after they can no longer be copied on the Beverages. At the peak propagation period, however, there is no noticeable or recordable differences between the two receive antenna systems.

4.0 Summary

The Eight Circle Vertical Array is a significant addition to the low band receive antennas at W5ZN. It is now the primary system used for receiving on 160 meters. It will not replace the other receive antennas because as unpredictable as 160 meters is, you never know when a propagation anomaly may occur that will present itself better to one of the other antennas, however that situation has not yet been seen.

An 80 meter version has now been constructed at W5ZN and is being evaluated during the Winter 2009/2010 low band season.

The amount of time and effort invested in this project was considerable. That was because only a very small amount of general information was available on this antenna array. Our hope is that this article will provide encouragement for others to try such an array, and that the time required to build one will be reduced significantly. For 160 meters, this array takes up a circle diameter of less than 350 ft, with an additional 65 feet for radials. That is less than a 1λ Beverage on 160 meters, and eight directions can be obtained. So, if you're space limited for a Beverage array but can afford the real estate for an Eight Circle Vertical Array, give it a try. You will *not* be disappointed!

Notes

¹ARRL DX Challenge Award: www.arrl.org/news/stories/2001/05/08/3/.

²John Devoldere, ON4UN, "ON4UN's Low Band DXing," Fourth Edition, ARRL — The National Association for Amateur Radio™, 2005. ARRL publications are available from your local ARRL dealer, or from the ARRL Bookstore. Telephone toll free in the US 888-277-5289 or call 860-594-0355, fax 860-594-0303; www.arrl.org/shop; pubsales@arrl.org.

³Joel Harrison, W5ZN, "Horns for the Holidays," *Proceedings of Microwave Update '97*, ARRL, 1997, pp 147-149.

⁴Joel Harrison, W5ZN, "W5ZN Dual Band 10 GHz / 24 GHz Feedhorn," *Proceedings of Microwave Update '98*, ARRL, 1998, pp 189-190.

⁵Joel Harrison, W5ZN, "Further Evaluation of the W5LUA and W5ZN Dual Band Feeds," *Proceedings of Microwave Update '99*, ARRL, 1999, pp 66-84.

⁶Paul Wade, W1GHZ and Joel Harrison, W5ZN, "Multi-band Feeds for Parabolic Dish Antennas," *W1GHZ Microwave Antenna Book*, Chapter 6, W1GHZ, 2000, www.w1ghz.org/antbook/chap6_9p1.pdf.

⁷Tom Rauch, W8JI, www.w8ji.com, www.w8ji.com/small_vertical_arrays.htm, W8JI, 2008.

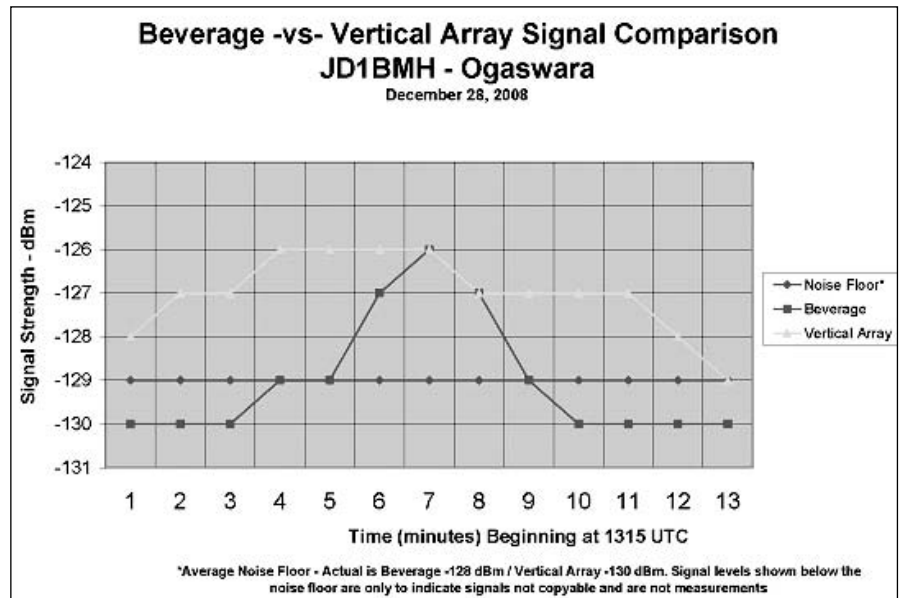


Figure 30 — This chart compares signal levels between the Eight Circle Vertical Array and a Beverage antenna for signals from JD1BMH, Ogaswara.

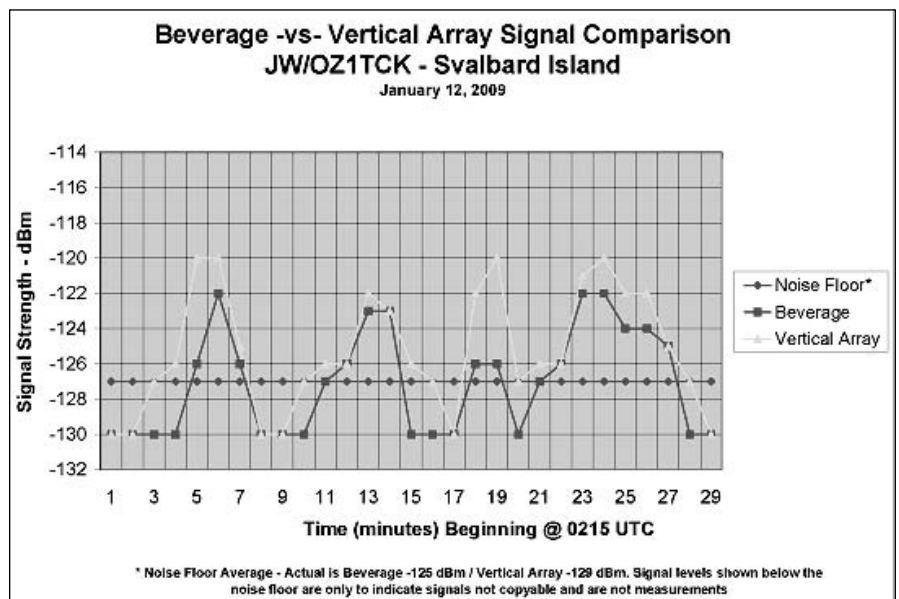


Figure 31 — This chart compares signal levels between the Eight Circle Vertical Array and a Beverage antenna for signals from JW/OZ1TCK, Svalbard Island.

⁸John Devoldere, ON4UN, "ON4UN's Low Band DXing," Third Edition, ARRL — The National Association for Amateur Radio™, 1999, pp 11-68 to 11-71.

⁹The authors' EZNEX 4 model files are available for download from the ARRL QEX web site. Go to www.arrl.org/qexfiles and look for [3x10_Harrison_McGwier.zip](http://www.arrl.org/qexfiles).

Joel Harrison, W5ZN, was first licensed as WN5IGF in 1972. He went on to acquire his General, Advanced and Amateur Extra licenses as WB5IGF. He's had his current call sign since 1996.

Joel has many interests in Amateur Radio including VHF/UHF/Microwave weak signal communication, EME, low band DXing and contesting. His Amateur Radio operating awards include DXCC Honor Roll, DXCC Challenge, 9 Band DXCC, 11 Band VUCC (50 MHz through 24 GHz), 6 meter WAS and WAC, 2 meter WAS and WAC and Satellite WAS and WAC. He held the ARRL June VHF Contest Single Operator World Record from 1996 to 2006 and held the 80 meter record for the W5 call area in the ARRL International DX Contest, CW, from 2006-2009. In 2001, the Central States VHF Society awarded him the

Mel S. Wilson Award for continuous service and dedication toward promoting VHF and UHF activity, in 2008 La Federacion Mexicana de Radioexperimentadores awarded him the prestigious Azteca Diploma for 25 years of service to Amateur Radio and in 2010 the ARRL Board of Directors awarded him the ARRL Outstanding Service Award for over 25 years of volunteer service to ARRL, including two terms as ARRL President. He is a member of the Collierville Millimeter Wave Society, a life member of the Central States VHF Society, a Life Member of ARRL and just retired as President of ARRL, The National Association for Amateur Radio™.

Joel began his formal education studying industrial electronics at Arkansas State University and then traveled overseas to further his education in Germany, Norway and Denmark, completing his curriculum at the Electric Power Research Institute. In 1983 he became the first person in the world to qualify an automated ultrasound imaging system for use in the nuclear power industry, and in 1995 received Special Recognition for Contributions from the American Society for Nondestructive Testing.

In 2008 he was appointed by Arkansas Governor Mike Beebe to serve on the Board of Directors of the Arkansas Science and Technology Authority. Joel is Manager, NDE Technology for URS (United Research Services) Corporation in Princeton, NJ, which serves the nuclear power, government, space and infrastructure markets. More information about Joel can be found at www.w5zn.org.

Dr. Robert McGwier, N4HY, has been licensed since the early 1960s when he was WN4HJN. He received N4HY in 1976 when he decided he did not want to be N4BM (with apologies to the current owner of that call).

Bob holds a BSEE and BS in Mathematics from Auburn and Ph.D. in Applied Mathematics from Brown University. He serves as Chairman of the ARRL Software Defined Radio Working Group. Bob is the immediate past Vice President of Engineering for AMSAT. Bob's early work included writing the Quiktrak satellite tracking software package for the Commodore, RadioShack, and then PC computers. He has worked on several satellite projects and was a co-designer of the Microsat satellites and on the early design teams for AO-40. With Tom Clark, K3IO, he started the AMSAT/TAPR digital signal processing project. Bob received the 1990 Dayton Hamvention® Award for Technical Achievement for his work with AMSAT, TAPR, and the ARRL. Recent DSP and software-defined radio activities include authoring the DSP software (DttSP: in PowerSDR) along with Frank Bickle, AB2KT.

Bob is employed with the Center for Communications Research in Princeton, New Jersey.

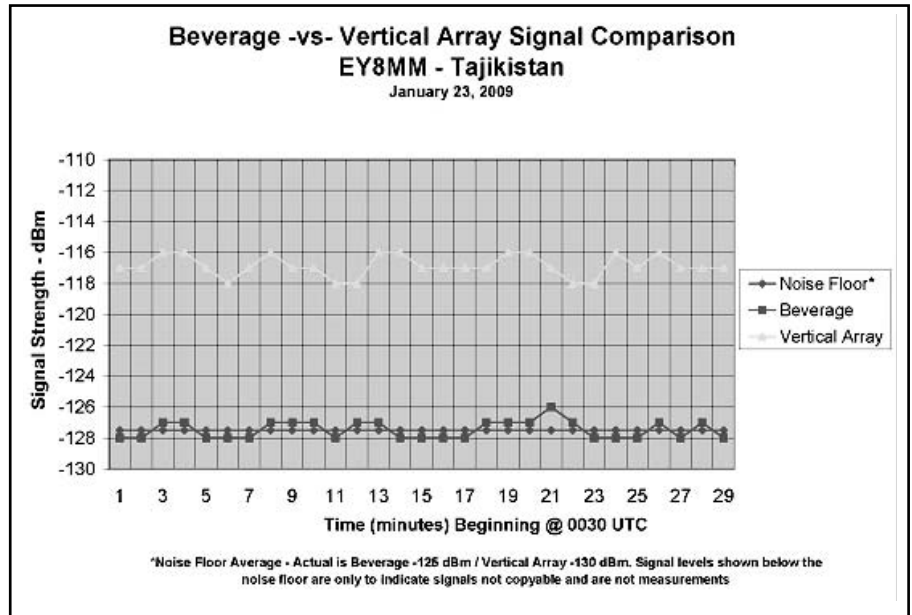


Figure 32 — This chart compares signal levels between the Eight Circle Vertical Array and a Beverage antenna for signals from EY8MM, Tajikistan.

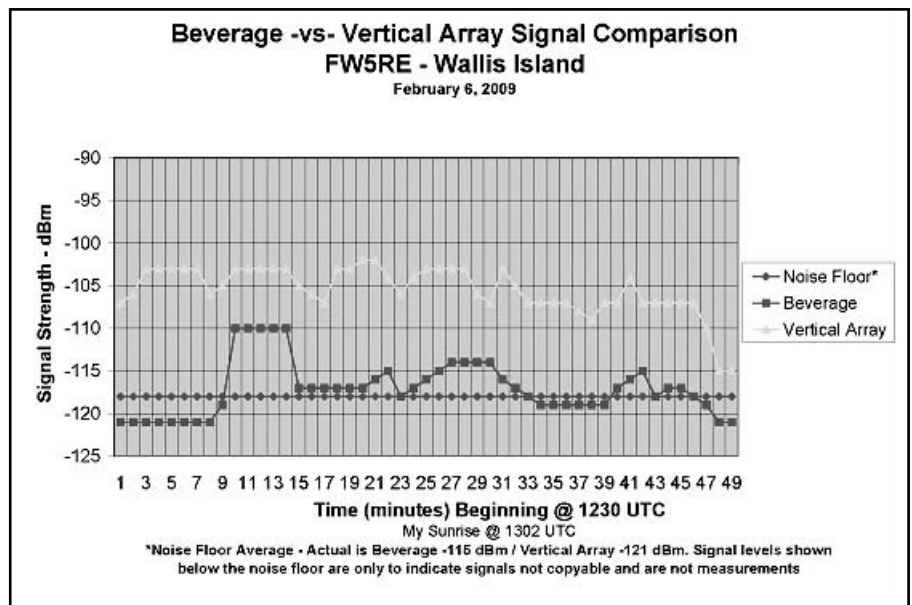


Figure 33 — This chart compares signal levels between the Eight Circle Vertical Array and a Beverage antenna for signals from FW5RE, Wallis Island.

QEX

Amateur Radio Astronomy Projects—A Whistler Radio

The author takes us for a ride into the amazing world of natural radio signals!

[In the author's Jan/Feb 2010 *QEX* article, there was an error in Figure 5, the schematic diagram of the Gyrator II VLF receiver. When our Graphics Department created the schematic, a 0.001 μF capacitor, C4, was omitted between sections U1A and U1B of the op amp. When I reviewed the schematic for accuracy, I failed to notice that missing capacitor, and I apologize for the error. Several readers wrote to point out the omission, and we thank them. A corrected

version of that schematic diagram is reproduced here. — Ed.]

I wanted to continue my project articles with my favorite, a “whistler” radio.¹ “Whistler” radios (named for the whistle-like sound heard when radio signals from lightning travel along magnetic field lines

and disperse) detect the electromagnetic radiation at about 10 Hz to 20 kHz from lightning, aurora, solar flares and other effects on the Earth as they react with the atmosphere. These signals are easily detected and create a variety of sounds, which I will discuss in this article. This gives the “whistler” radio data a distinctive sound quality that no other radio astronomy project has, and makes them much more enjoyable to use and share with others.

¹Jon Wallace, “Amateur Radio Astronomy Projects,” *QEX*, Jan/Feb 2010, pp 3-8.

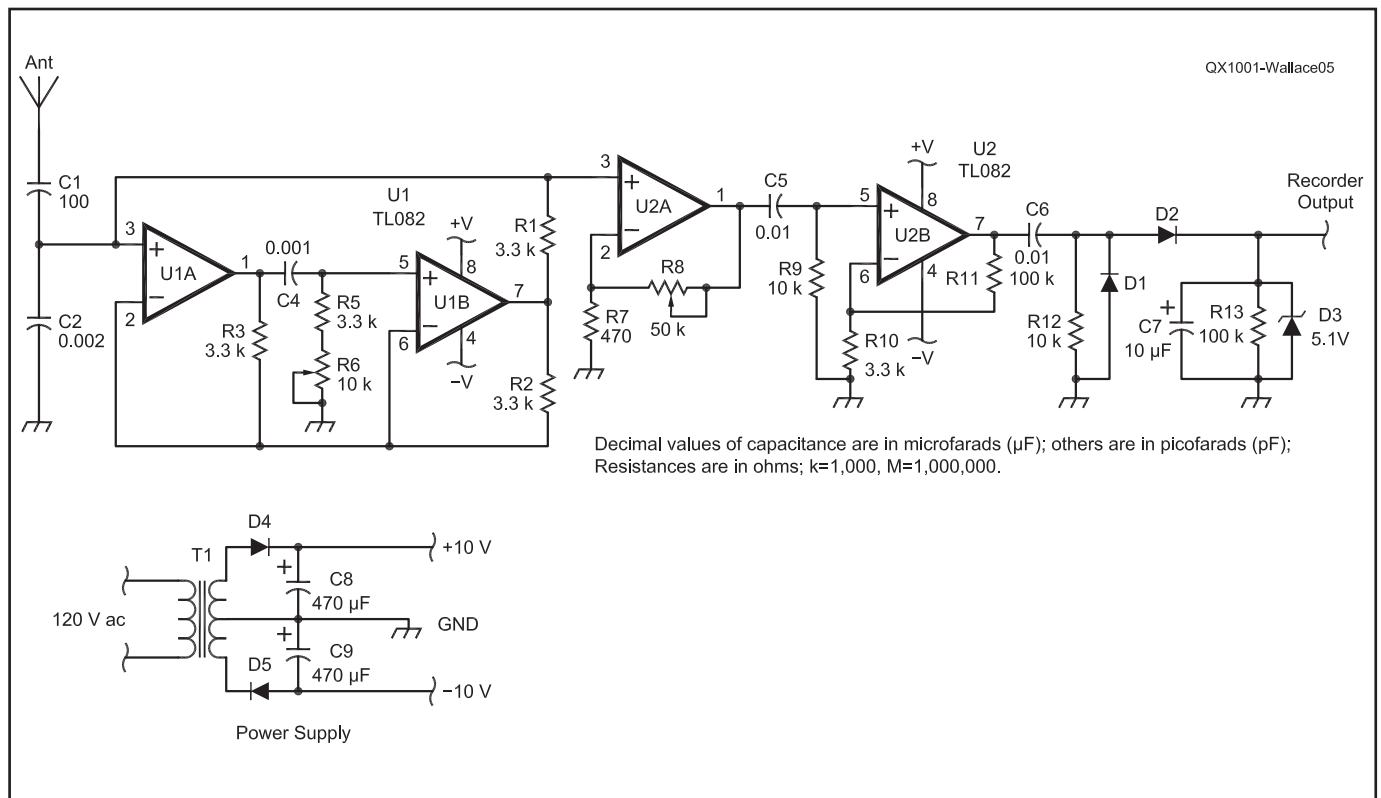


Figure 5 from Jan/Feb 2010 *QEX*, p 5 — This corrected schematic diagram shows the Gyrator II VLF receiver. (Capacitor C4 was omitted.) There is more information, including a complete parts list at www.aavso.org/images/fullgyrator.gif.

Background

VLF and the Ionosphere

The ionosphere is the region of the atmosphere which is ionized by solar and cosmic radiation. It ranges from 70 to 500 km (about 40 to 300 miles) above the surface of the Earth, and is generally considered to be made up of three regions, or layers D, E, and F. Some also include a C region and most experts split the F region into two (F1 and F2) during the daylight hours. Ionization is strongest in the upper F region and weakest in the lower D region, which basically exists only during daylight hours. As I mentioned in the Jan/Feb *QEX* article, solar flare and coronal mass ejection events can strengthen the Ionospheric regions and they then act as a wave guide for VLF. This is due to the fact that the wavelengths of the signals we are monitoring are a significant part of the height of these regions. (Remember that $\lambda = c / f$ thus $(300,000 \text{ km/s}) / (2000 \text{ Hz}) = 150 \text{ km}$). This allows signals from lightning to be heard from nearly half way around the Earth.

Geomagnetic Storms

A geomagnetic storm is a disturbance created by a coupling of the Earth's magnetic field with the magnetic field of the solar wind, caused by solar flares, coronal mass ejections, coronal holes, and so on. They can induce large currents into Earth's magnetosphere and as a result can induce currents into long wire antennas and power lines, leading to damaged equipment and blackouts. Given a powerful storm, these events often generate beautiful auroral displays, which can be seen as far south as Florida. Geomagnetic storms have been linked to many VLF emissions such as *chorus* and *risers* (described in more detail below).

Signals Detected

Lightning Induced Signals: Sferics

Sferics is short for "atmospherics" and these signals are caused by the burst of radio energy emitted by lightning strikes. They cover the entire range of frequencies we are monitoring and are by far the easiest signals to detect. They sound like cracks, pops, and snaps, and are characterized by vertical lines on a spectrogram (see Figure 1). Sferics from lightning can be heard from as far as a thousand miles because of the ionospheric ducting mentioned earlier.

Tweaks

Tweaks are generated when lightning occurs at greater distances from the receiver than those of sferics. Distances can be as great as half way around the Earth. While traveling through the ionospheric duct from these distances, the signal experiences dis-

persion — a process in which higher frequencies travel faster than lower frequencies. This yields a sound for tweaks like a musical saw being plucked, or a musical "twang." They are characterized by vertical lines with "hooks" on their bases, around 2 kHz on a spectrogram (see Figure 1).

Whistlers

Whistlers are created when energy generated by lightning travels away from Earth along magnetic field lines, toward conjugate areas on the Earth. They can sometimes travel back and forth several times between conjugate areas. Since the path along magnetic field lines is very long (as much as three Earth diameters) the dispersive effects are great and the signal sounds like a descending whistle or a bomb dropping. The whistler sound can last for as long as a couple of seconds because of the great dispersion experienced. They are characterized by long descending arcs on a spectrogram (see Figure 1). Whistlers can consist of pure tones if they travel along single paths or be much more diffuse if they travel more complex paths. As mentioned earlier, they can sometimes travel between conjugate areas on Earth, so more than one whistler can be heard from the same lightning event, each experiencing more and more dispersion and therefore spread out more with each trip.

Geomagnetic Signals:

Geomagnetic effects can induce large amounts of energy into the Earth's magnetosphere and generate a number of signals that we can detect. Monitoring the Space Weather Web site (www.swpc.noaa.gov/today.html) and looking for a planetary K index over 5 gives you warning of a geomagnetic storm. The planetary K index is a weighted average

of the maximum deviations on magnetometers compared to a "quiet day" in several locations worldwide. It is calculated every three hours from near-real-time data from these geomagnetic observatories. It ranges from 0 — very quiet to 9 — very large geomagnetic storm. Any K index over 5 is considered a geomagnetic storm and may generate signals we can detect (see Table 1).

Chorus

Chorus seem to be associated with auroral activity caused by geomagnetic storms (there is more study being done on this effect). Chorus signals have a very distinctive sound, which sounds like crickets or birds chirping, many times sounding like a tropical rainforest soundtrack. The signals are characterized by quick rising arcs of less than a second each in duration on a spectrogram, and they tend to be more prevalent during the early morning hours (see Figure 2).

Triggered Emissions

Other signals can be detected and are lumped together here. They include single

Table 1
Planetary K index, Geomagnetic Index and Magnetic Field Intensity in nT

K	nT	G
0	0 - 5	0
1	5 - 10	0
2	10 - 20	0
3	20 - 40	0
4	40 - 70	0
5	70 - 120	1
6	120 - 200	2
7	200 - 330	3
8	330 - 500	4
9	>500	5

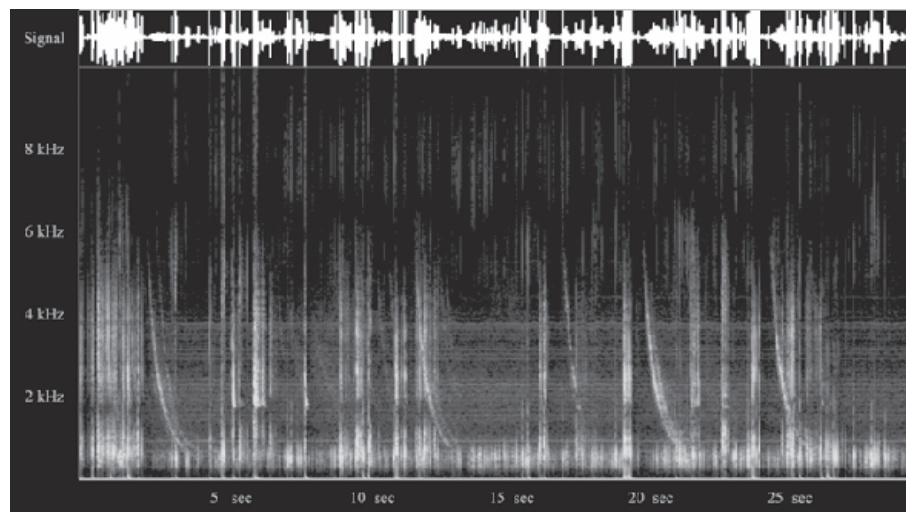


Figure 1 — A sample spectrogram display of natural radio signals. In this display you can see sferics (vertical lines), tweaks (vertical lines with hooks at 2 kHz) and whistlers (downward arcs). Original sound file from NASA INSPIRE: www.theinspireproject.org/index.php?page=types_vlf_signals.

rising tones, hissing, periodic emissions (non-whistler related), and short tonal signals (non-whistler related).

Man-Made Signals:

60 Hz Hum

By far the most readily heard signal and the curse of natural radio listeners is 60 Hz hum. The power lines in the US radiate radio energy at 60 Hz and many harmonics above this, which make it particularly difficult to filter out. This is why you must find a location that is about ¼ mile from normal power lines and at least a mile from major lines to begin to hear the much weaker signals from natural radio sources. On a spectrogram you will notice horizontal rows on your chart, which represent the hum and its harmonics.

Other Electrical Noise

Devices such as electronic ballasts for fluorescent lighting and computer monitors generate distinctive sounds as well. Again, try to get far away from these signal sources so you can detect the weaker natural radio signals.

Loran

LORAN navigation signals can be detected and appear as horizontal dots on a spectrogram. [Recent news stories indicate that the US Coast Guard will stop transmitting US LORAN-C signals as of 2000 UTC on 8 February 2010. See, for example, www.navcen.uscg.gov/loran/default.htm. — Ed.]

Russian Alpha and Coast Guard Omega Navigational Signals

Alpha and the now inactive Omega signals can/could also be detected at the upper range of our receiver. They appear on a spectrogram as horizontal rows of dashes.

Other Signals:

Tire Noise

Tire noise can be detected whenever a car drives by. A brief signal is heard, which appears to be generated by static charge on the tire. These signals can only be detected within about a hundred feet or less of the vehicle. It sounds like a short swish or buzzing.

Flying Insects

Apparently, the flapping of insect wings near an antenna can disrupt the signals detected. It is a very distinctive signal and sounds like ... an insect flying. Normally it is not a problem unless there are swarming insects or an insect that remains close to the antenna for extended periods of time.

Equipment Needed

The Receiver

Whistler radios operate at the ELF and

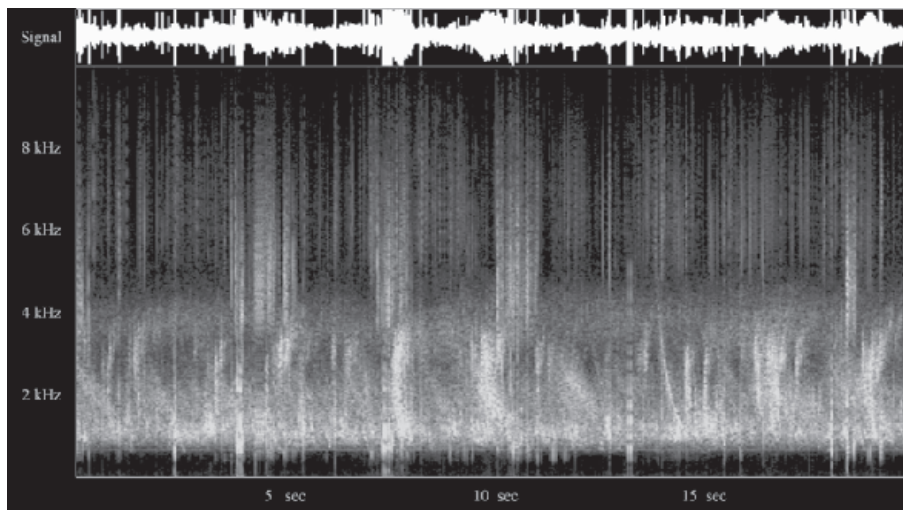


Figure 2 — In this sample spectrogram display you can see chorus signals. Original sound file from NASA INSPIRE: www.theinspireproject.org/index.php?page=types_vlf_signals.

VLF range (typically 10 Hz to 20 kHz). This band of frequencies is known as the audible band, not because you can hear them (you can't hear radio frequencies directly) but because you can feed them into an amplified speaker with a long wire antenna input and hear them. This explains how people in the 19th century knew about some of these phenomena; they were heard on telegraph lines. Unfortunately, due to the ac power grid and other modern innovations, you now

need a receiver that has filtering and more sensitivity than just an amplified speaker. Several sources are available for these radios, all of which work well. Links are included at the end of this article. I currently use the Kiwa Earth Monitor and a small portable unit built by Brian Lucas in England. The Lucas receiver has a ferrite loop antenna that cancels most 60 Hz electrical interference but at a cost to sensitivity (few whistlers will ever be heard with this radio). See Figure

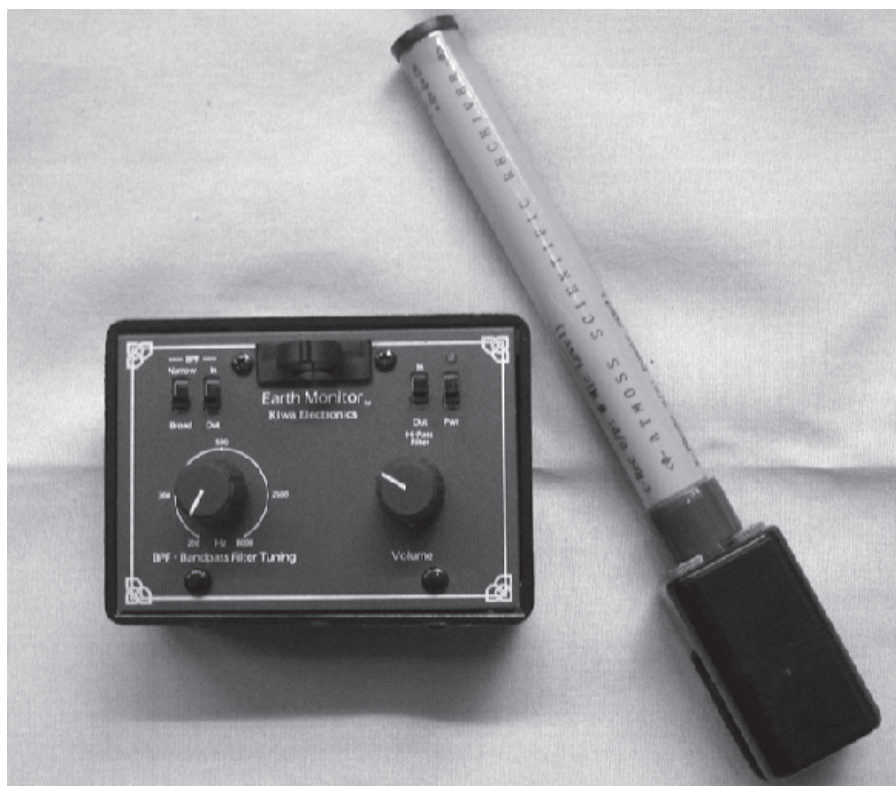


Figure 3 — This photo shows the Kiwa Earth Monitor (left) and Brian Lucas' ATMOSS (right) VLF receivers. (Photo by author.)

Table 2
Sample INSPIRE Data Form

INSPIRE Data

INSPIRE Observer Team _____ Team Number: _____

Coordinated Observation Date: _____ Receiver _____

Tape/Recording Start Time (UT) _____ Tape/Recording Start Time (Local) _____

Local Weather: _____

Codes: M – Mark (WWV or Voice), S – sferics, T – tweek, W – whistler, A – Alpha, C – chorus

Sferic density: D: _____ Scale of 1-5 (1 – Very Low, 3 – Medium, 5 – Very High)

Time (UTC)	Entry	Observer
_____ M – WWV or V	S T W C A _____	D: _____
_____ M – WWV or V	S T W C A _____	D: _____
_____ M – WWV or V	S T W C A _____	D: _____
_____ M – WWV or V	S T W C A _____	D: _____

3. I've also built an INSPIRE (Interactive NASA Space Physics Ionosphere Radio Experiments) VLF radio (though not the newest version, which is available as a kit from INSPIRE at: <http://theinspireproject.org/>). The receivers are quite simple to build and operate, usually with just some simple filtering options and antenna and headphone inputs. I have tried a bunch of antennas and find that the longer the antenna, the better the signal. There is a trade-off, though, since it is difficult to travel with and erect a long wire antenna (I've been stopped by police officers and people driving by and asked what I was doing), so I've settled for a long whip antenna mounted to a tripod and find this satisfactory for most observing sessions. Grounding is also a necessity. Lastly, be aware that signals can range from barely audible to extremely loud crashes of lightning. Adjust your headphones appropriately so you don't damage your hearing.

Data Recording

I have used cassette tape for years, but with the advent of portable digital recorders I hope to transfer to this type of recording. Be sure the device you use doesn't have an automatic level control, or has one that can be turned off, since this will limit your ability to hear weak signals over loud lightning crashes.

Data Analysis

There are many spectrogram programs available on the web. I currently use the program *Spectrogram 12* by Richard Horne (www.brothersoft.com/publisher/richard-horne.html) to view sonograms of my data and visualize natural radio signals. It is a

freeware program and is easy to use. Simply input the file you recorded using the function/scan file options and then choose your file. The scan file screen then appears and allows you to adjust all aspects of your sound file. Once you've chosen your preferences for this file, it creates the spectrogram with the sound file shown on top. Of course, what you hear is much better than anything you will be able to create with a spectrogram, so be sure to listen to the recorded data, preferably as you record it, and make notes about what you hear for later analysis. INSPIRE has a format they recommend. Table 2 shows a sample of this form.

When and How to Listen

Generally, whistler activity seems greatest late at night, and the hours from midnight to dawn seem best. I've found my best activity near dawn, and sunrise can be a great time to observe. I've also found that winter and spring are the best times for activity. The INSPIRE program used to schedule coordinated observations during the spring. For geomagnetic activity, you must check the planetary K index and see when it rises above 5. This will give you the best chance to hear chorus and other geomagnetic emissions. These rules aren't written in stone, and some great observing can be had at any time. My suggestion is: if you have the time and the inclination, observe.

I hope you will enjoy listening to natural radio signals as much as I have.

Sources for VLF Whistler Radios and Additional Information

NASA INSPIRE Radio Kits: http://theinspireproject.org/index.php?page=order_vlf_receiver_kits

[inspireproject.org/index.php?page=order_vlf_receiver_kits](http://theinspireproject.org/index.php?page=order_vlf_receiver_kits)

Kiwa Earth Monitor: www.kiwa.com/ethmon.html

LF Engineering Co.: www.lfengineering.com/products.htm

Steve Mc Greevy's Web site: <http://n6gkj.blackpage.net/vlf/mcgreevy/VLFRadio.htm>

The Society of Amateur Radio Astronomy (SARA): www.radio-astronomy.org/

Jon Wallace has been a high school science teacher in Meriden, Connecticut for over 28 years. He is past president of the Connecticut Association of Physics Teachers and was an instructor in Wesleyan University's Project ASTRO program. He has managed the Naugatuck Valley Community College observatory and run many astronomy classes and training sessions throughout Connecticut. Jon has had an interest in 'non-visual' astronomy for over twenty-five years and has built or purchased various receivers as well as building over 30 demonstration devices for class use and public displays. He is currently on the Board of the Society of Amateur Radio Astronomers (SARA) and developed teaching materials for SARA and the National Radio Astronomy Observatory (NRAO) for use with their Itty-Bitty radio Telescope (IBT) educational project. Other interests include collecting meteorites, raising arthropods ("bugs") and insectivorous plants. Jon has a BS in Geology from the University of Connecticut; a Master's Degree in Environmental Education from Southern Connecticut State University and a Certificate of Advanced Study (Sixth Year) in Science from Wesleyan University. He has been a member of ARRL for many years but is not a licensed Amateur Radio operator.



Waveguide Filters You Can Build—*and* Tune

Part 3

Evanescent Mode Waveguide Filters

In the last of his three part series, the author introduces us to a filter with which many Amateur Radio operators are not familiar.

The only amateur publication of evanescent mode waveguide filters, to the best of my knowledge, is by Reed Fisher, W2CQH, in 1993.¹ I noticed the paper when it first appeared, but I recall thinking that they couldn't be very good filters, since evanescent modes have high loss.

Evanescent modes occur in waveguides at frequencies below the cutoff frequency, where attenuation is very high. The energy decays exponentially along the guide, so that attenuation is linear with distance (~30 dB per waveguide diameter for circular guide. For example, a circular guide with an inner diameter of one inch would have an attenuation of about 30 dB per inch). This phenomenon has been used for precision attenuators.²

Recently, I was looking for references on waveguide filters and came across several for evanescent mode filters. Apparently they actually work, and offer good performance in a compact package. What I hadn't realized is that evanescent modes in waveguide are reactive, so that the attenuation is due to reflection, not dissipation, of energy — the energy is not lost.³ When we make them resonant structures, they behave much differently than non-resonant evanescent mode waveguides. After perusing a few papers, I went back to Reed's paper to look for practical dimensions.

Starting with some of Reed's examples, I did some simulation with Ansoft HFSS

¹Notes appear on page 29.

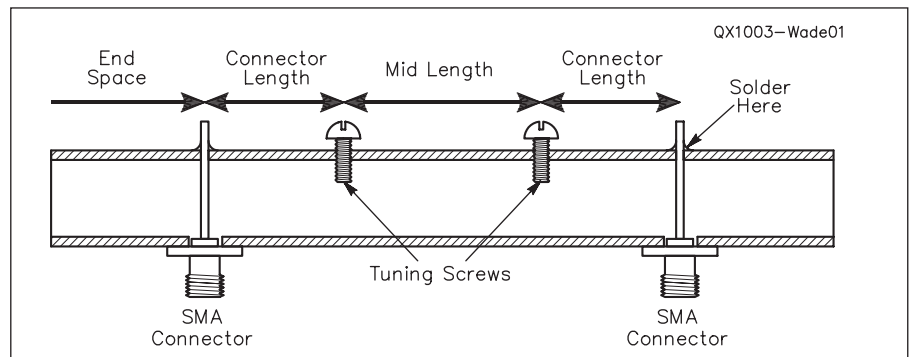


Figure 1 — This sketch shows a two section evanescent mode waveguide filter.

electromagnetic software, and fiddled the dimensions until a reasonable filter response appeared.⁴ Then it was time to make one. Construction is really simple — two SMA connectors with a tuning screw or two between them, as sketched in Figure 1, all on the centerline of the broad side of the waveguide. The critical dimensions are the distances between the screws — the *Mid Length*, and from the screws to the SMA connectors — the *Connector Length*. The SMA connector center pin connects to the far wall of the waveguide. This is the micro-wave version of a coupling loop.

The first filter I made was for 3456 MHz in WR-90 (X-band) waveguide. The cutoff frequency for WR-90 is about 6.5 GHz, so this is way below cutoff. Nothing should get through the waveguide at this frequency. However, the filter works pretty well — the

response is plotted in Figure 2. It is a pretty sharp filter, with less than 2 dB of loss. The filter was tuned and measured in my basement with surplus test gear, recording the data by hand, so the range is limited and the curve in Figure 2 has some glitches. Later, I was able to measure the filters on fancy vector network analyzers (VNA) from Agilent and Rhode & Schwarz, who are kind enough to bring these instruments to ham conferences. All the later plots are from these measurements. It is still easier to tune the filters on the old analog readout gear, however, rather than wait for a computerized measurement after each adjustment.

Construction is exceedingly simple: drill holes for the connectors and screws, tap the screw holes, solder the connector pins to the far wall, and tune it up. Since energy doesn't travel far in the evanescent guide without

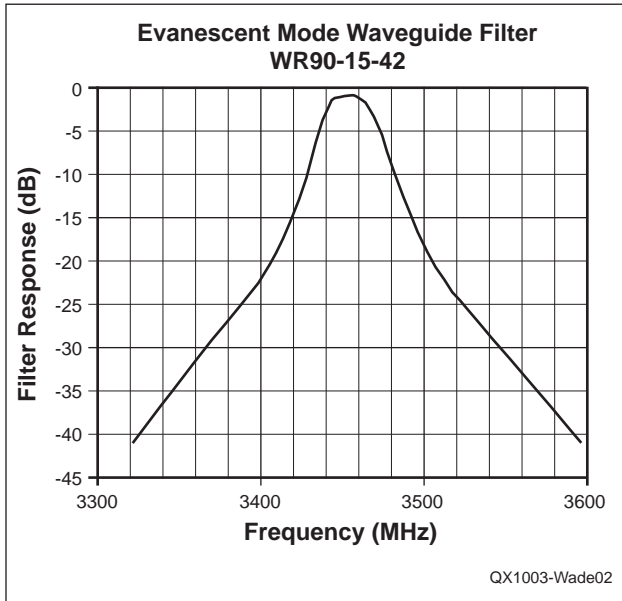


Figure 2 — The frequency response of the 3456 MHz filter.

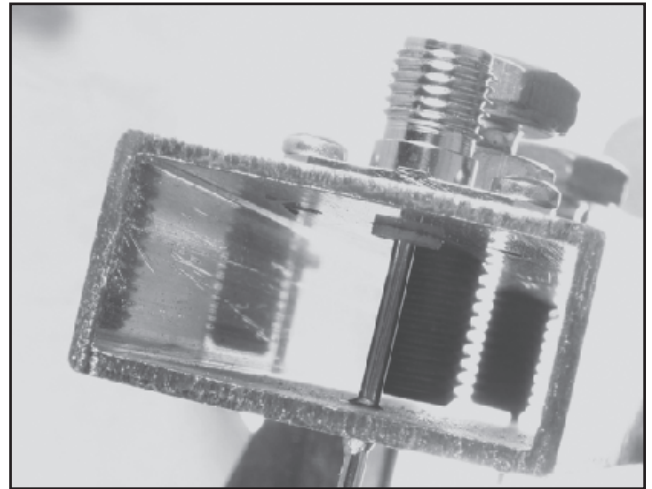


Figure 3 — Here is a view inside an evanescent mode filter.

something resonant, the ends may be left open. I was amazed to stick my finger in the end with no effect! The length of the *End Space* in Figure 1 should be more than half of the waveguide width. I usually leave about 20 mm as a convenient length.

Figure 3 is a photo looking in the end of the finished filter, showing the two screws sticking into the waveguide. These screws are tuning capacitors, so I used a couple of ¼-28 brass screws that I had in my junk box, with the ends faced flat on a lathe. The flat end might make the tuning smoother, but it was still pretty touchy even with the fine-thread screw. I also learned that putting the screw head on the same side as the coax connectors is a bad idea — there isn't much room in which to work. Later versions have the screws on the opposite side, as shown in Figure 1.

Evanescent Mode Filter Theory

So how do these filters work? Basically, a section of evanescent mode waveguide, well below cutoff, acts as an inductor. We add a capacitor to make a resonant circuit.

The simple equivalent circuit of a short length of evanescent mode waveguide is shown in Figure 4, a series inductance with a shunt inductance at each end. If we put connections at each end and a screw in the middle, like Figure 5, it forms the single resonator shown schematically in Figure 6.

The tuning capacitor resonates with the two L_{shunt} inductors, one on each side, and the L_{series} inductor provides coupling to the SMA connectors, to set the loaded Q_L of the resonator. Thus, making L_{series} larger, by increasing the spacing, reduces the coupling and there-

fore the loading from the 50 Ω source and load, making the Q_L higher.

The inductances are calculated from the length of waveguide, from the connector to the tuning capacitor (*Connector Length* in Figure 1, center-to-center) and the cutoff wavelength. First, the cutoff frequency of a rectangular waveguide is when the width of the guide equals a half-wavelength. For

WR-90, the width is 0.9 inch = 22.86 mm, so the cutoff wavelength $\lambda_c = 45.72$ mm. Thus, the cutoff frequency is $300/45.72 = 6.56$ GHz.

Craven & Mok show a graph of unloaded Q for WR-90 waveguide.⁵ The theoretical Q is higher than 10,000 at 10 GHz in a normally propagating TE_{10} mode, but slightly lower for the TE_{10} evanescent mode, perhaps 6,000 just below cutoff, and falling to around 1,000 at 1 GHz. This Q is still high enough to use the lossless transmission line assumption, which simplifies calculations.

For a lossless TE_{10} evanescent mode, the characteristic impedance, X_0 , is calculated from the cutoff wavelength, λ_c , the free space wavelength, λ , and the waveguide width a and height b . (See Note 5.)

$$X_0 = \frac{b}{a} \times \frac{120\pi}{\sqrt{\left(\frac{\lambda}{\lambda_c}\right)^2 - 1}} \quad [\text{Eq 1}]$$

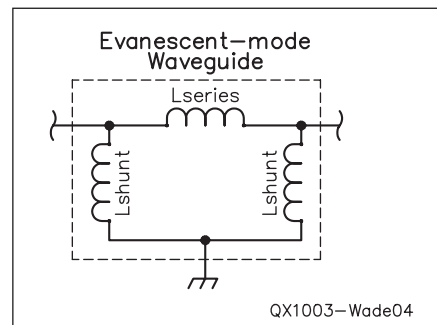


Figure 4 — A schematic representation of the equivalent circuit of an evanescent mode filter.

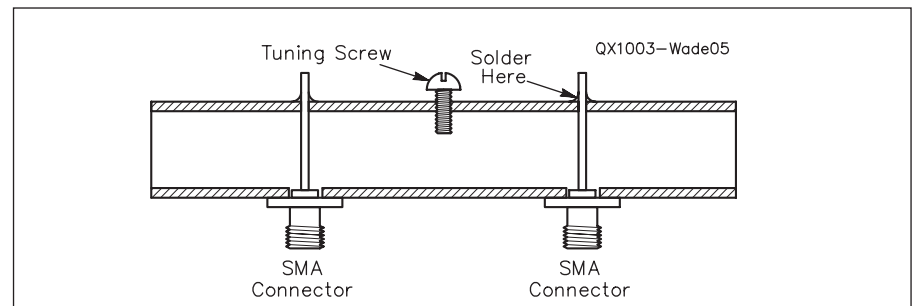


Figure 5 — Evanescent mode waveguide single resonator.

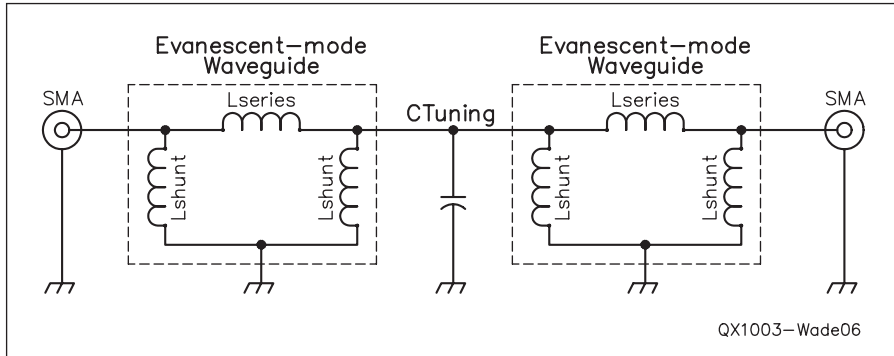


Figure 6 — A schematic of the equivalent circuit of an evanescent mode waveguide resonator.

And the propagation constant, γ , is:

$$\gamma = \frac{2\pi}{\lambda} \sqrt{\left(\frac{\lambda}{\lambda_c}\right)^2 - 1} \quad [\text{Eq 2}]$$

For a waveguide length, ℓ , the reactances of the inductors are then calculated:

$$X_{L_{series}} = jX_0 \sinh \gamma \ell \cong \frac{jX_0}{2} e^{\gamma \ell} \quad [\text{Eq 3}]$$

$$X_{L_{shunt}} = jX_0 \coth \frac{\gamma \ell}{2} \cong \frac{jX_0}{2} \quad [\text{Eq 4}]$$

where \sinh and \coth are the hyperbolic sine and cotangent functions, respectively.

The approximations on the right side are from W2CQH. He uses them for a further approximation to estimate the loaded Q_L :

$$Q_L \approx \frac{R_0}{X_0} e^{\gamma \ell}$$

where $R_0 = 50 \Omega$ for a coax termination.

All these approximations have some error, and the errors add up, so that the estimated Q_L is lower than the apparent values from simulation and measurement. The discrepancy is as much as a factor of two, which could lead to filters much sharper or lossier than expected. Also, the Johanson trimmer capacitors used to make the lower frequency filters are not nearly as high- Q as the waveguide, so the loss of the lower-frequency filters is higher.

Another factor is the inductance of the SMA connector pin. The inductance creates an additional impedance transformer, further reducing the loading and raising the loaded Q .

With waveguide post filters, we found that a double-tuned filter was adequate for many applications. For a double-tuned filter, we need not only the evanescent mode

waveguide length at each end, but also an additional length in the center, with an L_{series} calculated for the *Mid Length* in Figure 1 that provides the desired coupling between the two resonators tuned by the two capacitors. The double-tuned filter is shown schematically in Figure 7 and sketched in Figure 1. The two *Connector Lengths* should be identi-

cal, but the *Mid Length* is longer — increasing the length decreases the coupling.

The result of all the approximations and errors is that we cannot calculate the parameters accurately enough using these equations to design a filter — even a simple double-tuned filter. Snyder has more equations, but I have not had a chance to evaluate them.⁶ Instead, I have resorted to professional 3D electromagnetic software, the Ansoft *HFSS* program, to analyze various trial dimensions, and then to build some of the promising ones. Even then, some of the filters have a measured bandwidth slightly narrower than predicted.

More Examples

I have made a number of successful evanescent mode filters in all sizes of X-band waveguide, WR-90, WR-75, and WR-62, for frequencies from 5.76 GHz down to below 1 GHz. Figure 8 is a photo of several of the filters; the small physical size of these filters should be apparent. The limiting factor for low frequencies is the tuning capacitance – a

Table 1
Evanescent Mode Waveguide Filters

Designation	Band (MHz)	Connector Length (mm)	Mid Length (mm)	Tuning Screw USA	Bandwidth (MHz)	Insertion Loss (dB)
WR-62 Waveguide						
WR62-12-33	5760	12	33	#10	37	1.8
WR62-12-28	3456	12	28	conc #10	31.5	1.64
"	2304	12	28	conc #10	20	2.07
WR62-12-28J	3456	12	28	Johanson	36	3.13
"	2304	12	28	Johanson	18.5	4.5
"	1296	12	28	Johanson	10.5	7.1
"	1152	12	28	Johanson	9	7.9
WR62-10-24J	3456	10	24	Johanson	73	1.69
"	2304	10	24	Johanson	41	2.15
"	1296	10	24	Johanson	21.5	3.37
"	1152	10	24	Johanson	18.5	3.26
WR62-9-22J	3456	9	22	Johanson	109*	1.47
"	2304	9	22	Johanson	63	1.76
"	1296	9	22	Johanson	33	2.75
"	1152	9	22	Johanson	29.5	3.44
WR-75 Waveguide						
WR75-15-45	5760	15	45	1/4 - 28	32	1.3
WR75-13-34	3456	13	34	conc #10	37	0.8
WR75-13-32	2304	13	32	conc #10	26	1.08
WR-90 Waveguide						
WR90-12-30J	3300	12	30	Johanson	130*	1.48
"	2304	12	30	Johanson	69*	1.3
"	1296	12	30	Johanson	33	1.8
"	1152	12	30	Johanson	29	1.82
"	903	12	30	Johanson	23	2.36
"	720	12	30	Johanson	18	2.9
"	581	12	30	Johanson	15	3.7
WR90-14-35	2304	14	35	conc #10	(not built)	
WR90-15-42	3456	15	42	1/4 - 28	35	1.3

Note: End Space typically 20 mm

* - Over-coupled response

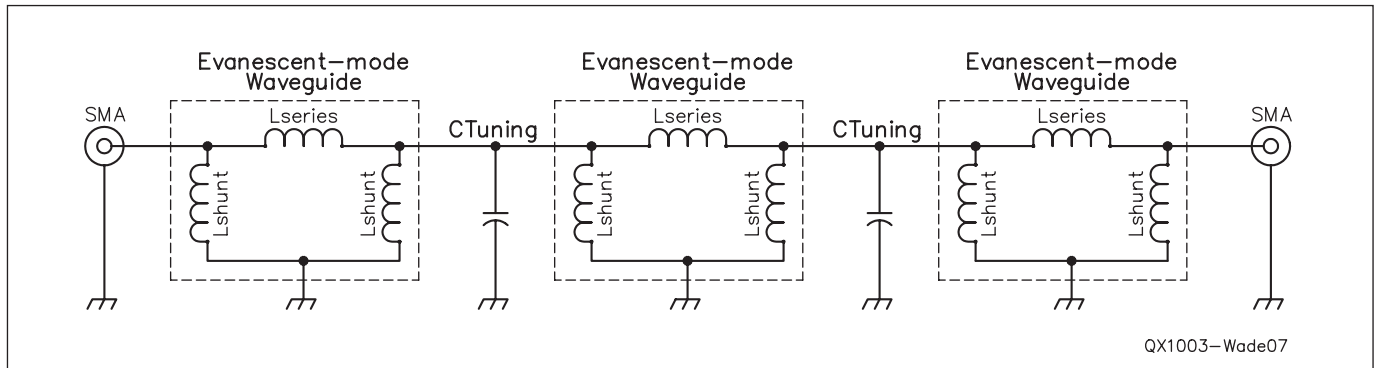


Figure 7 — This schematic represents a double-tuned (two section) evanescent mode waveguide filter.

simple screw provides only a fraction of a picofarad, and even the Johanson trimmer capacitors are limited to 10 pf or so. For 2.3 and 3.4 GHz, I increased the screw capacitance by soldering a ¼" diameter piece of hobby brass tubing to the opposite wall, so the #10 screw inside the tubing forms a concentric capacitor. This is sketched in Figure 9, and used in the bottom filter in Figure 8.

The performance is shown in Figure 10 of two 5760 MHz filters with plain tuning screws, like the top two filters in Figure 8. These are pretty sharp, good enough for better than 30 dB of LO rejection with a 144 MHz IF, yet the loss is under 2 dB.

These filters have a narrow passband with fairly low loss, and a wide stopband — there are no significant spurious responses below the cutoff frequency for the waveguide. Figure 11 shows the WR-75 filter for 5760 MHz over a very wide band. Above the cutoff frequency, calculated as 7.87 GHz for WR-75, normal propagation can occur in the waveguide and the filter is less effective, with a few spurious responses. Thus, a WR-90 filter for 5760 MHz could have an additional response starting at about 6.5 GHz, so it would be less effective for this band than one with smaller waveguide. On the other hand, a WR-62 filter would not have any significant spurious response below about 10 GHz, so it can be an effective harmonic filter as well as bandpass filter for 2304 or 3456 MHz. Figure 12 shows this for a 3456 MHz filter in WR-62. Any spurious response below 10 GHz is more than 60 dB down. There is plenty of surplus WR-62 waveguide around; it is not as good for 10.368 GHz operation since it is very close to cutoff, but very useful for these filters.

The filter in Figure 12 looks exceedingly sharp in the wideband plot. Figure 13 zooms in to look at the passband of a half-dozen filters tuned to 3456 MHz. Most of these filters can be tuned over a wide range, so I was able to tune and measure some of them at several different bands. Table 1 lists all the successful filters I made and the different bands at

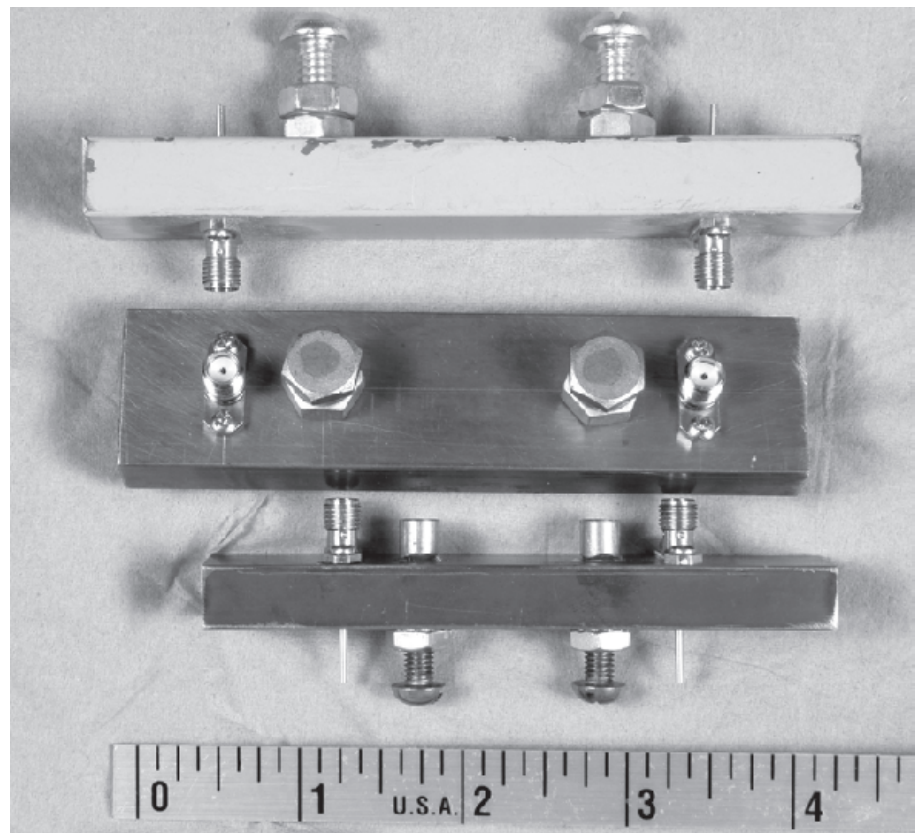


Figure 8 — This photo shows some examples of two section evanescent mode waveguide filters using three sizes of X-band waveguide.

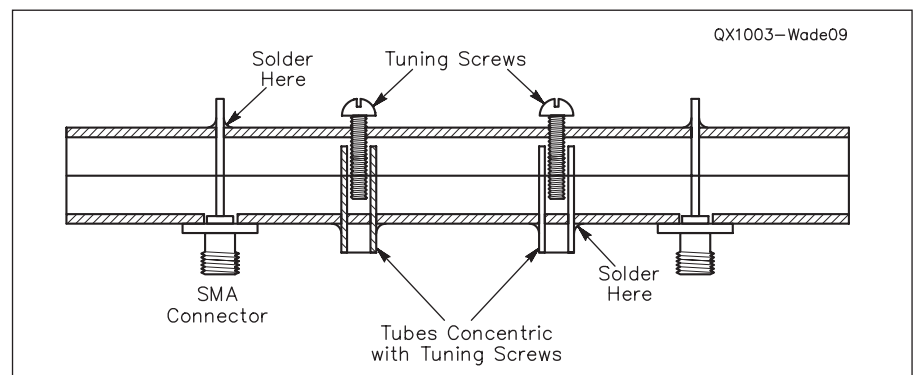


Figure 9 — This filter uses a concentric screw-inside-tubing capacitor.

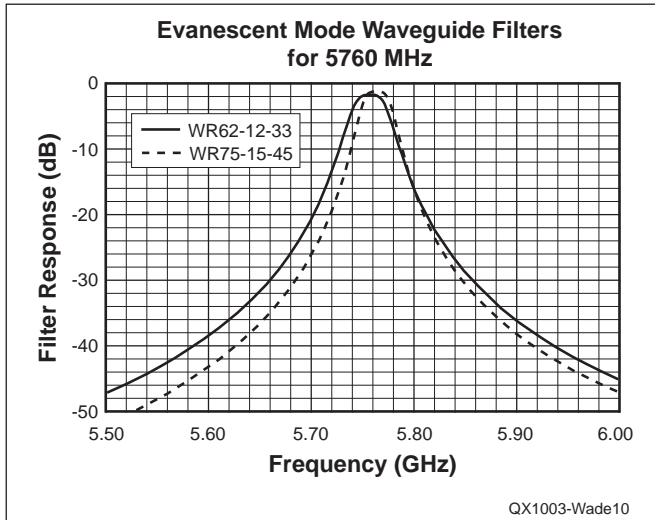


Figure 10 — This graph shows the response of a two section 5760 MHz filter, using two different types of waveguide.

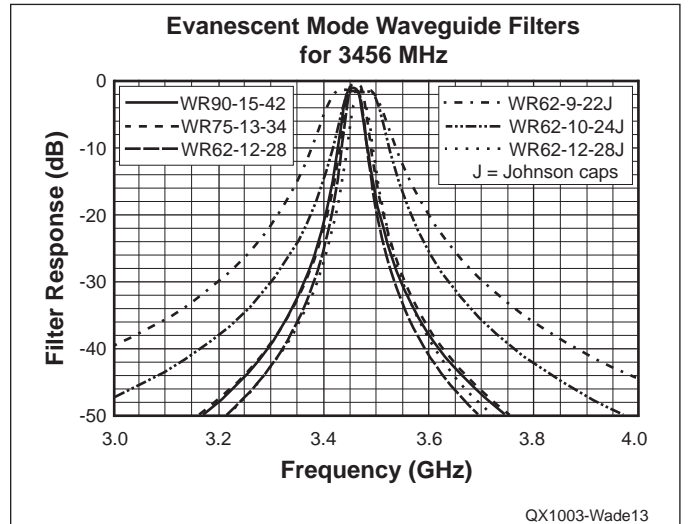


Figure 13 — This graph shows the frequency response of several two section 3456 MHz filters.

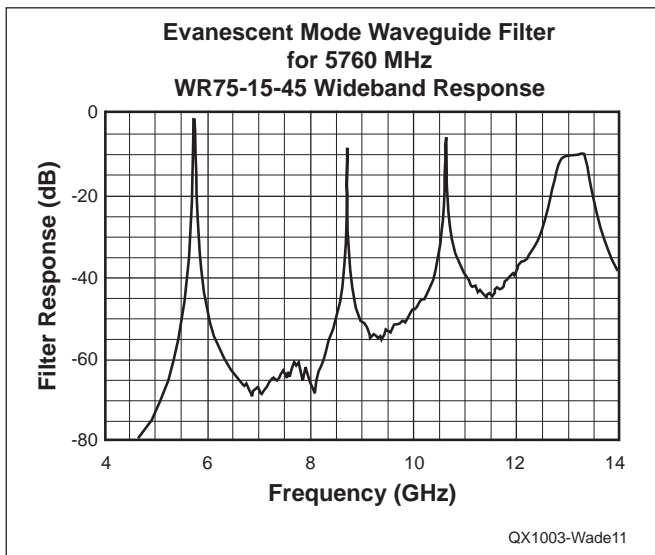


Figure 11 — This plot gives the wideband response for a 5760 MHz filter built with WR75-15-45 waveguide.

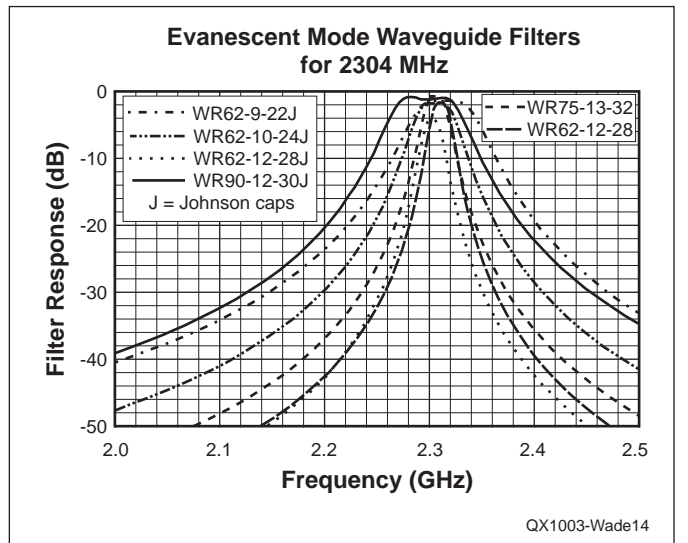


Figure 14 — Here is the frequency response of several two section 2304 MHz filters.

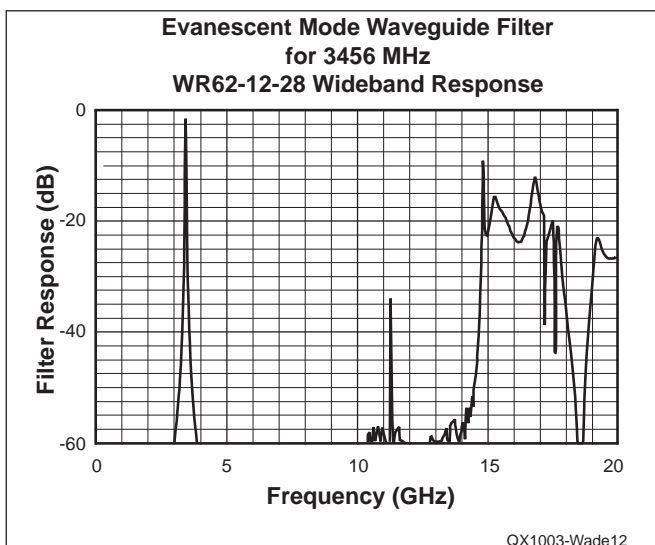


Figure 12 — Here is the frequency response of a 3456 MHz filter built with WR62-12-28 waveguide.

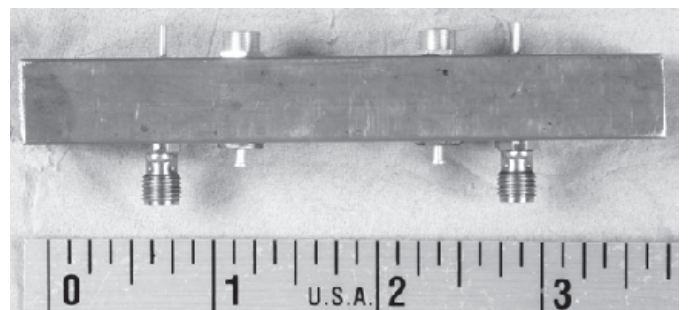


Figure 15 — This photo shows an evanescent mode filter tuned with Johnson capacitors.

which they were tested. For one set of dimensions, the WR62-12-28, I made one with concentric tuning screws and another with Johanson capacitors — the difference in loss is clear at 3456 MHz, as shown in Figure 13 and at 2304 MHz, as shown in Figure 14.

The filters plotted with solid lines in Figure 13 have tuning screws, either plain or concentric. All have loss under 2 dB and would provide more than 30 dB of LO rejection for a 2 meter IF. The dashed lines are for filters using Johanson piston-trimmer capacitors. These were intended for lower frequencies, but I wanted to see how high they would tune. The wider ones still have low loss, while the narrowest one has more

loss, about 3 dB. We expect narrower filters to have more loss, since the loaded Q_L is higher, and the Johanson capacitors probably have a lower Q than a tuning screw.

The filters for 2304 MHz are small, the same size as 3456 MHz. Many of them are the same filters with the screws farther in, but they still have good performance, as shown in Figure 14. The filters with concentric screws have loss under 2 dB, while the narrow WR-62 filter with Johanson trimmers has more loss at 2304 MHz.

With the higher capacitance of the Johanson trimmers, the lower end of the tuning range is extended. A WR-90 filter with large Johanson trimmers, model 5502, tunes

from about 3.3 GHz down to 580 MHz. Figure 15 is a photo of the filter, and Figure 16 shows the tuning range, retuning the filter and measuring at several frequencies across the range. The loss increases as we go down in frequency. I don't know whether this is due to lower Q of the evanescent mode waveguide, the trimmer capacitors, or both. At the upper end of the tuning range, the filter starts to become over-coupled, with a double-hump response.

WR-62 filters with the more common Johanson capacitors, models 2954 and 5202, tune from 3456 MHz down to about 980 MHz. I tuned several of them, as well as the WR-90 filter from Figure 15, to

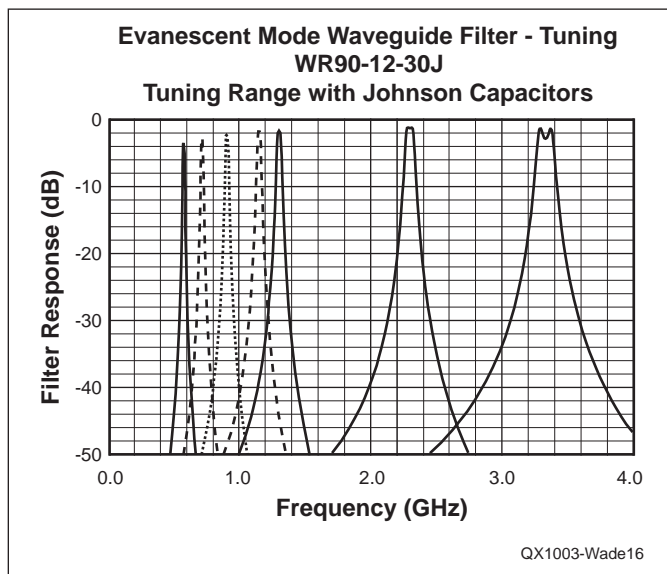


Figure 16 — A graph of the frequency response of the filter shown in Figure 15. The filter was retuned for several frequencies across its range, from about 580 MHz to about 3.3 GHz.

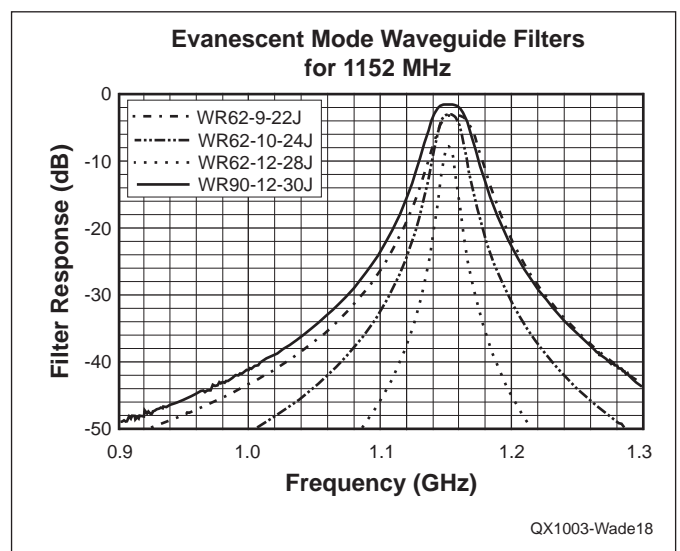


Figure 18 — Here is the frequency response of various two section filters tuned to 1152 MHz.

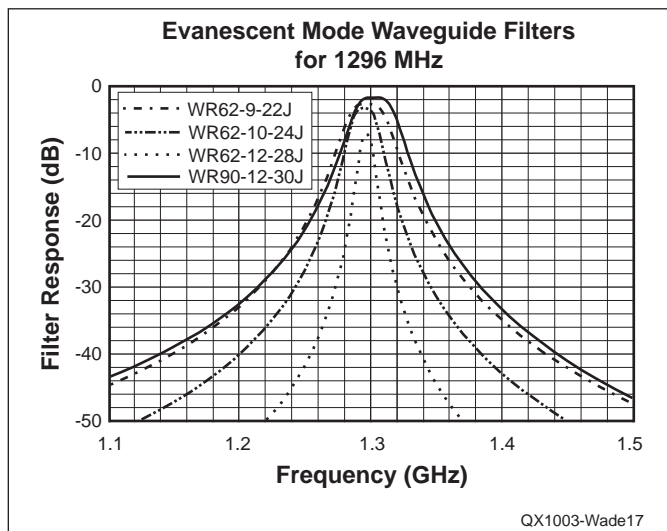


Figure 17 — This graph shows the frequency response of several two section filters for 1296 MHz.

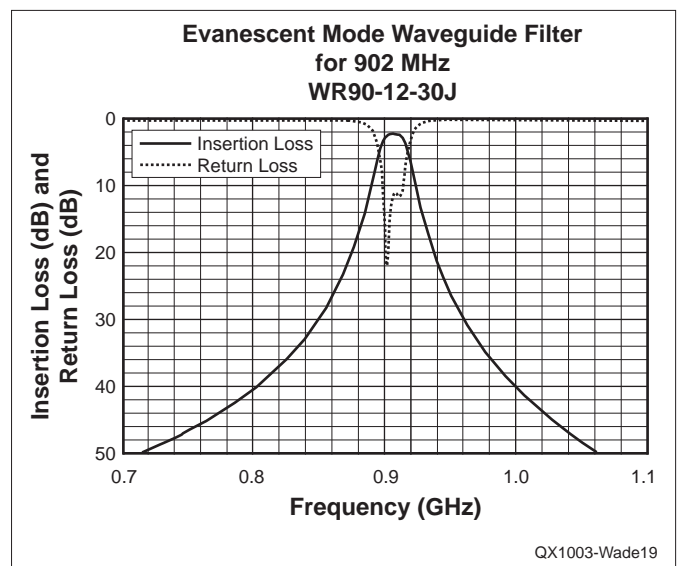


Figure 19 — This graph shows the insertion loss and the return loss for a two section filter built from WR90 waveguide and tuned to 902 MHz.

1296 MHz. Results are shown in Figure 17. The WR-90 filter has less than 2 dB loss, while the WR-62 filters have slightly more loss. As expected, the narrower filters have higher loss.

The same four filters have similar performance when retuned to 1152 MHz, a common LO frequency for 1296 MHz, as shown in Figure 18.

The WR-62 filters will not tune as low as 902 MHz, but the WR-90 filter from Figure 15, with the larger Johanson capacitors, will tune much lower in frequency, as we saw in Figure 16. Performance of this filter tuned for 902 MHz is shown in Figure 19. Loss has increased to around 2.5 dB, but the filter might be sharp enough for a 28 MHz IF at 902 MHz. The upper trace shows that the input return loss is much narrower than the bandpass, but it is still fine for our use.

A summary of dimensions for all the successful filters is shown in Table 1, along with frequencies at which each was tested — some of them work at 3 or 4 different bands.

Tuning these filters can be tricky, unless a swept-frequency test is available, since the

filters tune over a wide range. If only fixed frequency testing is possible, it is necessary to slowly tune both screws together until some output is noted. Then it is simply a matter of tuning for maximum output and minimum SWR. Most of them tune with the screws inserted quite far into the guide, so it might be easier to start with the screws nearly shorting and back them out slowly.

The performance shown is tuned to ham bands, but several of the filters can be tuned to more than one band. Obviously, they can be tuned to any frequency in between, and more. Thus, the examples shown above and in Table 1 should fulfill most requirements.

Summary

Evanescence mode waveguide filters offer very good performance in a compact package, and are easy to build for several of the lower microwave bands. While we have not worked out design formulas, a table of dimensions for a number of working filters is included. These examples utilize small lengths of any of the common X-band waveguides, including WR-62, which is of other-

wise limited usefulness.

Notes

¹Reed Fisher, W2CQH, "Evanescence Mode Waveguide Filters," *Proceedings of Microwave Update '93*, ARRL, 1993, pp. 10-16.

²David H. Russell, "The Waveguide Below-Cutoff Attenuation Standard," *IEEE Transactions on Microwave Theory and Techniques*, December 1997, pp. 2408-2413.

³George F. Craven & Richard F. Skedd, *Evanescence Mode Microwave Components*, Artech, 1987.

⁴HFSS is a simulation tool for 3D full-wave electromagnetic field simulation: www.ansoft.com

⁵G. F. Craven & C. K. Mok, "The Design of Evanescence Mode Waveguide Bandpass Filters for a Prescribed Insertion Loss Characteristic," *IEEE Transactions on Microwave Theory and Techniques*, March 1971, pp. 295-308.

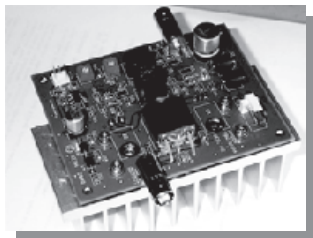
⁶Richard Snyder, "New Application of Evanescence Mode Waveguide to Filter Design," *IEEE Transactions on Microwave Theory and Techniques*, December 1977, pp. 1013-1021.



HPSDR is an open source hardware and software project intended to be a "next generation" Software Defined Radio (SDR). It is being designed and developed by a group of enthusiasts with representation from interested experimenters worldwide. The group hosts a web page, e-mail reflector, and a comprehensive Wiki. Visit www.openhpsdr.org for more information.

TAPR is a non-profit amateur radio organization that develops new communications technology, provides useful/affordable hardware, and promotes the advancement of the amateur art through publications, meetings, and standards. Membership includes an e-subscription to the *TAPR Packet Status Register* quarterly newsletter, which provides up-to-date news and user/technical information. Annual membership costs \$25 worldwide. Visit www.tapr.org for more information.

NEW!



PENNYWHISTLE
20W HF/6M POWER AMPLIFIER KIT

TAPR is proud to support the HPSDR project. TAPR offers five HPSDR kits and three fully assembled HPSDR boards. The assembled boards use SMT and are manufactured in quantity by machine. They are individually tested by TAPR volunteers to keep costs as low as possible. A completely assembled and tested board from TAPR costs about the same as what a kit of parts and a bare board would cost in single unit quantities.

HPSDR Kits and Boards

- **ATLAS** Backplane kit
- **LPU** Power supply kit
- **MAGISTER** USB 2.0 interface
- **JANUS** A/D - D/A converter
- **MERCURY** Direct sampling receiver
- **PENNYWHISTLE** 20W HF/6M PA kit
- **EXCALIBUR** Frequency reference kit
- **PANDORA** HPSDR enclosure



TAPR

PO BOX 852754 • Richardson, Texas • 75085-2754

Office: (972) 671-8277 • e-mail: taproffice@tapr.org

Internet: www.tapr.org • Non-Profit Research and Development Corporation

Doppler Tracking

The author combines some simple electronics with a physics principle to measure speed and height of his model rocket launches.

The “Doppler effect” is responsible for frequency shifts of the received signal just by virtue of movement of the reflecting or transmitting source.¹ It almost seems like you get something for nothing. By this I mean that no complex electronics are required to produce the frequency shift, and those that are required are familiar to the typical ham operator. The system that I will discuss uses some of my ham equipment.

Most applications of the Doppler frequency shift have one thing in common: the object being measured is moving. These applications include radar to track incoming storms or fast moving motorists, medical applications to measure blood flow in arteries and veins, and astronomy applications to measure the speed of stars moving toward or away from Earth. Although the frequencies used, be they audio, RF, or optical, may differ for each application, the effect is the same.

But what can Joe Ham do with the Doppler effect? My own interest in using the Doppler effect comes from a secondary hobby, model and high power rocketry. Do you think you have too many hobbies? While attending rocket launches at the Black Rock desert in Nevada, I all too often observed rockets that would make great ascents but have ballistic descents caused by parachute deployment problems. The result was a destroyed rocket and, electronics embedded in the desert floor. The thought occurred to me that if these rockets had some sort of inexpensive and sacrificial RF system, in case of a crash, maybe we could learn something about the speed and altitude of these imperfect flights.

I didn’t want the project to be so sophisticated that it required extremely high RF power levels or specialized tracking antennas. For example, Doppler weather radars



use many kilowatts of power. I was more interested in milliwatts. I did not consider a transponder because I thought it too complex. I was after simplicity. There was some previous work on transponder systems done by Steve Bragg, KA9MVA. Steve referred to his experimental work as the “Digital Amateur Rocket Tracking System.”² I also wanted to make use of ham radio equipment I already owned or could easily build. I decided early on to make use of the 23 cm band, and this decision was primarily based on owning an older ICOM IC-1271, which is a multi-mode 23 cm. transceiver. The SSB mode was very important to make these measurements, as this mode produces a tone from a CW signal. I was already familiar with the 23 cm band since I had worked ATV and FM repeaters on that band. It helps with Doppler to use as high a frequency as possible, since the Doppler frequency shift is proportional to the operating frequency.

So, is the 23 cm band high enough in frequency to make some measurements? We shall see.

Theory

The Doppler shifted frequency is given by this formula:

$$f_{\text{rec}} = f(1 + v/c) \quad [\text{Eq 1}]$$

where:

f is the transmitted frequency

f_{rec} is the frequency of the wave arriving at the receiver

v is the velocity of the transmitter relative to the receiver in meters per second.

(v is positive when the transmitter and receiver move towards one another and negative when they move away from each other)

c is the speed of the wave (3×10^8 m/s for electromagnetic waves traveling in air or a vacuum)

Δf is the Doppler frequency shift.

This equation assumes that we are using radio frequencies that propagate at the speed of light, and that the relative velocities of the transmitter and receiver are a small percentage of the speed of light. These are good assumptions for the applications I had in mind.

What kind of frequency shift can we expect for 23 cm signals? For a velocity $v = 25$ m/s — which is about 56 mph — a frequency shift of 108 Hz should result. Is this enough shift? Do we need higher speeds? Do we need higher frequencies? Frequency stability ultimately determines the frequency resolution and thus velocity resolution of the measurement. It turns out 100 Hz is enough shift for short-term — 1 minute or less — measurements. At 1200 MHz, 100 Hz corresponds to a stability of 0.08 parts per million (ppm). Modern transceivers, particularly those designed for SSB and CW, have stability specifications of at least 3 ppm. For example, my older IC-1271 has a stability

¹Notes appear on page 37.

of 3 ppm, and a newer transceiver like the IC-9500 has 0.05 ppm stability. I have found the short-term stability, particularly when the temperature is constant, is much better than the specified values. The specified values assume long-term measurements over a 50°C temperature range.

Hardware and Software

Figure 1 shows a simple experiment. The transmitter and receiver are close enough so the receiver can hear the transmitter at the low desired power levels. The car can be driven away from the receiver for one test and toward the receiver for another test. We need a receiver with SSB capability because we are basically tracking the tone produced in the receiver as it hears the unmodulated carrier from the transmitter. This is the same tone you hear when you listen to someone tune their transmitter. The bandwidth of most SSB receivers can handle the expected velocities and corresponding Doppler frequency shifts. For example a 2.4 kHz bandwidth, typical for an SSB receiver, would allow velocities as great as 581 m/s at 23 cm. Incidentally, Mach 1 (the speed of sound) is 340 m/s at 15°C. I used the previously mentioned IC-1271 for the receiver, but any modern day 23 cm multimode receiver or transceiver would suffice.

The transmitter was custom built, but only because I had some specialized requirements. The transmitter needs only to generate a CW carrier of reasonable spectral purity and low drift. This is fairly easy to accomplish with modern phase-locked-loop circuits and crystal oscillators. The transmitter consists of a crystal reference oscillator, a PLL chip with self contained EEPROM, and a power amplifier chip. Size (23 mm × 100 mm) and power supplied <10 mW are low and allow use of small, lightweight batteries. Figure 2 shows a picture of the transmitter as well as the schematic. Cost, in case the transmitter is lost or destroyed, is low (about \$35). The total transmitter weight is 1 oz, including batteries. If the transmitter platform is larger, such as an automobile for example, a larger and heavier transmitter can be tolerated.

I was concerned about transmitter stability under acceleration, particularly the G forces on the 32 MHz crystal oscillator that is the reference for the PLL transmitter. The data from the actual launches, however, looked very similar to predicted velocity profiles from computer programs such as *RockSim*.³ My conclusion was that G forces and short term temperature effects were not enough of an issue to use more sophisticated reference schemes.

A key requirement for analyzing the

Doppler data is a computer program that can measure frequency versus time. This is called a spectrogram. I used a shareware computer program, in fact, called *Spectrogram* to both record as well as analyze the data.⁴ This program runs on either a PC laptop or desktop and makes use of the sound card for audio input. The program allows for adjustments of the time window and maximum and minimum frequencies of the spectrogram. The data displayed on the screen can simultaneously be stored to a file by selection with a pull-down menu and a mouse driven record on-off feature. *Spectrogram* also allows replaying or analysis of the previously recorded files. There are probably other programs that can perform this task but I found *Spectrogram* met all my needs.

Procedure for Taking and Analyzing Data

The hardware and software setup for all the applications is as follows:

- 1) Turn on the transmitter.
- 2) Turn on the receiver.

3) Tune the receiver VFO until the transmitter is making a pleasant tone somewhere between 800 and 1500 Hz. The frequency of this tone is arbitrary. This is just like tuning in your favorite CW signal.

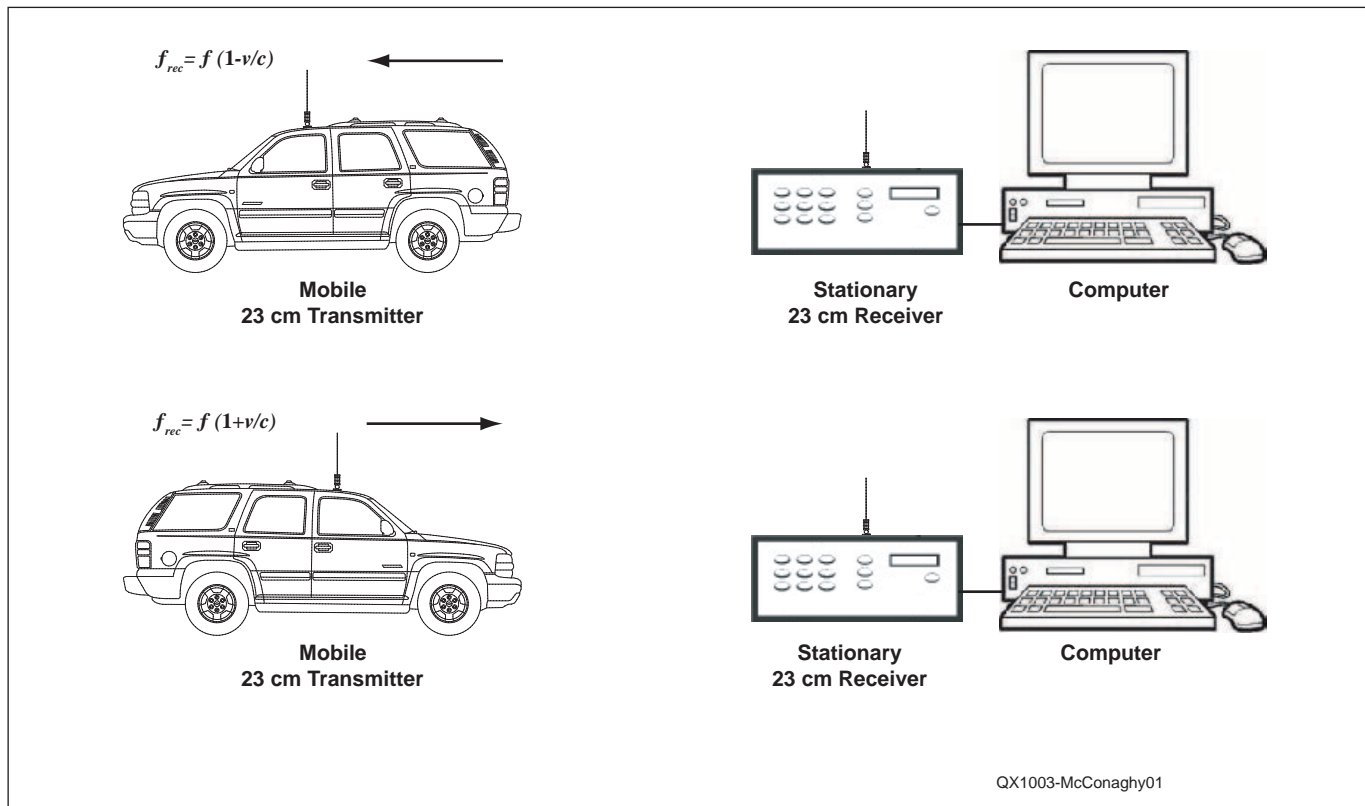
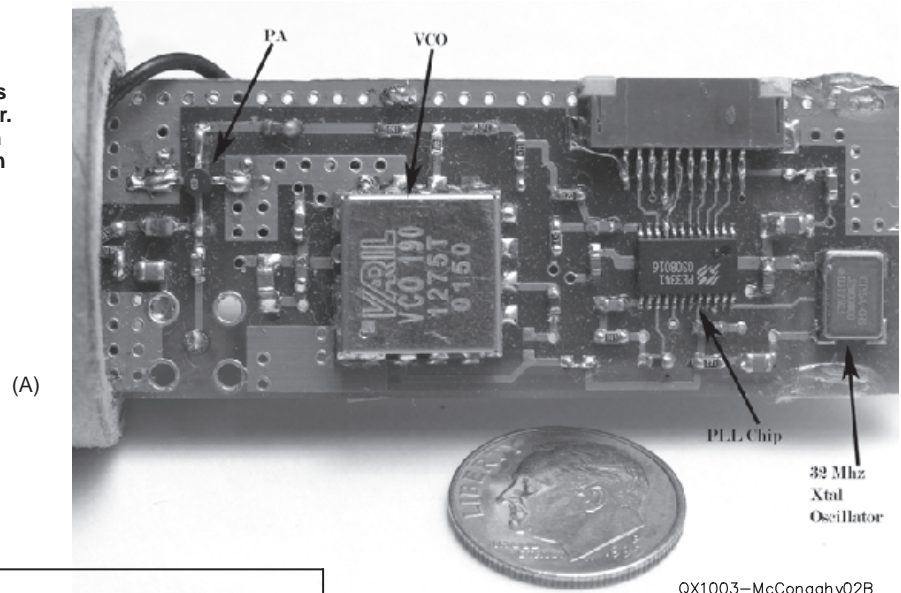


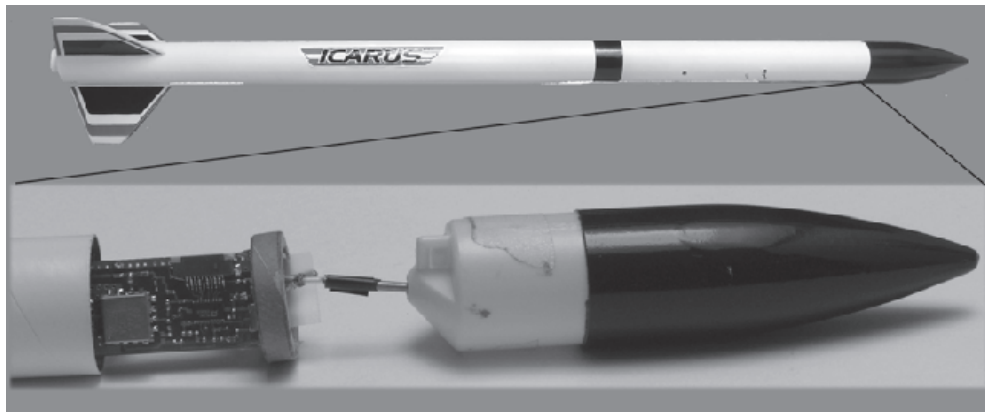
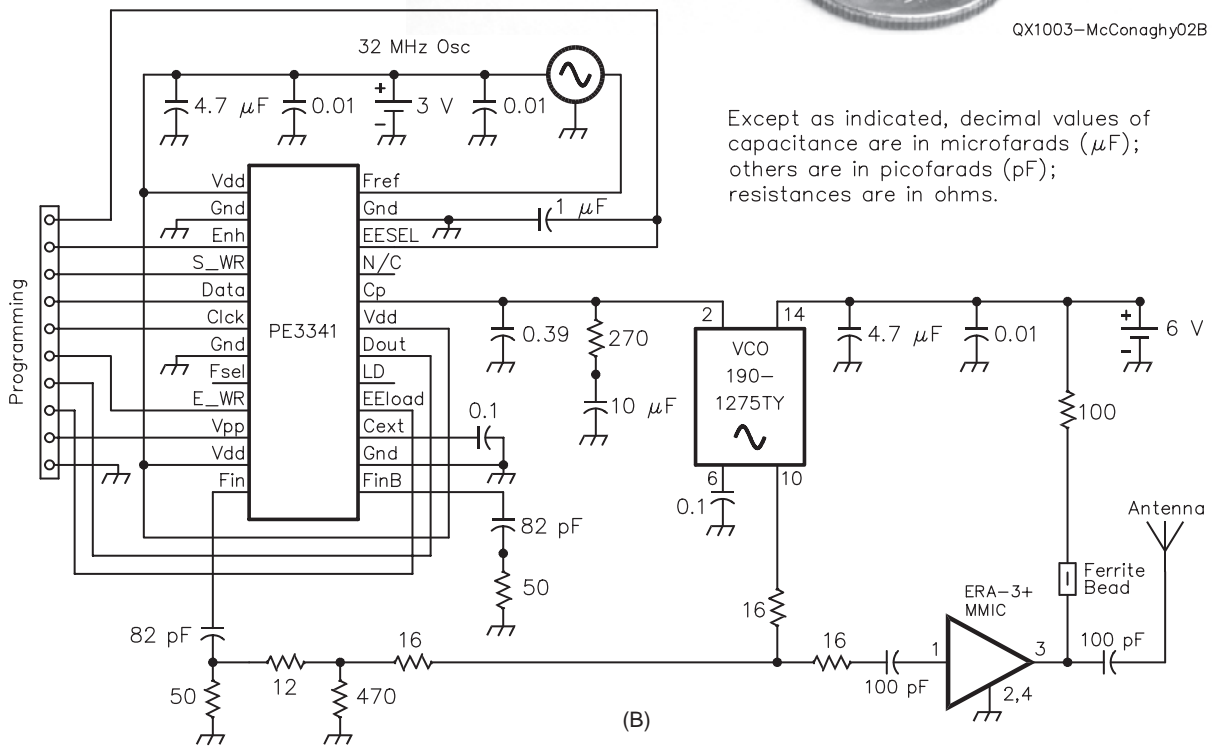
Figure 1 — Drawing showing mobile transmitter moving away from (top) or toward (bottom) a fixed receiver.

Figure 2 — Part A shows the transmitter circuit board, and Part B is a schematic diagram of the transmitter. Part C shows a model rocket, with an expanded photo showing the location of the transmitter board



QX1003-McConaghy02B

Except as indicated, decimal values of capacitance are in microfarads (μF); others are in picofarads (pF); resistances are in ohms.



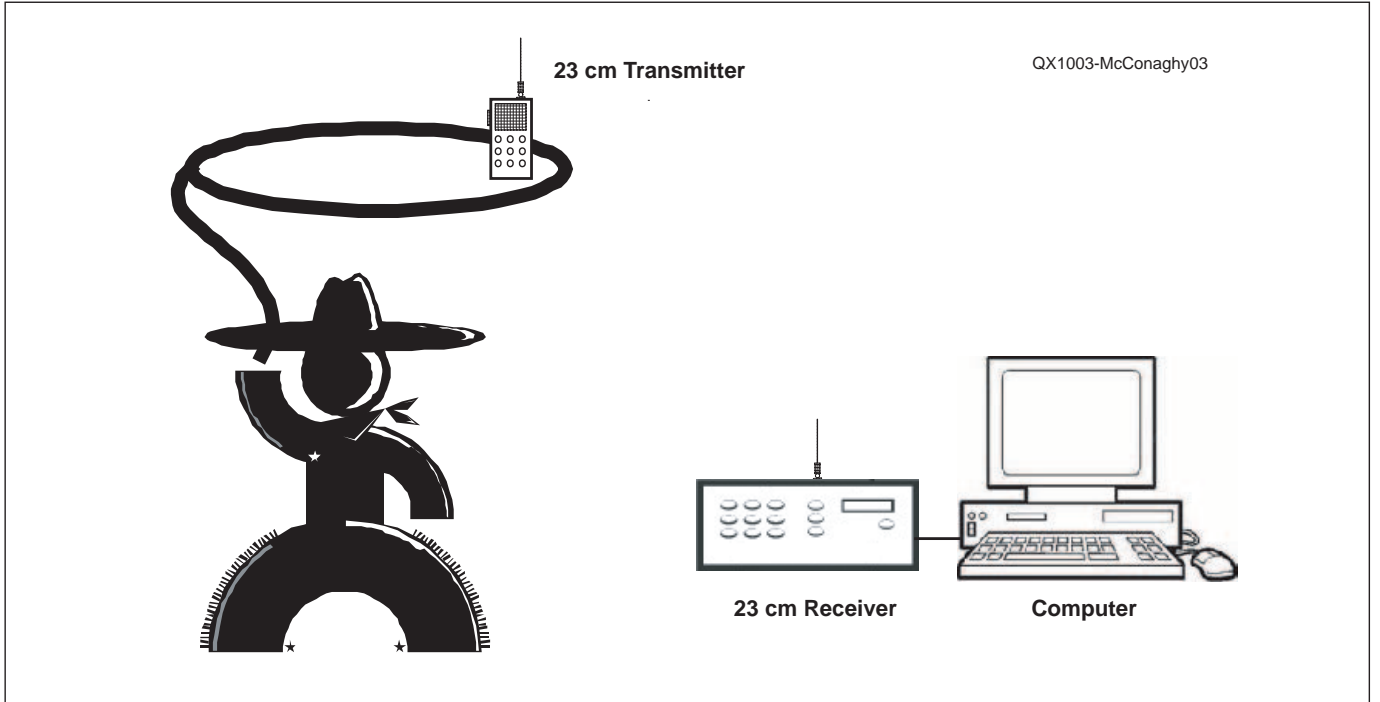


Figure 3 — This drawing shows a transmitter spinning on the end of a lasso.

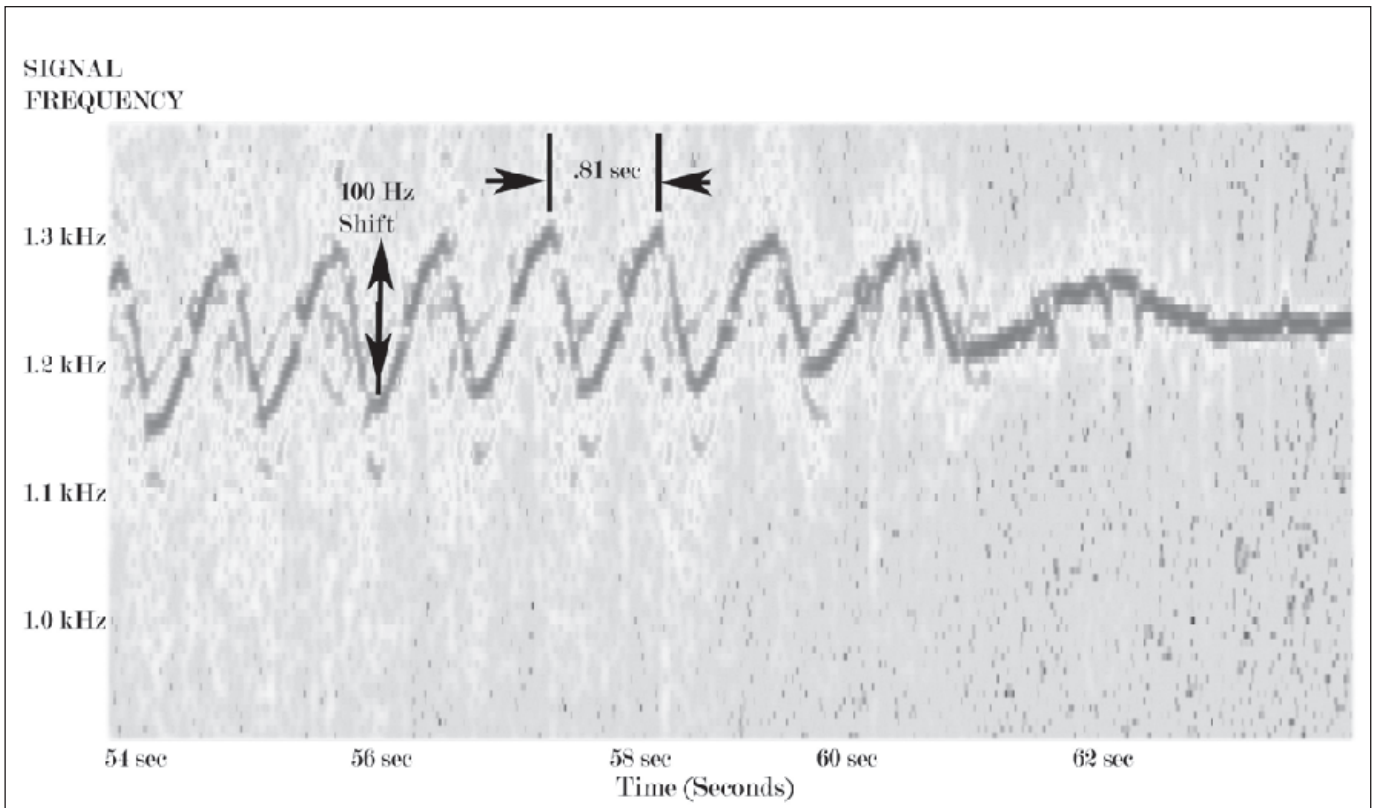


Figure 4 — This spectrogram shows the data for the example of Figure 3. You can measure the rotation period of 0.81 s over most of the waveform, with a peak to peak Doppler shift near 100 Hz. This corresponds to a velocity of 11 m/s.

4) Start the Spectrogram software and you will see it displaying a horizontal line at the frequency of the tuned tone. There may be some drift to this line if the transmitter is drifting.

The analysis of the data requires establishing a reference line, that is, a frequency when the object being measured is standing still. This frequency is arbitrary and just needs to be in the audio pass-band of both the receiver as well as the computer sound card. What we are interested in is the frequency changes from this reference value. For example, the baseline value in Figure 7 was 1382 Hz. Everything is referenced to this baseline value. The peak frequency is 1703 Hz. The difference between peak and baseline is 321 Hz. The conversion to velocity is done using Equation 1, $f_{rec} = f(1+v/c)$, which can be simplified to

$$v = c \times \Delta f / f \quad [\text{Eq 2}]$$

for small Doppler shifts in comparison to the radio frequency. For a 1260 MHz RF signal:

$$v = \Delta f \times 0.238 \text{ m/s} \quad [\text{Eq 3}]$$

Applications

As previously mentioned, my original motivation came from tracking rockets but my first proof of principle experiment

involved putting the transmitter at the end of a 5 foot long string and swinging the transmitter in a circular pattern above my head, much like a cowboy about to rope a steer. For this test, the receiver is located several feet outside and away from the circular trajectory of the transmitter. In fact, the receiver can be located as far away from the transmitter as signal levels will permit and the same spectrogram will result. Figure 3 shows this arrangement. Swinging the transmitter in a circle results in a Doppler frequency increase as the transmitter moves toward the receiver and then a Doppler frequency decrease as the transmitter moves away from the receiver. This produces a roughly sinusoidal pattern, which repeats for every circle the transmitter traces out. The faster you swing the transmitter, the greater the Doppler shift.

The data I collected in this experiment is shown in Figure 4. It is possible to interpret the rotation period as 0.81 s, the frequency shift as 100 Hz, or about 50 Hz positive as the transmitter moves toward the receiver and 50 Hz negative as the transmitter moves away from the receiver. Finally, the velocity from the Doppler data is about 11 m/s. For a 5 ft (1.5 m) rope and a 0.84 s period, we can verify by calculation that the frequency shift is ± 50 Hz. The same effect could also be

achieved with the transmitter at a fixed location and swinging the antenna. The antenna is located at the end of a coaxial cable tether. In fact, the latter is the basis of a popular direction finding (DF) antenna, but in the DF Doppler antenna, rotation is accomplished using electronic switching rather than mechanical motion as was done here.⁵

A second application I tried was to have the receiver and receive antenna at a fixed location on the side of a road and to mount the transmitter inside a vehicle as shown in Figure 1. I then drove the vehicle, initially located several hundred feet from the receiver, at a constant velocity, say 60 mph, toward the receiver and continued on at this constant velocity several hundred feet down the road past the receiver. When the vehicle is at zero velocity there is no frequency shift. Upon accelerating to 60 mph, however, and then remaining at this velocity there is a positive frequency shift (from the zero velocity frequency). As the vehicle passes the receiver, the received signal makes an abrupt drop in frequency to a new frequency that is negative (below the zero velocity frequency) because now the vehicle has passed the receiver and is moving away from it. Figure 5 shows the spectrogram for this data. The velocity doesn't have to be constant and

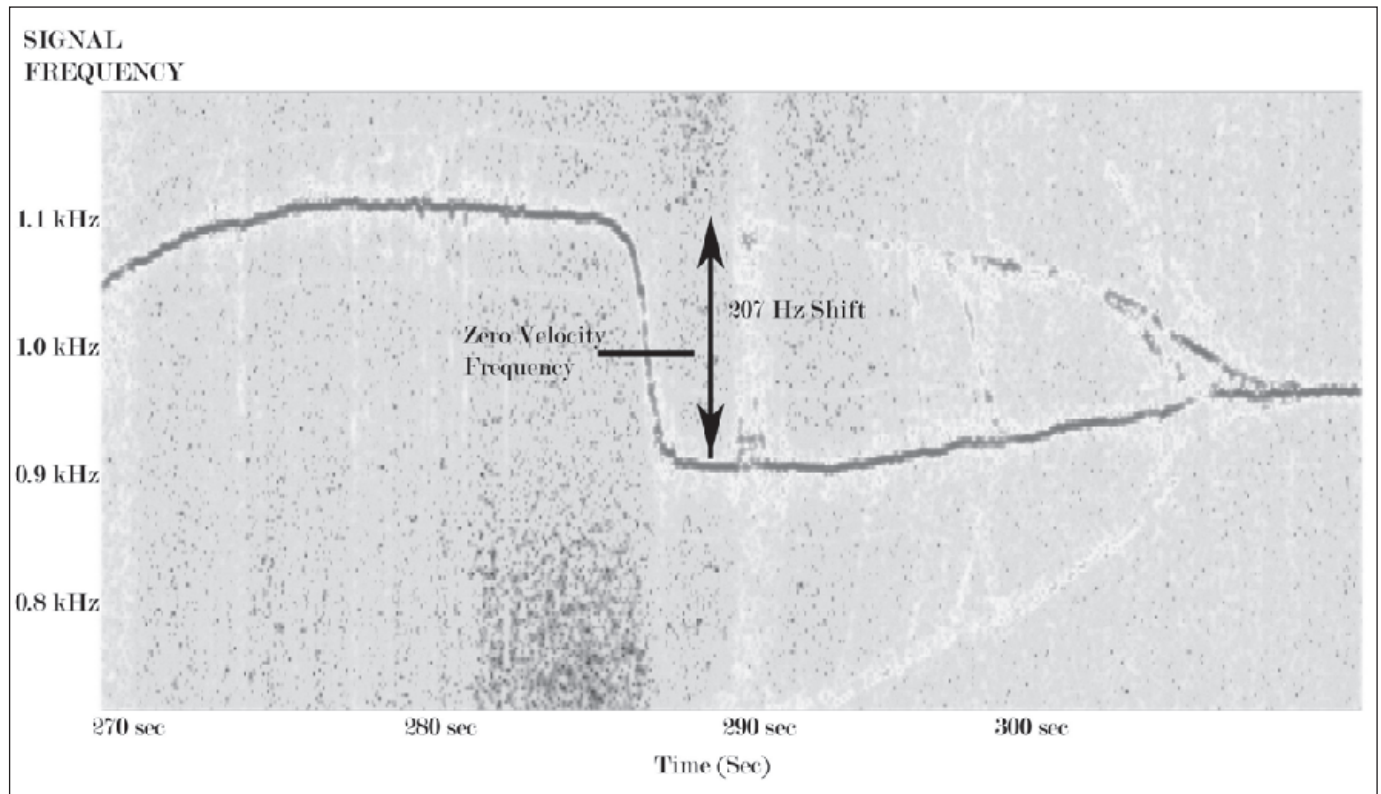


Figure 5 — This spectrogram shows data for the moving car experiment. The transmitter is in car moving past the receiver at near constant velocity after an initial acceleration. The abrupt frequency change is 207 Hz. The velocity of the car is 24 m/s (55 mph). The frequency change is twice the Doppler shift, since it goes from positive to negative as the car passes the receiver. You can also see a region of deceleration as the car slows down after passing the receiver.

definitely is not during the acceleration and braking portions. The spectrogram provides a direct readout of the velocity profile. This might be useful for telling how long it takes to brake a vehicle as well as how fast a vehicle might go from 0 to 60 mph.

The third application is model rocketry tracking, which most definitely uses a variable velocity profile. From this profile such things as fuel burnout time, peak velocity, altitude and time to the ejection charge can be directly observed. Since I began this work several years back and in the intervening years a number of manufacturers have come up with on-board data recorders that use MEMS sensors to measure both acceleration and atmospheric pressure to come up with these same parameters. Although these on board measurement units work fine, they are more complex than a simple transmitter, and also do not have real-time readout. Some of them do have additional telemetry transmitters. Again my goal was to keep the on-board electronics portion simple and inexpensive.

In rocketry, the Doppler frequency shift is always downward upon liftoff. This of course assumes the rocket is moving away from the receiver as shown in Figure 6. If it isn't, that is a completely different problem since I normally locate the receive antenna near the launch pad. If the ejection charge occurs at

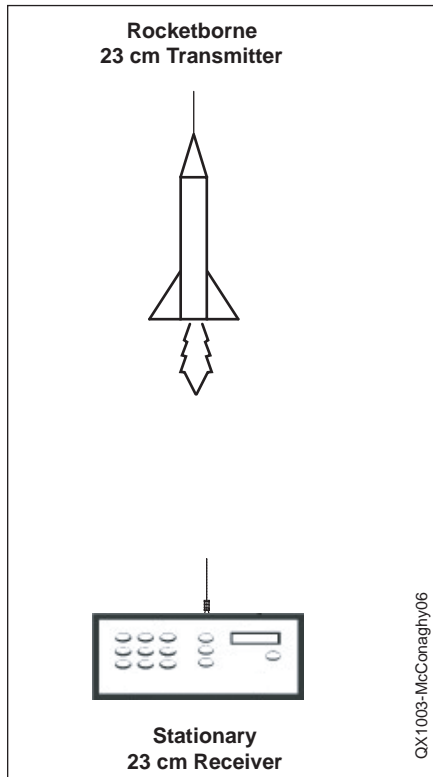


Figure 6 — Here is a drawing that shows the model rocketry application. The transmitter in the rocket is moving away from the receiver, which is on the ground.

or before apogee, the frequency shift will be negative through the entire flight. In general there isn't enough resolution to measure the positive velocity seen as the rocket slowly descends back under a parachute. Of course if the rocket comes in ballistic, that would easily be visible on the spectrogram.

Some of the data I took showed a positive frequency shift upon launch but that was only from accidentally using the LSB (lower sideband) selection on the receiver rather than the USB (upper sideband) selection. The LSB selection causes a frequency inversion of the data.

Figure 7 shows the spectrogram for a single stage rocket. The maximum frequency change is 321 Hz, which corresponds to the peak velocity of 76.4 m/s (171 mph). From the peak velocity, which occurs just as the engine burns out, there is a gradual decrease in velocity to a 74 Hz frequency change which corresponds to 17.6 m/s (39 mph). At this point an ejection charge goes off slowing the rocket to near zero frequency shift. The ejection occurred fairly close to apogee, as the rocket was approaching zero velocity.

The spectrogram for a two stage rocket is shown in Figure 8. From this spectrogram, we can determine that the first stage burned for 1.5 s with a Doppler shift of 119 Hz, corresponding to a speed of 28.3 m/s (63.4 mph)

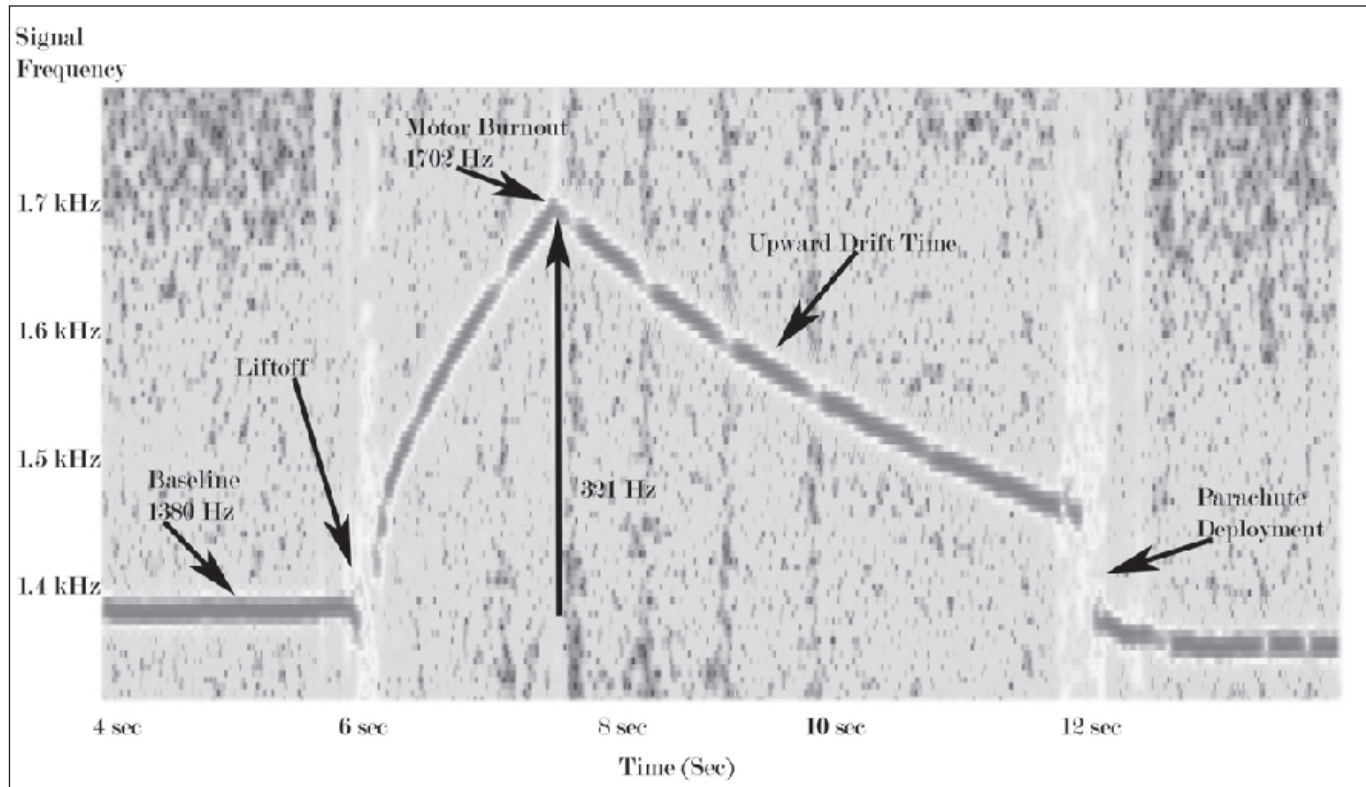


Figure 7 — Here is a spectrogram showing the data for a single stage rocket. The transmitter is on a rocket. The maximum frequency change is 321 Hz and corresponds to a peak velocity of 76.4 m/s (171 mph), at which point the engine shuts down and the velocity slows down to 17.6 m/s (39 mph) as indicated by only a 74 Hz Doppler shift. At 5.6 s after launch the ejection charge fires slowing the velocity back to the baseline. When the rocket is dropping safely under a parachute, there will be little Doppler shift.

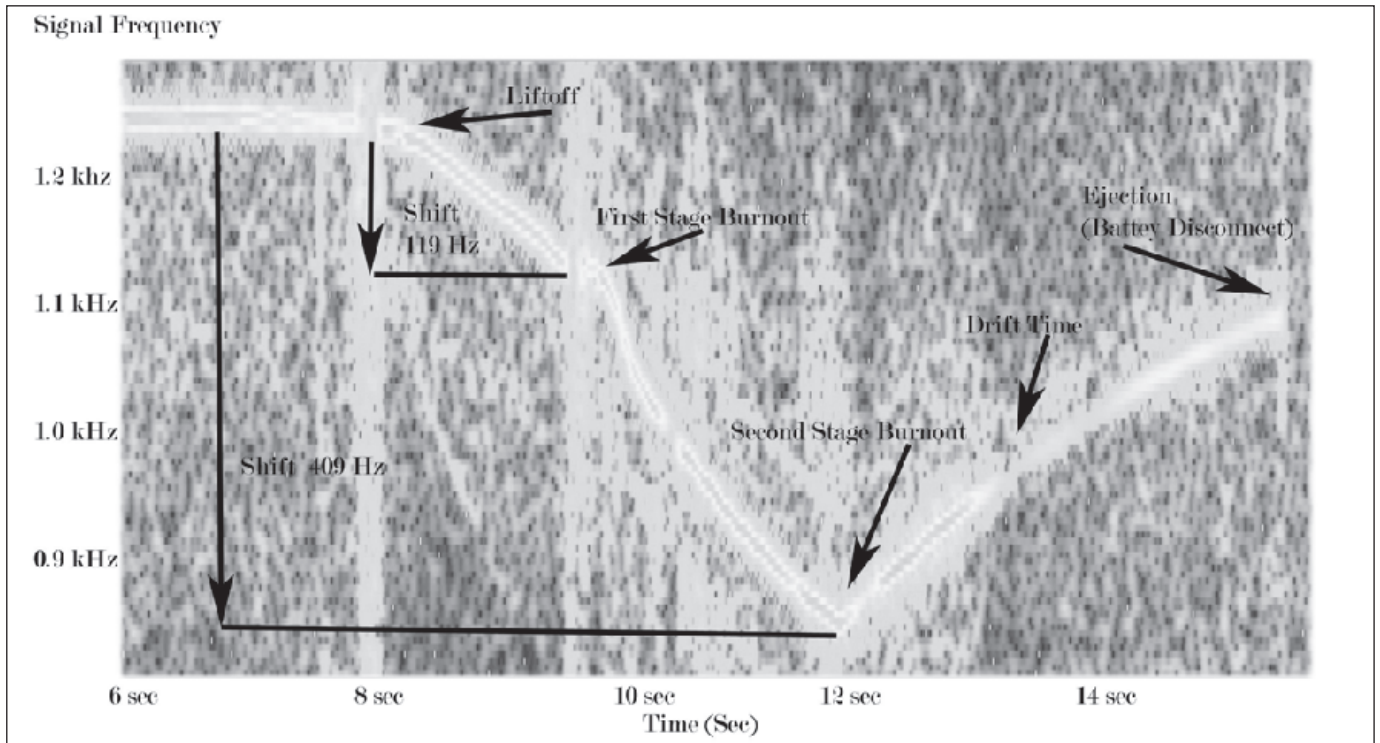


Figure 8 — This spectrogram shows the data for a two stage rocket. The transmitter is on a two stage rocket. The first stage burns for 1.5 s and at this point the Doppler shift is 119 Hz or 28.3 m/s (63.4 mph). The second stage burns for an additional 2.5 s, at which point the Doppler shift is 409 Hz or 97.3 m/s (218 mph) at this point all the fuel is burned and a slow down occurs for an additional 3.4 s, at which time the Doppler shift is 160 Hz or 38 m/s (85.2 mph) . At this point the ejection charge fired but shook the battery connection disabling the RF transmitter

at the end of first stage burnout. Further, the spectrogram shows the second stage burned for an additional 2.5 s with a Doppler shift of 409 Hz, which corresponds to a speed of 97.3 m/s (218 mph) before the second stage fuel was fully burned. After that, a gradual decrease in speed is observed for an additional 3.4 s, at which time the ejection charge fired but shook the battery connection, disabling the RF transmitter. Just prior to the ejection, the rocket was still traveling upward at a speed of 38 m/s (85.2 mph) as evidenced by the Doppler shift of 160 Hz.

Further analysis of the velocity curves can produce altitude data, or more generally, distance data. This is accomplished by integrating the data shown in Figures 7 and 8 with a simple Microsoft Excel spreadsheet. The altitude plots are shown in Figures 9 and 10. A peak altitude of 250 m (820 ft) is achieved by the single stage flight and a peak altitude of 370 m (1213 ft) is achieved by the two stage flight.

Summary

The Doppler effect can be used by hams to make speed measurements of cars, swinging transmitters, rockets and other moving platforms. By separating the transmitter and receiver, using readily available computers and software, these measurements can be

performed by hams with off-the-shelf radios and lower power levels. It is a lot less complex than you might normally expect for a “Doppler radar” system.

Acknowledgements

I would like to thank both Asher Blum and Rick Schnetz, WA6RAI, for taking time

to read this article and for making suggestions to clarify the content.

Chuck McConaghy, WA6SYE, has been a ham since 1971, when he was originally licensed as WN9IBX. He currently holds an Advanced class license. Over the years, Chuck’s Amateur Radio activities have included UHF repeater construction, ATV, amateur satellites

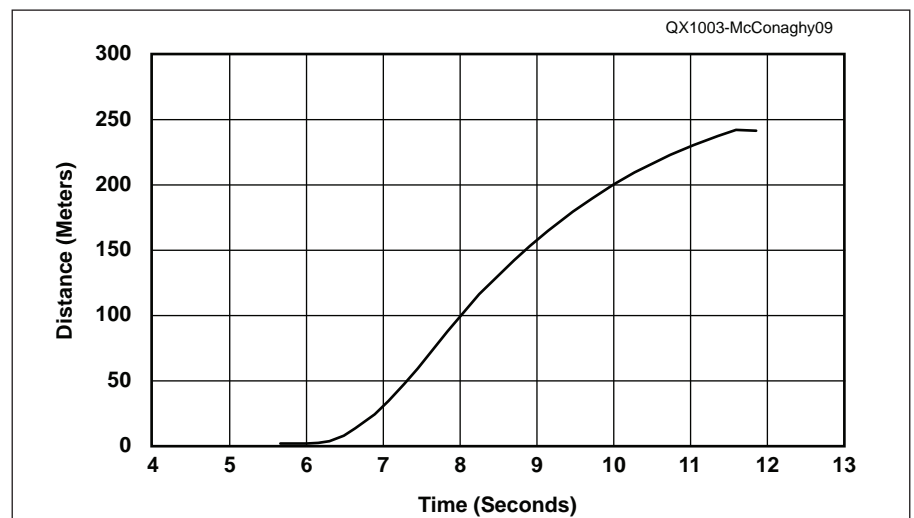


Figure 9 — This data is produced by integrating Figure 7. It shows that a peak altitude of just near 250 meters (820 ft) occurs at the 12 s point. (The launch began at the 6 s point)

and PSK31. He retired in 2007 after 35 years at Lawrence Livermore National Laboratory, where he worked on everything from high speed X-ray diagnostics, integrated optics, ASIC design and MEMS sensors. He holds a BSEE degree from Purdue University and an MSEE degree from Stanford University.

Notes

¹For more information about the Doppler effect, see: [//en.wikipedia.org/wiki/Doppler_effect](http://en.wikipedia.org/wiki/Doppler_effect).

²There is more information about the DARTS

project at www.hamhud.net/darts.

³For information about the RockSim software and other model rocketry information and supplies, see: www.apogeerockets.com

⁴You can obtain more information and download a 10-day trial version of the Spectrogram software at the Visualizations Software Web site at: www.visualizationsoftware.com/gram.html (At press time this Web site was listed as "Under Construction." You can also download an older version (5.17) of the Spectrogram software free at: www.dxzone.com/cgi-bin/dir/jump2.cgi?ID=2056.

⁵Terrence Rogers WA4BVY, "A DoppleScAnt," QST, May 1978, pp 24-28.

We Design And Manufacture To Meet Your Requirements

**Prototype or Production Quantities*

800-522-2253

This Number May Not Save Your Life...

But it could make it a lot easier! Especially when it comes to ordering non-standard connectors.

RF/MICROWAVE CONNECTORS, CABLES AND ASSEMBLIES

- Specials our specialty. Virtually any SMA, N, TNC, HN, LC, RP, BNC, SMB, or SMC delivered in 2-4 weeks.
- Cross reference library to all major manufacturers.
- Experts in supplying "hard to get" RF connectors.
- Our adapters can satisfy virtually any combination of requirements between series.
- Extensive inventory of passive RF/Microwave components including attenuators, terminations and dividers.
- No minimum order.



NEMAL ELECTRONICS INTERNATIONAL, INC.
 12240 N.E. 14TH AVENUE
 NORTH MIAMI, FL 33161
 TEL: 305-899-0900 • FAX: 305-895-8178
 E-MAIL: INFO@NEMAL.COM
 BRASIL: (011) 5535-2368

URL: WWW.NEMAL.COM

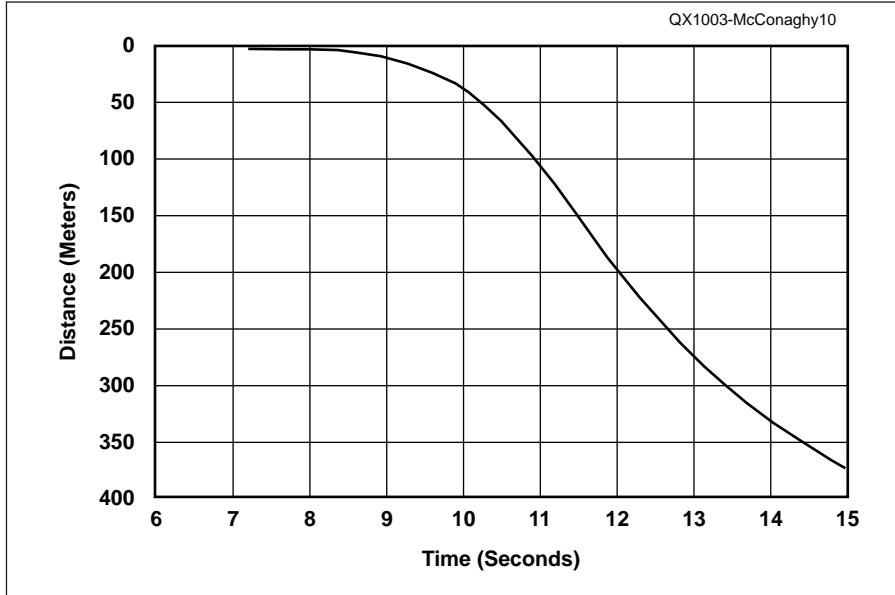


Figure 10 — This data is produced by integrating Figure 8. It shows that a peak altitude of just near 370 meters (1200 ft) occurs at the 15 s point. (The launch began at the 8 s point)



On Maximizing the Tuning Range of SA/NE 602 IC Colpitts Oscillators

This article reports the results of a theoretical and experimental investigation of SA/NE 602 Colpitts oscillator circuits for application at MF, HF, and VHF.

A number of years ago I embarked on the project of designing an experimental AM superheterodyne (superhet) radio receiver using the SA/NE 602 IC as the front end. One of the most challenging tasks involved designing a local oscillator (LO) that would tune over the 2.17:1 frequency range (995 kHz to 2155 kHz) required to receive the entire AM band (540 kHz to 1700 kHz). I found the oscillator design information provided in the manufacturer's application notes so sketchy that it provided little assistance in completing this task. The article that follows is my attempt to place the design of SA/NE 602 Colpitts oscillator circuits on a more rigorous foundation.

This article will first review the operating principle of the Colpitts oscillator circuit. Next, we will derive the small signal model for the oscillator in order to determine the conditions required to begin oscillations. The equations resulting from this model provide a quantitative basis for analysis and design of Colpitts oscillator circuits. Finally, we will compare the results of theoretical predictions and oscillator measurements for three Colpitts oscillator circuits constructed to operate in the MF, HF and VHF bands.

Colpitts Oscillator Circuit

Figure 1 depicts a Colpitts oscillator circuit similar to that shown in Figure 2 of AN1982, *Applying the Oscillator of the NE602 in Low Power Mixer Applications*, the application note produced by Signetics.¹ In order to broaden the analysis so that it also applies to a tuned transformer, the circuit in Figure 1 includes a coupled inductor with

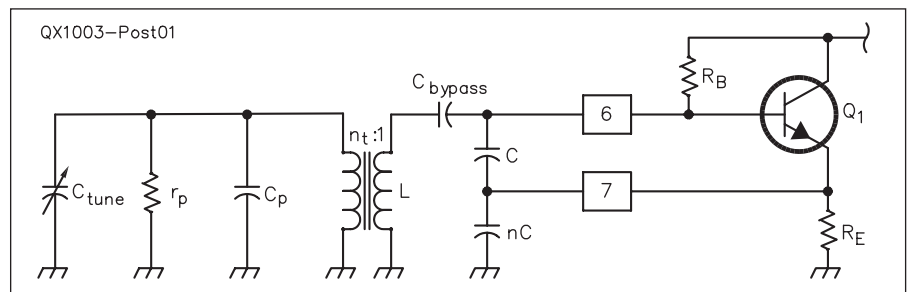


Figure 1 — A typical design applying the SA/NE 602 IC as a Colpitts oscillator. Capacitor C_{bypass} is selected so that is a short at the frequency of oscillation. (Note that the blocks labeled 6 and 7 represent connections to those pins of the IC. Connection to V_{cc} (pin 8) and ground (pin 3) are not shown in this figure, but are also required.)

a turns ratio of $n_t:1$, as well as a resistor r_p and capacitor C_p that account for the finite Q and self-resonant frequency of all practical inductors and transformers. It is possible to eliminate the transformer by reflecting the components connected to the transformer primary into the secondary as shown in Figure 2. Doing so decreases the inductance L and the resistance r_p by the square of the turns ratio while increasing the total capacitance $C_{\text{tune}} + C_p$ by the square of the turns ratio. The resonant frequency of the LC tank is unchanged, however, because the turns ratio n_t cancels out when taking the product of L and C .

Neglecting C_p for the moment, the tuning range of the LC tank is set by the square root of the maximum value of C_{tune} divided by the minimum value of C_{tune} . For example in the case of an AM radio LO, a typical oscillator tuning capacitor might have maximum and minimum C_{tune} values of 60 pF and 10 pF, which implies a tuning range of 2.45:1 — just adequate to cover the entire AM band. Any additional capacitance that is connected

across the tank, for example, C_p , adds a greater proportional amount to the minimum value of C_{tune} compared to what is added to the maximum value of C_{tune} , thus reducing the tuning range.

It is well known that in order for oscillations to begin, the gain around the oscillator's feedback loop, the so-called "loop gain", must be greater than unity at a frequency where the phase shift is 0° , or some integral multiple of 360° , so that the feedback signal constructively reinforces the initial signal. For the Colpitts oscillator in Figure 2, Q_1 is connected as an emitter follower (common collector) amplifier, which has a voltage gain less than unity and a phase shift of 0° . This implies that the feedback network shown on the left side of the drawing must have sufficient voltage gain in order to overcome this loss, along with a phase shift of 0° so that the feedback signal reinforces the original signal. The feedback network for the Colpitts oscillator consists of a capacitive voltage booster (in other words, a capacitive volt-

¹Notes appear on page 42.

age divider operated backwards) so that the amplitude of the signal at the transistor emitter is boosted before it appears at the transistor base. The capacitive voltage booster is formed by the series connection of capacitors C and nC . Here n is some positive number in order to facilitate the circuit analysis. The series equivalent of C and nC appears in parallel with the LC tank, which serves to reduce the oscillator's tuning range for the same reason discussed previously for C_p .

Maximizing the tuning range of the oscillator requires understanding the following conundrum: In order for the series connected capacitors to act as a voltage booster their reactances at the low end of the tuning range should be small compared with the resistances that load them — which implies a relatively larger value of series capacitance. But, in order to maximize the oscillator's tuning range the voltage booster capacitors should be made small in comparison with the minimum value of C_{tune} — which implies a relatively smaller value of capacitance. The essence of the design problem then is to achieve an acceptable tradeoff between these two competing requirements. This allows us to maximize the tuning range of the oscillator while simultaneously achieving a loop gain greater than unity in order to sustain oscillations.

Now that the Colpitts oscillator has been discussed qualitatively, the next step is circuit analysis in order to develop a quantitative basis for understanding the tradeoffs discussed above. This is shown in Appendix 1, in which the technique of node voltage analysis is applied in order to solve for the loop gain. From this result it is possible to determine the frequency where the loop gain is greater than unity with the correct phase, which implies that the circuit will start to oscillate.

In order to illustrate these concepts, an LO for an AM superhet receiver will be designed using the component values given in Table 1. In this case the coupled inductor is the ubiquitous "red can" commonly used as a tuned transformer in AM superhet LOs. The variable capacitor in this case is a small trimmer capacitor with capacitance ranging between 6.8 pF (minimum) and 45 pF (maximum), which substitutes for the oscillator tuning capacitor.

First, the values in Table 1 are evaluated using Equations A.8 through A.11, with $n = 0.5, 1, \text{ and } 2$ in order to find the divider capacitance, C , to achieve loop gains of $A_v = 0.9, 1.0, \text{ and } 1.1$,

Table 1
Component Values for AM Superhet LO.

Component	Value
L	500 μH
n_t	11
C_{tune}	6.8 – 45 pF
r_p	300 k Ω
C_p	3.6 pF

Table 2
Value of Voltage Booster Capacitor C Required to Achieve Loop Gains of $A_v = 0.9, 1.0, \text{ and } 1.1 \text{ V/V}$ with $n = 0.5, 1, \text{ and } 2$ at the Low-Frequency End of the Range ($C_{tune} = 45 \text{ pF}$).

n	$A_v = 0.9 \text{ V/V}$	$A_v = 1.0 \text{ V/V}$	$A_v = 1.1 \text{ V/V}$
0.5	409 pF	489 pF	605 pF
1.0	301 pF	340 pF	386 pF
2.0	221 pF	243 pF	267 pF

and 1.1 V/V at the low-frequency end of the range ($C_{tune} = 45 \text{ pF}$). These results are shown in Table 2. Table 2 clearly demonstrates that larger values of both the capacitance, C , and the divider ratio, n , increase the loop gain, A_v , at a given frequency of oscillation.

Once the value of capacitance C is found for a given minimum loop gain, A_v , and divider ratio, n , it is possible to plot the loop

gain, A_v , as the tuning capacitance, C_{tune} , is varied from maximum to minimum. Figure 3 shows this result for the nine values of capacitance, C , listed in Table 2. Additionally, Equation A.5 has been used so that in the figure the loop gain is plotted versus the oscillation frequency instead of versus the tuning capacitance. The figure shows that the loop gains all begin at either $A_v = 0.9, 1.0, \text{ or } 1.1 \text{ V/V}$ at the low-frequency end of the range and rise monotonically, but relatively slowly, with steeper slopes for larger values of the divider factor, n .

Consider the three curves that begin at $A_v = 1.0$. The curves all begin at almost the same point and have about the same tuning range for any choice of divider ratio, n . For this reason there is little advantage to choosing a divider ratio n other than unity in this case.

It is important to note that under any condition the minimum loop gain occurs at the low-

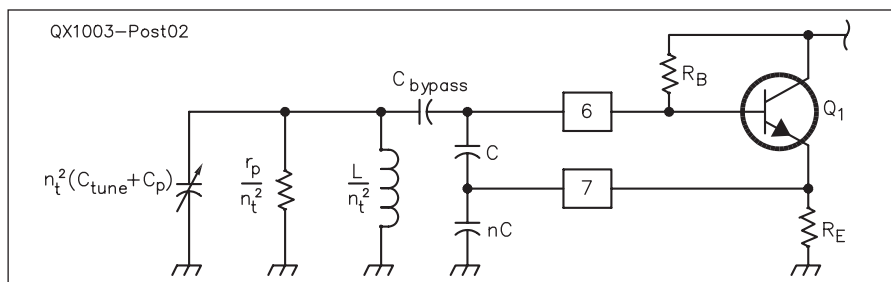


Figure 2 — The SA/NE 602 Colpitts oscillator circuit after reflecting components connected to the secondary of the transformer into the primary circuit of the transformer. (Note that the blocks labeled 6 and 7 represent connections to those pins of the IC. Connection to V_{cc} (pin 8) and ground (pin 3) are not shown in this figure, but are also required.)

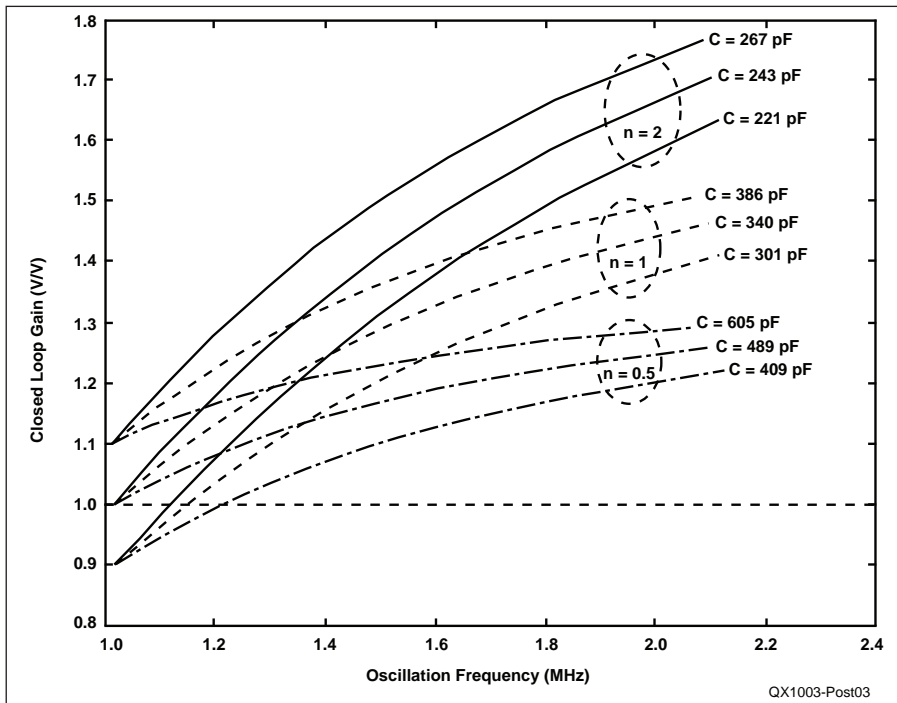


Figure 3 — Plot of Colpitts oscillator loop gain $A_v = 0.9, 1.0, \text{ and } 1.1 \text{ V/V}$ versus frequency of oscillation for $n = 0.5, 1 \text{ and } 2$ using values of capacitance C as shown. Note the slight variation in tuning range for any choice of n or C .

Table 3**Predicted and Measured Results for the MF Colpitts Oscillator Constructed Using the Components Listed in Table 1.**

<i>C</i> (pF)	<i>A_v</i> (V/V)	Predicted		Measured				Error
		<i>f_{low}</i> (MHz)	<i>f_{high}</i> (MHz)	<i>TR</i> (MHz)	<i>f_{low}</i> (MHz)	<i>f_{high}</i> (MHz)	<i>TR</i> (MHz)	<i>TR error</i> (%)
340	1.00	1.0184	2.0959	1.0775	1.195	1.930	0.735	31.8
373	1.07	1.0160	2.0818	1.0659	1.051	1.916	0.865	18.8
426	1.17	1.0124	2.0603	1.0479	0.929	1.900	0.971	7.34
470	1.24	1.0097	2.0433	1.0336	0.925	1.890	0.965	6.64
556	1.34	1.0049	2.0119	1.0070	0.920	1.860	0.940	6.65
800	1.50	0.9929	1.9322	0.9393	0.908	1.80	0.892	5.04

frequency end of the oscillator's tuning range. This effect may cause several practical problems. First of all, if *C* is undersized for any choice of the divider ratio *n*, the bottom curves in Figure 3 show that the loop gain will fall below unity at the lower end of the frequency range and oscillations cannot occur. Another phenomenon results from the fact that for practical oscillators, the loop gain required to sustain oscillations once they have begun is slightly smaller than that required for oscillations to begin in the first place. Because of this, if the loop gain is just greater than unity at the lowest frequency of oscillation, it is possible to start the oscillator at the high frequency end of the tuning range and tune to the low frequency end of the tuning range while maintaining oscillation. But the oscillator will not start if it is switched on at the low frequency end of the tuning range until it is tuned above the starting frequency. The solution for this problem is to design for sufficient loop gain at the low frequency end of the tuning range, so that the starting frequency is below the lowest frequency in the tuning range.

Experimental Results

In order to validate the theoretical analysis just presented, I constructed SA/NE 602 Colpitts oscillators for operation in the MF, HF and VHF bands according to the design in Figure 1. See Figure 4. Prior to construction, each inductor was characterized to determine *L*, *n*, *C_p*, and *r_f* using the impedance measurement capability of an HP4195A network/spectrum analyzer. Next, capacitors were measured for the voltage boosting capacitance *C* and the resulting loop gain, *A_v*, calculated from Equation A.6. Then the tuning range was calculated according to Equation A.5. Finally, the spectrum analysis capability of an HP4195A network/spectrum analyzer was employed along with the HP 41800A active probe to measure the oscillation frequency after power was applied to the circuit, to measure the lowest (*f_{low}*) and highest (*f_{high}*) oscillation frequencies for each circuit.

A direct connection of the probe to the oscillator circuit was not necessary because the signal power produced by the oscillators was sufficient that placing the probe adjacent to the circuit provided adequate signal level

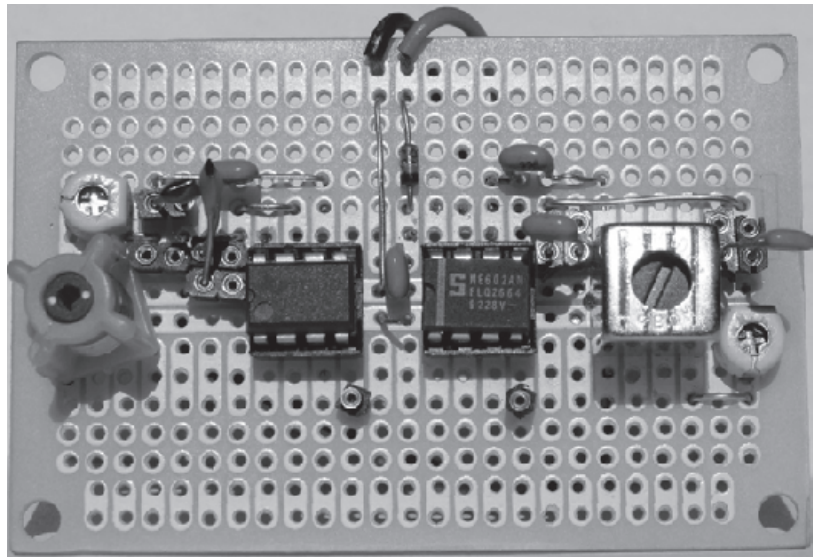


Figure 4 — Experimental Colpitts oscillator circuits designed after Figure 1. The oscillator on the right operates on the MF band while the oscillator on the left operates on the HF/VHF bands. Sockets are installed to facilitate installation and removal of the voltage booster capacitors, *C*, during testing.

for measurement. This arrangement served to eliminate possible loading effects caused by the probe.

The first experimental circuit is the MF band oscillator shown on the right side of Figure 4. This oscillator was constructed using the component values listed in Table 1. Applying Equation A.8 with these component values and *n* = 1, *A_v* = 1, and *C_{tune}* = 45 pF results in *C* = 340 pF, as shown previously in Figure 3. The left most column in Table 3 lists the values of capacitance that were used for the voltage boosting capacitance, *C*, in the circuit. For each case, capacitors were selected using a Philips PM 6303 RCL analyzer so that they matched within a few picofarads of the same value. Capacitor values in between standard values were obtained by connecting two capacitors in parallel.

The next four columns in the table record the predicted minimum loop gain, *A_v*, at the lowest oscillation frequency (*f_{low}*) computed using Equation A.6, the lowest and highest oscillation frequencies predicted from Equation A.5, and the tuning range, which is the difference between these two frequencies. The next three columns record the lowest and

highest oscillation frequencies measured for the circuit, as well as the measured tuning range, which is the difference between these two frequencies. The final column reports the percentage error between the measured and predicted tuning range results.

As the final column shows, the difference between the predicted and measured tuning ranges narrows to only a few percent beginning at a loop gain of 1.17 V/V. Additionally, the measured tuning range initially grows as the loop gain increases to 1.17 V/V and then declines for loop gains above that value. This is because a practical oscillator requires a loop gain somewhat larger than unity in order for oscillations to begin, which results in a slightly larger lower oscillation frequency, *f_{low}*. As the loop gain increases, the tuning range initially begins to rise as *f_{low}* falls. At some point, however, the tuning range begins to fall with increasing loop gain because of the progressively larger voltage booster capacitor, *C*, that appears across the *LC* tank.

The second experimental circuit is the HF band oscillator similar to the one shown on the left side of Figure 4, but using the inductor value listed in Table 4. If a single

inductor is used instead of a tuned transformer then Figure 2 applies, with $n_t = 1$. In this case, applying Equation A.8 with these component values and $n = 1$, $A_v = 1$, and $C_{tune} = 45$ pF results in $C = 8.2$ pF. The left most column in Table 5 lists the values of capacitance or parallel combinations of capacitance between 8.2 pF and 22.7 pF that were used for the voltage boosting capacitance, C , in the circuit, which were selected after the manner previously described. As before, the three columns listed under the predicted heading contain the minimum loop gain A_v at the lowest oscillation frequency computed using Equation A.6, the lowest and highest oscillation frequencies predicted from Equation A.5, and the tuning range, which is the difference between these two frequencies. Again, the next three columns record the lowest and highest oscillation frequencies measured for the circuit, as well as the measured tuning range which is the difference between these two frequencies. Finally, the rightmost column again reports the percentage error between the measured and predicted tuning range results. As this column shows, the difference between the predicted and measured tuning ranges narrows to a few percent for loop gains above about 1.20 V/V.

Once again, the measured tuning range initially grows as the loop gain increases to 1.20 V/V and then declines for loop gains above that value. In this case, however, the oscillator would not start reliably below 11.75 MHz when the loop gain was set at 1.2 V/V ($C = 10.3$ pF). Increasing the loop gain to 1.41 V/V ($C = 13.3$ pF) provided reliable oscillator starting at f_{low} , with a concomitant reduction in tuning range.

The final experimental circuit is the VHF band oscillator shown on the left side of

Figure 4 with component values listed in Table 6. In this case, applying Equation A.8 with these component values and $n = 1$, $A_v = 1$, and $C_{tune} = 45$ pF results in $C = 2.8$ pF. The left most column in Table 7 lists the values of capacitance or parallel combinations of capacitance between 2.8 pF and 15.1 pF that were used for the voltage boosting capacitance, C , in the circuit. The columns listed under the predicted and measured headings record the predicted and measured values obtained in the manner identical to that previously described. As shown in the Table, the percentage error for the tuning range shown in the last column falls below 10% for the largest loop gain.

As before, the measured tuning range initially grows as the loop gain increases to 1.17 V/V and then declines for loop gains above that value. In this case, the oscillator would not start reliably below 40.0 MHz when the loop gain was set at 1.17 V/V ($C = 3.4$ pF). Once again, increasing the loop gain to 1.51 V/V ($C = 5.2$ pF) resulted in reliable oscillator starting at f_{low} .

In all three oscillators, the measured oscillation frequency is somewhat below the predicted oscillation frequency, and the discrepancy grows at the HF and VHF bands as the oscillation frequency increases. This discrepancy is attributed to a few picofarads of parasitic stray capacitance present in the actual circuit that was not accounted for in the circuit model in Figure 2. The unmodeled parasitic capacitance ultimately appears in parallel with the LC tank, which lowers the measured frequency of oscillation compared to the predicted frequency of oscillation. The effect is less noticeable at the MF band because the small parasitic capacitance is

swamped by the much larger capacitance, C . The effect becomes very noticeable at the HF and VHF bands, where C is much smaller.

Conclusion

This article presents the results of a theoretical and experimental investigation of a Colpitts oscillator constructed using the SA/NE 6021C — widely used in Amateur Radio and experimental transmitter and receiver circuits. The theoretical analysis resulted in equations useful for the analysis and design of Colpitts oscillator circuits. Three experimental examples demonstrated the accuracy of the equations to determine the oscillator tuning range to within a few percent error for the MF and HF oscillators, and to within approximately ten percent error for the VHF oscillator.

Additionally, in each of the three cases, designing for a minimum loop gain of approximately $A_v = 1.2$ V/V appears to maximize the tuning range. Starting considerations, however, indicate that for the HF and VHF oscillators, a minimum loop gain of $A_v \approx 1.4$ to 1.5 V/V is necessary to ensure reliable oscillator starting at the low end of the tuning range. In any case, increasing the loop gain above $A_v = 1.5$ V/V reduces the tuning range of the oscillator without noticeable improvement of any other aspect of the oscillator's performance.

I have created a Microsoft Excel spreadsheet that applies the equations derived in Appendix 1 to compute the necessary loop gain, minimum and maximum oscillation frequencies and tuning range as a function of the component values for each oscillator. That spreadsheet file is available for download from the ARRL QEX files Web site.² The

Table 4
Component Values for HF Colpitts Oscillator.

Component	Value
L	3.39 μ H
n_t	1
C_{tune}	6.8–45 pF
r_p	23.16 k Ω
C_p	0.739 pF

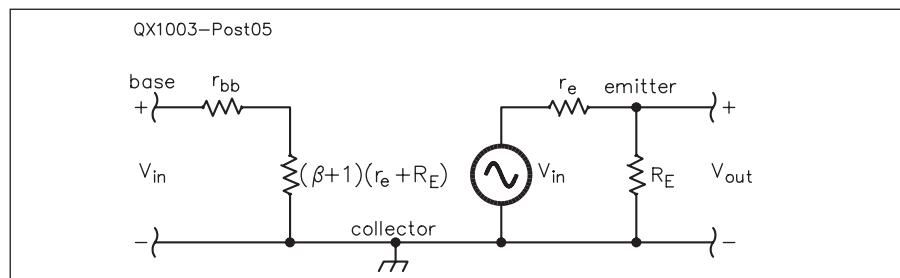


Figure 5 — Alternate emitter follower equivalent circuit. See Note 2.

Table 5
Predicted and Measured Results for the HF Colpitts Oscillator Constructed Using the Components Listed in Table 4.

C (pF)	A_v (V/V)	Predicted			Measured			Error
		f_{low} (MHz)	f_{high} (MHz)	TR (MHz)	f_{low} (MHz)	f_{high} (MHz)	TR (MHz)	
8.2	1.00	12.7653	26.4286	13.6633	12.000	22.850	10.850	20.6
10.3	1.20	12.5266	25.0859	12.5594	10.620	22.040	11.420	9.07
13.3	1.41	12.2561	23.5503	11.2942	10.440	20.860	10.420	7.74
15.1	1.49	12.1156	22.7684	10.6528	10.350	20.360	10.010	6.03
22.7	1.70	11.6174	20.1967	8.5793	10.050	18.630	8.5800	-0.01

default component values in the spreadsheets compute the predicted results shown in the first lines of Tables 3, 5 and 7 for the MF, HF and VHF oscillators. To view the results for the other lines in the tables, change the value of C in picofarads shown in cell B12 to match the value in the first column of the table for the appropriate oscillator. In order to design your own oscillator, insert the appropriate component values in cells B2 to B11. Next, notice that cell E10 displays the capacitance C required to achieve the loop gain shown in cell B9 at the lowest frequency. Finally, enter the capacitance value from cell E10 in picofarads into cell B12, or choose your own value to observe the loop gain and tuning range variations with changes in capacitance, C .

John E. Post is an assistant professor of electrical and computer engineering with Embry-Riddle Aeronautical University in Prescott, AZ. He holds an Amateur Extra class license, KA5GSQ, and has BS, MS, and PhD degrees in electrical engineering.

Notes

¹Philips Semiconductors Applications Note AN1982, *Applying the Oscillator of the NE602 in Low Power Mixer Applications*, Dec, 1988. This Ap Note is available as a PDF file at: www.datasheetarchive.com/SA602-datasheet.html.

²A Microsoft Excel spreadsheet to calculate oscillator design parameters is available for download from the ARRL QEX files Web site. Go to www.arrl.org/qexfiles/. Look for the file **3x10_Post.zip**.

³David J.Comer, *Modern Electronic Circuit Design*, Reading Massachusetts: Addison-Wesley, 1976.

Table 6
Component Values for VHF Colpitts Oscillator.

Component	Value
L	0.308 μ H
n_t	1
C_{tune}	6.8–45 pF
r_p	17.64 k Ω
C_p	0.843 pF

Appendix 1 — Derivation of Loop Gain Equation

Before analyzing the Colpitts oscillator, first consider an alternate equivalent circuit for the emitter follower circuit shown in Figure 5.³ In this model, the voltage source in the collector-emitter circuit reproduces the input voltage v_{in} that appears between the base and ground, while the output voltage v_{out} appears across the voltage divider formed by resistors r_e and R_E . For the SA/NE 602, the nominal value for R_E is given as 20 k Ω in the application note, while the value of the dynamic resistor r_e is estimated from the 0.25 mA of typical bias current as $r_e = 26 \text{ mV} / 0.25 \text{ mA} = 104 \Omega$. These values are such that it is possible to assume in Figure 5 that the multiplication of the series connection of r_e and R_E by $\beta + 1$ for all practical purposes results in an open circuit looking into the base. The bias resistor, R_B , is also neglected in the analysis because based on bias conditions it is estimated to be larger than 2 M Ω . Thus, no additional loading on the LC tank circuit is incurred due to the connection to the base of the transistor.

Figure 6 shows the complete Colpitts oscillator ac model after incorporating the alternate emitter-follower equivalent circuit and substituting

$$r'_p = \frac{r_p}{n_t^2}, \quad L' = \frac{L}{n_t^2}, \quad C' = n_t^2 (C_{\text{tune}} + C_p).$$

If a single inductor is used instead of a tuned transformer, then Figure 2 applies with $n_t = 1$. In order to determine the voltage gain around the feedback loop A_v , which is defined as the ratio of V_{out} to V_{in} , it is necessary to open the feedback loop by disconnecting the base of the transistor from the LC tank and then determine the voltage V_{out} at Node A assuming the output voltage source is V_{in} . As stated previously, since the base connection appears to be an open circuit the load resistance on the LC tank circuit does not change when the feedback loop is opened.

The first equation comes from enforcing Kirchhoff's Current Law at Node A in Figure 6. Summing currents exiting the node from left to right results in

$$\frac{V_{out}}{r'_p} + \frac{V_{out}}{\frac{1}{j\omega C'}} + \frac{V_{out}}{j\omega L'} + \frac{V_{out} - V}{\frac{1}{j\omega C}} = 0 \quad [\text{Eq A.1}]$$

The second equation comes from summing the four currents exiting Node B, or

$$\frac{V - V_{in}}{r_e} + \frac{V}{R_E} + \frac{V}{\frac{1}{j\omega nC}} + \frac{V - V_{out}}{\frac{1}{j\omega C}} = 0 \quad [\text{Eq A.2}]$$

Combining Equations A.1 and A.2 to eliminate V , and solving for the loop gain yields:

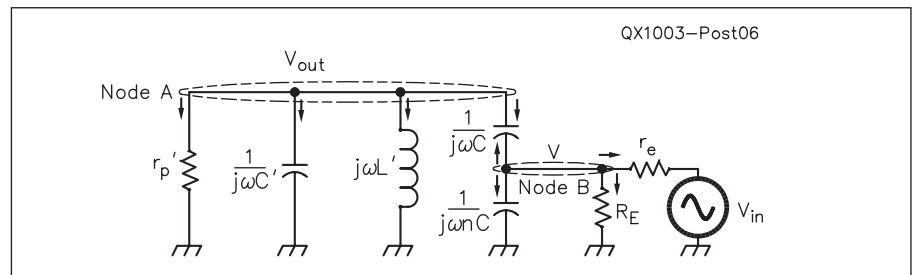


Figure 6 — Colpitts oscillator ac equivalent circuit.

Table 7

Predicted and Measured Results for the VHF Colpitts Oscillator Constructed Using the Components Listed in Table 6.

		Predicted			Measured			Error
C (pF)	A_v (V/V)	f_{low} (MHz)	f_{high} (MHz)	TR (MHz)	f_{low} (MHz)	f_{high} (MHz)	TR (MHz)	TR error (%)
2.8	1.00	42.3333	96.6923	54.3590	42.125	79.125	37.000	31.9
3.4	1.17	42.1042	94.9785	52.8743	35.35	77.175	41.825	20.9
5.2	1.51	41.5360	90.3289	48.7929	33.55	74.175	40.625	16.7
7.9	1.72	40.8571	84.6748	43.8177	33.10	70.30	37.2	15.1
10.3	1.80	40.3238	80.5064	40.1826	33.33	67.75	34.42	14.3
15.1	1.87	39.3562	73.7791	34.4229	32.40	63.65	31.25	9.22

$$A_v(\omega) = \frac{V_{out}}{V_{in}} = \frac{1}{r_e \left[\left(\frac{1}{j\omega C r_p'} - \frac{1}{\omega^2 L' C} + \frac{C'}{C} + 1 \right) \left(\frac{1}{r_e} + \frac{1}{R_E} + j\omega C(n+1) \right) - j\omega C \right]} \quad [\text{Eq A.3}]$$

The frequency of oscillation is where the imaginary portion of the denominator of Equation A.3 is zero, or:

$$\frac{1}{j\omega C r_p'} \left(\frac{1}{r_e} + \frac{1}{R_E} \right) + j\omega C(n+1) \left(-\frac{1}{\omega^2 L' C} + \frac{C'}{C} + 1 \right) - j\omega C = 0 \quad [\text{Eq A.4}]$$

Solving Equation A.4 for the frequency of oscillation, ω_0 , gives:

$$\omega_0 = \sqrt{\frac{\frac{1}{L'C} + \frac{1}{r_p' C^2} \left(\frac{n+1}{r_e} + \frac{R_E}{r_e} \right)}{n + (n+1) \frac{C'}{C}}} \quad [\text{Eq A.5}]$$

Then the loop gain at the oscillation frequency, ω_0 is found by setting the imaginary portion of the denominator of Equation A.3 to zero, or

$$A_v(\omega_0) = \frac{V_{out}}{V_{in}} = \frac{1}{r_e \left[\frac{n+1}{r_p'} + \left(1 - \frac{1}{\omega_0^2 L' C} + \frac{C'}{C} \right) \left(\frac{1}{r_e} + \frac{1}{R_E} \right) \right]} \quad [\text{Eq A.6}]$$

Equations A.5 and A.6 are useful for analyzing the Colpitts oscillator circuit shown in Figure 1, but we are more interested in obtaining an equation that will allow us to determine the capacitance C required to achieve a desired loop gain A_v at the frequency of oscillation ω_0 . This is obtained by solving Equation A.6 for C , which results in:

$$C = \frac{C' - \frac{1}{\omega_0^2 L'}}{\frac{1}{A_v} - \frac{r_e(n+1)}{r_p'} - 1 + \frac{r_e}{R_E}} \quad [\text{Eq A.7}]$$

Next eliminate ω_0 in Equation A.7 by substituting Equation A.5 and then manipulating the resulting expression in order to solve for C using the quadratic formula, which results in:

$$C = \frac{-b + \sqrt{b^2 - 4ac}}{2a} \quad [\text{Eq A.8}]$$

where


$$a = \left[\frac{(n+1) \left(\frac{1}{A_v} - \frac{r_e}{r_p'} (n+1) \right)}{1 + \frac{r_e}{R_E}} - 1 \right] \frac{r_p'}{L'} \quad [\text{Eq A.9}]$$

$$b = \frac{1}{A_v} - 1 - \frac{(n+1)}{r_p'} - \frac{1}{R_E} \quad [\text{Eq A.10}]$$

$$c = -C' \left(\frac{1}{r_e} + \frac{1}{R_E} \right) \quad [\text{Eq A.11}]$$

Equations A.8 through A.11 allow determination of the capacitance, C , necessary to obtain a desired loop gain, A_v , at a frequency determined by L' and C' . □EX□


From
MILLIWATTS to KILOWATTS
More Watts per Dollar



Taylor
TUBES

**Quality
Transmitting
& Audio Tubes**




- COMMUNICATIONS
- BROADCAST
- INDUSTRY
- AMATEUR



Immediate Shipment from Stock

3CPX800A7	3CX15000A7	4CX5000A	813
3CPX5000A7	3CX20000A7	4CX7500A	833A
3CW20000A7	4CX250B	4CX10000A	833C
3CX100A5	4CX250BC	4CX10000D	845
3CX400A7	4CX250BT	4CX15000A	866-SS
3CX400U7	4CX250FG	4X150A	872A-SS
3CX800A7	4CX250R	YC-130	5867A
3CX1200A7	4CX350A	YU-106	5868
3CX1200D7	4CX350F	YU-108	6146B
3CX1200Z7	4CX400A	YU-148	7092
3CX1500A7	4CX800A	YU-157	3-500ZG
3CX2500A3	4CX1000A	572B	4-400A
3CX2500F3	4CX1500A	807	M328/TH328
3CX3000A7	4CX1500B	810	M338/TH338
3CX6000A7	4CX3000A	811A	M347/TH347
3CX10000A7	4CX3500A	812A	M382

- TOO MANY TO LIST ALL -

ORDERS ONLY:
800-RF-PARTS • 800-737-2787


Se Habla Español • We Export

TECH HELP / ORDER / INFO: 760-744-0700

FAX: 760-744-1943 or 888-744-1943

An Address to Remember:
www.rfparts.com

E-mail:
rfp@rfparts.com



RF PARTS
COMPANY

An Inexpensive HF Power Meter with a Linear dB Scale

Here is an innovative use of an inexpensive LASER pointer.

A sensitive HF power meter is a handy instrument to have around the shack, particularly if you engage in home brew projects. The meter described here has a linear decibel response from +10 dBm (10 mW) to +20 dBm (100 mW) on a 1 mA analog meter movement. Components cost less than \$10, if you have a 1 mA meter in your junk box. With careful calibration, you may be able to achieve near “lab-quality” measurements. This power meter would be handy to have around the shack for adjusting and measuring the output power from your next oscillator or VFO project.

Theory

Wide bandwidth laser diodes have a flat response through VHF and beyond. Such diodes (red) are available from “dollar stores” in the form of laser pointers. The pointer in Figure 1 cost \$1.25 at such a store. These pointers contain laser diodes in the

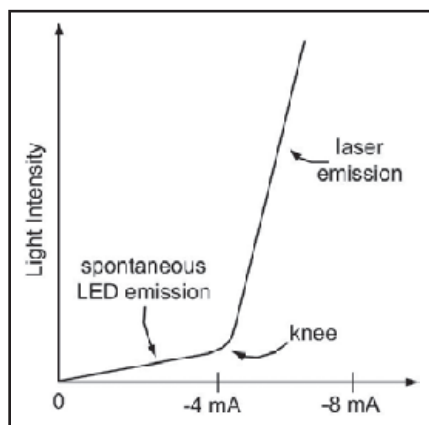


Figure 2 — Below the “knee,” the diode emits minor spontaneous LED radiation (incoherent). At the knee, laser action begins as internal losses in the diode are overcome. Above the knee, the laser light output (coherent) is linear with respect to drive current. The junction voltage at and above the knee is approximately -1.4 V dc.

form of individual laser chips (dye). More expensive laser pointers from RadioShack (\$15) contain laser diodes encapsulated in a transistor style can with an integral lens. These might be easier to work with, generally, but the price of the cheaper pointer was a driving force for me.

To obtain wideband response, the diode must be dc biased at the “knee,” as shown in Figure 2. Below the knee, there is a minor amount of LED radiation, which we do not use. At the knee and above, the diode begins to lase as internal losses are overcome. Light intensity increases rapidly and linearly with current.

The general biasing scheme is shown in Figure 3. The bias level is set by adjusting R_{bias} . For my unit, R_{bias} was 1800Ω with a 9 V battery, although I started initially with a 2.5 k Ω , ten-turn potentiometer.

The emitted laser light can be detected with a RadioShack cadmium-sulfide photoresistor, as shown in Figure 4. These are



Figure 1 — Laser pointer purchased at dollar store for \$1.25. The pointer comes with 4 holograms, which are not used.

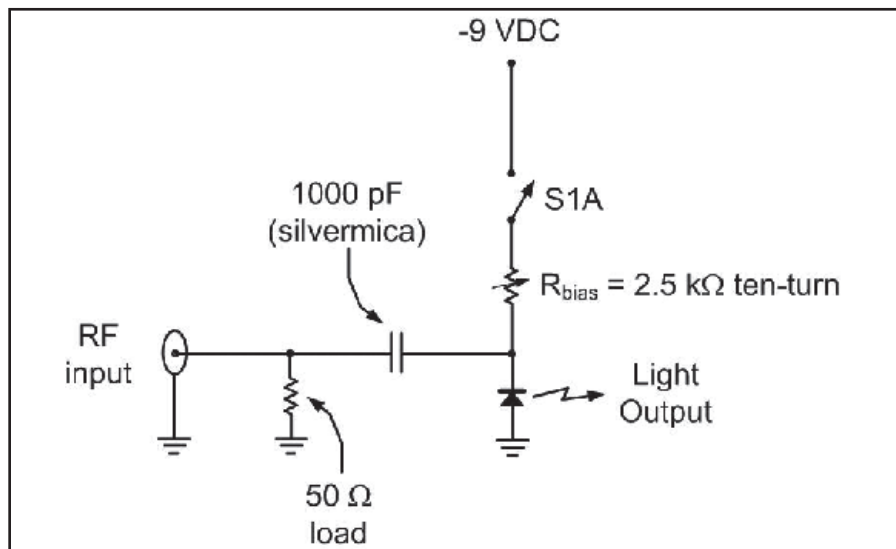


Figure 3 — The dc bias is set with R_{bias} , while the RF signal is coupled through the 1000 pF coupling capacitor (silver mica).



Figure 4 — Cadmium-sulfide photo-resistors available from RadioShack in a pack of five.

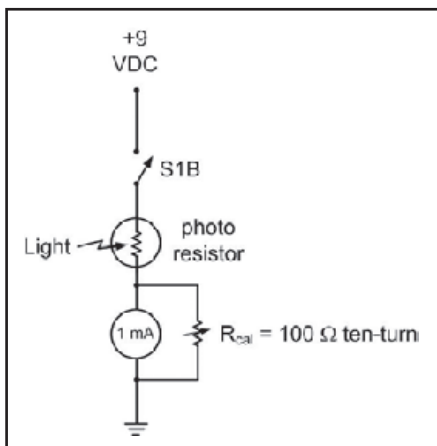


Figure 5 — Light detecting circuit using photo-resistor and 1 mA meter movement. Set R_{cal} initially to zero ohms. When laser is at full brilliance, the battery current is 25 mA.



Figure 6 — Individual photo-resistor used in power meter. This is the largest resistor in the pack of five. Note the serpentine structure of the resistor.

available in a pack of five for \$4.00. The complete light detector circuit is shown in Figure 5. The resistor shunting the meter is R_{cal} (100 Ω ten-turn potentiometer) and should be set initially to zero ohms.

Construction and Alignment

I used the largest photo resistor from the pack of five. This device goes from 360 k Ω in total darkness to about 400 Ω in bright light. The photo resistor is shown in Figure 6, where the serpentine structure can be seen.

The commercial laser pointer is shown in Figure 7A. In Figure 7B the aluminum tube is peeled away from the laser module with a pair of needle-nosed pliers. Part C shows the module itself. Note that the laser case is positive (+). Using a pair of sharp diagonal cutters, I removed the battery clip and push-button portion of the circuit card. Part D shows the photo resistor being mated to the laser module with a small amount of fast-setting epoxy. The epoxy should go around the periphery of the photo resistor and not on the sensitive face. Figure 7E is a photo of the first complete prototype. Keep lead lengths short. R_{bias} is shown as a fixed 1800 Ω resistor — this was done after first using a 10 turn potentiometer to determine the proper value of R_{bias} for a 9 V battery. The laser I used had a plated plastic case that could not be soldered; contact was made by tying a wire around the case and twisting tightly. The case is RF ground and positive bias. Before testing the power meter, set $R_{bias} > 1800 \Omega$ and R_{cal} to zero ohms.

Initial Alignment

- 1) Apply -9 V dc bias to the laser.
- 2) Decrease R_{bias} until some minor red light can be seen from the rear of the diode. There is a hole in the rear of the diode case for visual monitoring.

- 3) Set up a signal generator to provide 100 mW (+20 dBm) at 14 MHz by way of a 1 dB step attenuator. Don't forget the 50 Ω dummy load or you'll burn the diode immediately.
- 4) Apply the RF. The laser should shine brightly. Increase R_{cal} until there is a full-scale deflection on the milliammeter.

Final Alignment

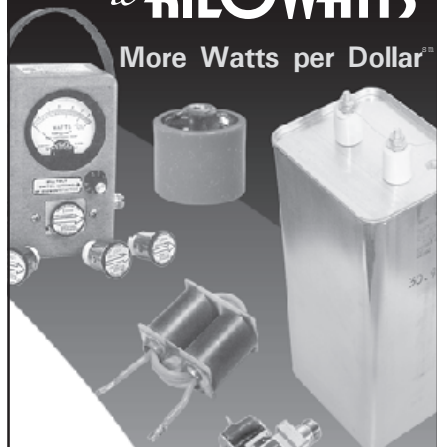
- 5) Reduce the RF level by 1 and 2 dB. Observe the meter response, looking for a decrease of 1 and 2 units.

- 6) If the decrease is more than 1 and 2 units, the laser is biased too lightly. Re-adjust R_{bias} for slightly higher bias. Go back to step 4. This time you will be decreasing R_{cal} to obtain a full deflection.

- 7) Conversely, if you obtain less than 1 and 2 units response on the meter, the bias level on the laser is set too high. Reduce the bias by increasing R_{bias} , and return to step 4; this time you will be increasing R_{cal} for full-scale deflection.

From
MILLIWATTS
to **KILOWATTS**

More Watts per Dollar



- **Wattmeters**
- **Transformers**
- **TMOS & GASFETS**
- **RF Power Transistors**
- **Doorknob Capacitors**
- **Electrolytic Capacitors**
- **Variable Capacitors**
- **RF Power Modules**
- **Tubes & Sockets**
- **HV Rectifiers**



ORDERS ONLY:
800-RF-PARTS • 800-737-2787

Se Habla Español • We Export

TECH HELP / ORDER / INFO: 760-744-0700

FAX: 760-744-1943 or 888-744-1943

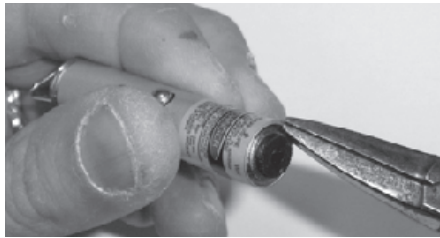
An Address to Remember:
www.rfparts.com

E-mail:
rfp@rfparts.com

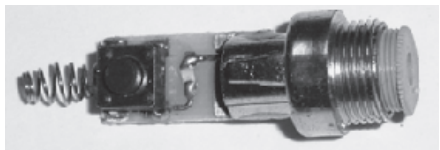




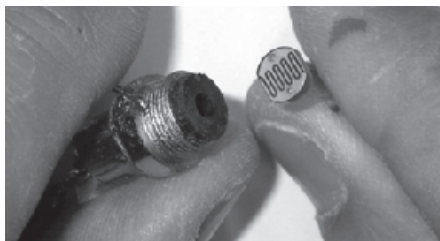
(A)



(B)



(C)



(D)



(E)

Figure 7 — Part A shows the commercial laser pointer. The photo at Part B shows the aluminum tube being peeled away from the laser module with needle-nosed pliers. The laser module was removed from aluminum case, as shown in Part C. The chip resistor in the center is a $62\ \Omega$ current limiting resistor in the negative lead. This is the lead to which the RF coupling capacitor and R_{bias} are attached. The plated plastic body is the ground for RF and bias — it cannot be soldered. In Part D, the photo-resistor is mated with the laser diode. Use a small amount of fast-setting epoxy, being careful not to get epoxy on the sensitive face of the photo-resistor. The completed prototype is shown in Part E. The coaxial line at left is the RF sensing line. The coaxial line at right is for application of the dc bias. Note that the case ground (+) is made by wrapping and twisting a fine copper wire around the case, and then soldering to the coaxial shield.

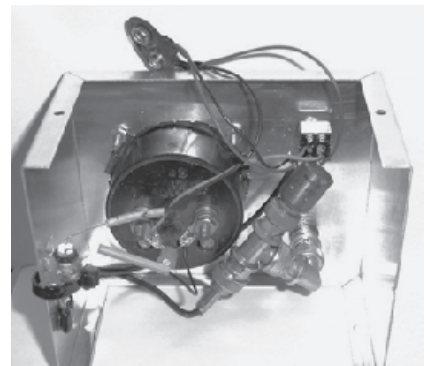
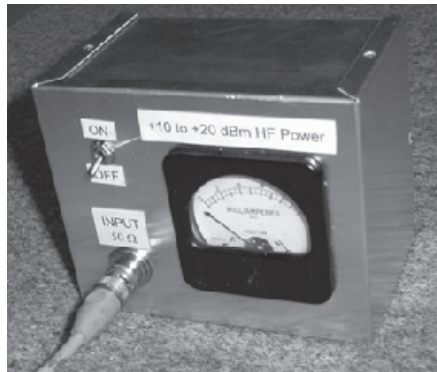


Figure 8 — The front panel of completed power meter is shown in Part A. Part B shows the internal view of the completed power meter. Note the $50\ \Omega$ load attached to the input connector with a BNC tee. The 10 turn ($100\ \Omega$) R_{cal} shunts the milliammeter. The laser head is secured to the case at left with a tie wrap and RTV rubber sealant. The switch is double-pole for the two 9 V batteries.

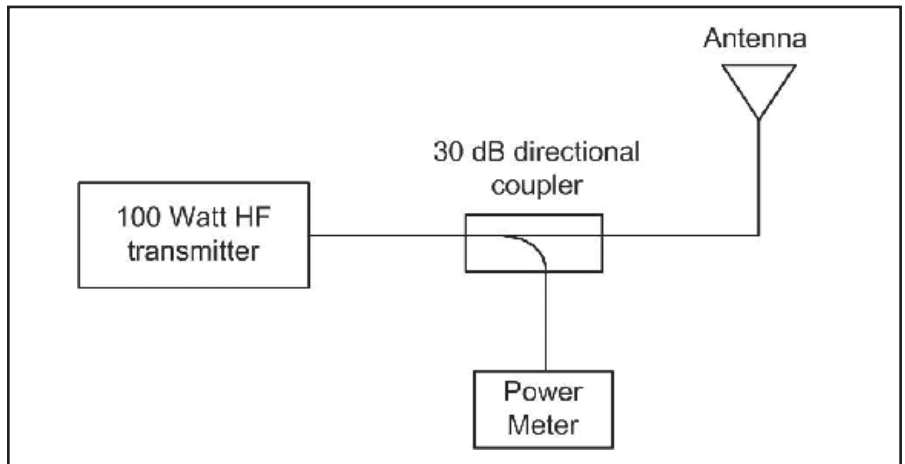


Figure 9 – Method of monitoring forward power from a 100 W HF transmitter.

One or two iterations of the calibration procedure, and the meter will read linearly from +10 to +20 dBm (0 to 1 on the analog meter scale). Verify the full meter response with a 1 dB step attenuator. You may find it desirable to adjust the meter zeroing screw so that the meter points below zero without bias and RF. Then when the bias is turned on with no RF applied, the meter will read zero (+10 dBm).

After calibration, you can check the meter response at different frequencies. My meter is flat to within half a decibel from 3 to 30 MHz. Figure 8 shows the completed power meter.

Summary

I find my laser power meter to be very handy around the shack. When not using it for experiments, I leave it connected to my HF rig with a 30 dB directional coupler to monitor forward power, as shown in Figure 9. If you are uncertain as to what power you expect to measure, always protect the power meter with a safety attenuator, for the laser can be burned out promptly with application of excessive power. As a final note, the power

meter may be built and calibrated for VHF and UHF use. If use at L-band is anticipated, it is better to buy a commercial laser diode from Digi-Key, to insure the laser has sufficient bandwidth. If the laser portion of the meter is realized in $50\ \Omega$ microstrip, a chip coupling capacitor, and a canned laser (for low parasitics), the meter can provide flat response from HF through the 23 cm band.

Robert K. Zimmerman, Jr. was born in 1951 in Dupou, Illinois. He graduated from Southern Illinois University, Edwardsville, with BS and MS degrees in physics (1973, 1975) and then attended the University of Illinois, Urbana-Champaign, where he was awarded the MSEE degree in 1980. He has spent his entire career in radio science, working for Cornell University (Arecibo Observatory), NASA Goddard Spaceflight Center, Los Alamos National Laboratory (accelerator division), and most recently as a radar engineer on Kwajalein Atoll. He is presently involved in microwave antenna research at McMaster University, Hamilton, Ontario. He has been licensed as WN9PXXG (1965), WA9ZSF, NP4B, V73BZ, and now as VE3RKZ. Zimmerman is active on 40 m and 23 cm.



Letters to the Editor

Experimental Determination of Ground System Performance for HF Verticals (Jan/Feb 2009 through Jan/Feb 2010)

Dear Larry,

As my series of QEX articles on ground system experiments were published I received a number of questions and comments. When I wrote the description of the experiment in Part 1, I only wanted to give an overview of the experiment and left out many details. Then of course there were questions about the omitted details! One frequent question concerned the power reflected from the vertical, back to the VNA due to mismatch at the antenna feed point. This mismatch varied as the ground system was changed. While most of the time this effect was very small, it still had to be taken into account, which it was for every measurement. I referred to this in Part 5 but not in detail. I also received a note from Paul Kiciak, N2PK, pointing out that I was misusing the term $|S_{21}|$ in some of the figure captions. He was right, I should have used the term transmission gain or something similar.

At the beginning of the experiments I wrote my initial thoughts in the experiment notebook. These notes were in the form of a conversation with myself, but with a little cleaning up they can be used to address the two points mentioned above. An excerpt from my notebook follows.

I hope this will help answer some of the questions.

Notebook Excerpt

The problem

In this series of experiments, I want to quantitatively determine the effect of various ground systems on the efficiency of a vertical. For example, if I add X number of radials to a given ground system, how much stronger is my signal at a distant receiver for the same power input to the antenna (P_i)? The power input to the antenna is defined as:

$$P_i = P_s - P_r \quad [\text{Eq 1}]$$

where:

P_s = forward or incident power at the antenna feed point.

P_r = reflected power at the feed point.

I will have to keep this distinction between P_i and P_s in mind later in the data analysis!

What I'm interested in is the power gain (G_T) expressed as:

$$G_T = \frac{P_L}{P_i} \quad [\text{Eq 2}]$$

where:

P_L = power in the receiver due to the excitation of the vertical with P_i . G_T in Equation 2 is a power ratio and I want to express it in dB:

$$G_T [\text{dB}] = 10 \log \left(\frac{P_L}{P_i} \right) [\text{dB}] \quad [\text{Eq 3}]$$

As I go through the experiments, I will be interested in the change in G_T [dB] from one ground system configuration to another. By taking the difference between G_T [dB] for one case and that for another I will have the "improvement" (or the lack thereof!) in dB for a given change in the ground system.

Solution to the Problem

After I had tried more conventional techniques, Paul Kiciak, N2PK, suggested a really slick way to determine G_T [dB]: use a vector network analyzer (VNA), excite the test antenna with the output of the VNA and measure the resulting signal via a remote antenna connected to the VNA input port. Repeat this for each change in the ground system.

What the VNA will give me is $|S_{21}|$ [dB] around the loop from the VNA output port to the test antenna, then out to the receiving antenna and back to the VNA detector port. $|S_{21}|$ is defined by:

$$|S_{21}| = \sqrt{\frac{P_L}{P_s}} \quad [\text{Eq 4}]$$

where:

P_L = power in the load, in this case the input to the VNA.

P_s = power supplied by the source, in this case the output of the VNA

The VNA gives $|S_{21}|$ [dB]:

$$|S_{21}| [\text{dB}] = 20 \log \left(\sqrt{\frac{P_L}{P_s}} \right) [\text{dB}] \quad [\text{Eq 5}]$$

I can pull the square root out of Equation 5 so that:

$$|S_{21}| [\text{dB}] = 10 \log \left(\frac{P_L}{P_s} \right) [\text{dB}] \quad [\text{Eq 6}]$$

That's very nice but what I really want is G_T [dB] as given in Equation 3. I can see that Equation 3 has the same form as Equation 6, therefore:

$$G_T [\text{dB}] \Leftrightarrow |S_{21}| [\text{dB}] \quad [\text{Eq 7}]$$

Be careful. There is a trap here! While G_T

[dB] may be numerically equal to $|S_{21}|$ [dB] (Note: for the moment only, we are assuming $P_r = 0$), G_T is not the same as $|S_{21}|$! There is a conceptual difference.

A Necessary Tweak on G_T [dB]

For Equations 6 and 7 I assumed that $P_i = P_s$, $P_r = 0$. However, we know that is true only if the feed point impedance of the vertical is exactly 50Ω (Z_0 for these experiments). In other words, $P_r = 0$, but in general that will not be true. What I want is:

$$G_T \Rightarrow |S_{21}'| = \sqrt{\frac{P_L}{P_i}} \quad [\text{Eq 8}]$$

where:

P_i = the power delivered to the input of the test antenna and $|S_{21}'|$ is the transmission from the input of the vertical to the input of the VNA via the receiving antenna, but $|S_{21}|$ is the transmission from the output of the VNA to the input of the VNA. The problem is that what I get from the VNA is $|S_{21}|$ [dB], not $|S_{21}'|$ [dB]. Due to reflection $P_i < P_s$ and that means $|S_{21}'| > |S_{21}|$. What I need to do is to determine the difference between the two and modify what the VNA gives me, to get the G_T [dB] I'm after.

I derived an expression for this additional term, incorporating SWR measurements, and Paul sent me another expression in terms of $|S_{11}|$.

$|S_{21}|$ to $|S_{21}'|$

I know from Equation 1 that:

$$P_i = P_s - P_r \quad [\text{Eq 9}]$$

I can eliminate P_r from Equation 9 and calculate P_i in terms of P_s and SWR at the feed point:

$$\frac{P_i}{P_s} = 1 - \left[\frac{\text{SWR} - 1}{\text{SWR} + 1} \right]^2 \quad [\text{Eq 10}]$$

Using Equations 4 and 8:

$$|S_{21}'| = \sqrt{\frac{P_L}{P_i}} = \sqrt{\frac{P_L}{P_s}} \sqrt{\frac{P_s}{P_i}} = |S_{21}| \sqrt{\frac{P_s}{P_i}} \quad [\text{Eq 11}]$$

Substituting Equation 10 into Equation 11:

$$|S_{21}'| = \frac{|S_{21}|}{\sqrt{1 - \left[\frac{\text{SWR} - 1}{\text{SWR} + 1} \right]^2}} \quad [\text{Eq 12}]$$

Paul sent me the following expression:

$$\frac{P_L}{P_i} = \frac{|S_{21}|^2}{1 - |S_{11}|^2} \quad [\text{Eq 13}]$$

which I will change to:

$$|S_{21}'| = \sqrt{\frac{P_L}{P_i}} = \frac{|S_{21}|}{\sqrt{1 - |S_{11}|^2}} \quad [\text{Eq 14}]$$

to make Equation 13 look like Equation 12.

It's not too hard to show that:

$$|S_{11}| = \frac{SWR - 1}{SWR + 1} \quad [\text{Eq 15}]$$

Equations 12 and 14 are equivalent. For these experiments I will use Equation 12.

One More Step

I need $|S_{21}'|$ [dB] not $|S_{21}|$. From Equation 12:

$$|S_{21}'| [\text{dB}] = |S_{21}| [\text{dB}] - 10 \log \left[1 - \left(\frac{SWR - 1}{SWR + 1} \right)^2 \right] \quad [\text{Eq 16}]$$

During these experiments I will record both $|S_{21}|$ [dB] (which the VNA gives me) and SWR (which the VNA also gives me) for every ground system configuration. One small thing to watch out for:

$$\left[1 - \left(\frac{SWR - 1}{SWR + 1} \right)^2 \right] \leq 1 \quad [\text{Eq 17}]$$

Therefore the log of Equation 17 will be negative. That means I will need to *add* the $10 \log[**]$ term to the value of $|S_{21}'|$ [dB] I get from the VNA. Also $|S_{21}'|$ [dB] < 0 dB for these experiments. For example, if $|S_{21}| = -42.6$ dB and the SWR is 2, $-10 \log[**] = +0.5$ dB. Then $|S_{21}'| = -42.1$ dB.

I will create a table of values for Equation 18:

$$K = -10 \log \left[1 - \left(\frac{SWR - 1}{SWR + 1} \right)^2 \right] \quad [\text{Eq 18}]$$

The table will have all positive numbers to modify the recorded values for $|S_{21}|$ [dB] to get $|S_{21}'|$ [dB].

— 73, Rudy Severns, N6LF, PO Box 589, Cottage Grove, OR 974249; n6lf@arrl.net

Hi Rudy,

Thank you for sending the detailed information about the derivation of the equations and the calculations used in your QEX series. There was a lot of interest in the series, and I am sure many readers will be interested to learn more about the calculations behind your results.

— 73, Larry Wolfgang, WR1B, QEX Editor; lwolfgang@arrl.org

SDR: Simplified (Jan/Feb 2010)

Larry,

Karl-Otto Müller, DG1MFT, found a couple of mistakes I made in my last column. The drawings for Figures 3B and 3C were swapped. Also, I am not sure what happened, but when I did the *gnuPlot* work for a couple of the figures, I was off by a factor of 2 times. The 400 Hz sine wave is actually 200 Hz and the 20 kHz wave is actually 10 kHz. The principle to be illustrated is still correct: the energy in the higher Nyquist zones is due to the size of the error between the samples and the true waveform, and gets progressively worse as the sampled wave approaches one half the sampling frequency.

There is no column for the March/April issue because of problems I faced in getting the software tools to work correctly. I owe the readers a lot of code and other supporting work for previous columns. In order to make that process easier, I have created a Web site at www.dsp-radio-resources.info so that I can post updates from readers, answer questions from readers, and supply an alternative to the ARRL Web site for file downloads. It is meant to be a forum for information exchange for the readers.

Down East Microwave Inc.

We are your #1 source for 50MHz to 10GHz components, kits and assemblies for all your amateur radio and Satellite projects.

Transverters & Down Converters, Linear power amplifiers, Low Noise preamps, coaxial components, hybrid power modules, relays, GaAsFET, PHEMT's, & FET's, MMIC's, mixers, chip components, and other hard to find items for small signal and low noise applications.

We can interface our transverters with most radios.

Please call, write or see our web site www.downeastmicrowave.com for our Catalog, detailed Product descriptions and interfacing details.

Down East Microwave Inc.
19519 78th Terrace
Live Oak, FL 32060 USA
Tel. (386) 364-5529

— 73, Ray Mack, W5IFS, 17060 Conway Springs Ct, Austin, TX 78717; w5ifs@arrl.net

Hi Ray,

Thanks for the information about your new Web site. I apologize for our layout error on Figure 3 of your Jan/Feb column.

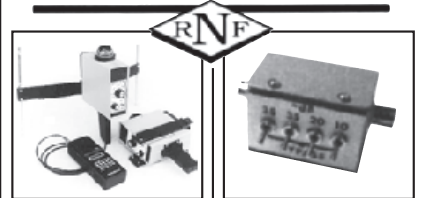
— 73, Larry, WR1B

QEX

Next Issue in QEX

David Bern, W2LNX, describes his first programming project with a Microchip PIC microcontroller — “A PS/2 Keyer: Using Keyer Paddles to Emulate a PS/2 Keyboard and Mouse.” Besides a desire to find a useful project to learn about programming a PIC microcontroller, David's motivation for this project was to make portable PSK-31 operation with the NUE-PSK modem even simpler. Now all he needs is his transceiver, NUE-PSK modem and a keyer paddle. No keyboard required!

NATIONAL RF, INC.

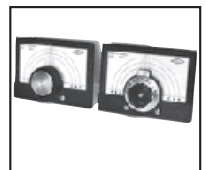


VECTOR-FINDER
Handheld VHF direction finder. Uses any FM xcvr. Audible & LED display
VF-142Q, 130-300 MHz \$239.95
VF-142QM, 130-500 MHz \$289.95

ATTENUATOR
Switchable, T-Pad Attenuator, 100 dB max - 10 dB min BNC connectors
AT-100, \$89.95



TYPE NLF-2
LOW FREQUENCY ACTIVE ANTENNA AND AMPLIFIER
A Hot, Active, Noise Reducing Antenna System that will sit on your desk and copy 2200, 1700, and 600 through 160 Meter Experimental and Amateur Radio Signals!
Type NLF-2 System: \$369.95



DIAL SCALES
The perfect finishing touch for your homebrew projects. 1/2-inch shaft couplings.
NPD-1, 3 1/8 x 2 3/4, 7:1 drive \$34.95
NPD-2, 5 1/8 x 3 3/8, 8:1 drive \$44.95
NPD-3, 5 1/8 x 3 3/8, 6:1 drive \$49.95

NATIONAL RF, INC
7969 ENGINEER ROAD, #102
SAN DIEGO, CA 92111

858.565.1319 FAX 858.571.5909
www.NationalRF.com

All the information you need to design your own complete antenna system.

The ARRL

The ARRL
ANTENNA BOOK

21st Edition

ANTENNA BOOK



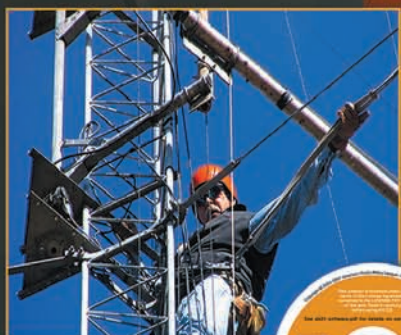
21st Edition

ARRL Order No. 9876

Only **\$44.95***

*plus shipping and handling

The *ultimate* reference for Amateur Radio antennas, transmission lines and propagation



Fully searchable CD-ROM included!



ARRL The national association for AMATEUR RADIO

SHOP DIRECT or call for a dealer near you.
ONLINE WWW.ARRL.ORG/SHOP
ORDER TOLL-FREE 888/277-5289 (US)

QEX 3/2010

The Totally New - Advanced Dual Band Mobile Radio

5.2" x 1.6" Large dot matrix (264 x 64 dots) LCD display

GPS / APRS® / Bluetooth® Features



NEW

144/(220)* /430 MHz 50 W
FM Dual Band Transceiver
FTM-350R

*220 MHz 1W (USA Version only)

NEW

Large (5.2" x 1.6"/130 x 40 mm) dot matrix (264 x 64 dots) LCD display for comfortable viewing for night and day. Choose your favorite LCD display from 8 vibrant color options

NEW

The Display Control Head is designed for easy separation from the main RF power unit built by tough aluminum die-cast; 10ft control cable included (Optional 20ft control cable available)

NEW

Multi-purpose Global Positioning System display (with optional FGPS-1 GPS Receiver and Antenna. Optional FGPS-2 External GPS Receiver and Antenna is also available)

NEW

Compatible with the worldwide standard data-communications system, APRS®, and SmartBeaconing™ capabilities

NEW

Huge memory channel management capability!
500 Independent Memory channels
+ 9 Programmable Band Limit Memory Scan channels
+ 1 Rewritable Preferred channel for each L and R Band

NEW

3 Speaker System
(including Built-in Dual Speakers on the rear of the Control Head for FM Broadcast in Stereo!)

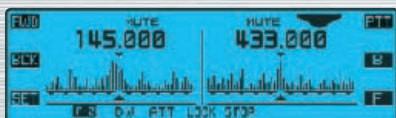
Exclusive

Dual Band AF Monitor for listening to FM/AM broadcast and monitoring ham bands as well

Exclusive

Built-in Barometric Pressure Sensor

Screen Example



Dual Band (Spectrum Scope function)



Navigation (with GPS antenna unit attached)



Mono Band (Spectrum Scope function)



APRS®



Barometer



Timer

* APRS® is a registered trademark of Bob Bruninga WB4APR.
* SmartBeaconing™ from HamHUD Nichetronix

For the latest Yaesu news, visit us on the Internet:
<http://www.vertexstandard.com>

Specifications subject to change without notice. Some accessories and/or options may be standard in certain areas. Frequency coverage may differ in some countries. Check with your local Yaesu Dealer for specific details.

YAESU
Choice of the World's top DX'ers™

Vertex Standard
US Headquarters
10900 Walker Street
Cypress, CA 90630 (714)827-7600

